HARRIS-NESBET METHOD FOR ELECTRON-Li^{2+} COLLISIONS: DETERMINATION OF THE SINGLET S-WAVE DOUBLY EXCITED STATES OF Li^{+} BELOW THE N=2 THRESHOLD OF Li^{2+}

KIET A. NGUYEN

Harris-Nesbet Method for Electron-Li^{2+} Collisions: Determination of the Singlet S-wave Doubly Excited States of Li^{+} below the N=2 Threshold of Li^{2+}

by

Kiet Nguyen A.

A thesis submitted to the School of Graduate Studies in partial fulfilment of the degree of Master of Science.

Department of Physics and Physical Oceanography

Faculty of Science

Memorial University of Newfoundland

May – 2008

St. John's Newfoundland

Abstract

The positions and widths of the singlet S-wave doubly excited state resonances $^1S^e$ of Li^- at energy below the N=2 threshold of Li^{2+} are determined, employing a numerical procedure developed earlier for electron collisions with hydrogenlike ions within the Harris-Nesbet variational method. Altogether, twenty of these singlet S-wave doubly excited states are located below this threshold with their widths determined. Some of these doubly excited states are determined for the first time by the present calculation. Our results are compared, with discussion, to those obtained by various other research groups using different numerical methods of approach for their calculations. Graphical presentation of all these twenty doubly excited states is given.

Acknowledgements

I would like to hold a special place for my gratitude towards Dr T. T. Gien, my supervisor. He, with the most patient and sympathy as well as vast knowledge in this physics field, has not only guided me as a professor through the whole program but also accompanied as a best friend during the life as graduate student. He has step by step improved my understanding about Atomic Physics, provided information and research procedure to emerge myself into a new environment and offered countless helps on organizing and writing this thesis. Without him, I may not ever finish this subject or even come across it in the first place.

I would also like to thank all the staff members of Department of Physics and Physical Oceanography, Memorial University of Newfoundland. They have provided assistances on many aspects of researching and working as a graduate student. I also appreciate the professors, who directly or indirectly instructed me on various problems. A lot of gratefulness goes to my new friends in St. John's, especially Bill Kavanagh and the Huu Anh Trans, whose welcome and caring have enlightened me a great deal during my working and studying in a completely new academic environment.

Not any less important, it is my family who provide me endless support spiritually and practically whenever I am in need, especially my mother and my life's friend, my wife.

I would also like to thank Mr. Lester Marshal as well as the members at the Counselling Center. During my most discouraging period, he has patiently listened and advised me the most possible solution so that I can come back and finish this thesis.

After all, I must express my appreciation to Memorial University of Newfoundland. The organization and its community in a whole has firstly granted me a fellowship, an opportunity to be a part of it; secondly, provided a healthful and active environment to do research; and lastly, acknowledged my very first project overseas.

Table of Contents

List of Tables

List of Figures

Chapter 1

Introduction

1.1 Introduction

Beside the singly excited states which have been well understood nowadays, a multi-electron atom when receiving appropriate energy from an external source can be doubly excited to higher energy states where two electrons of the atom are simultaneously excited. Throughout the years, doubly-excited states of two-electron (neutral or ionic) atoms have been studied intensively by various experimental as well as theoretical research groups. In particular, the study of doubly excited states of Li^+ has been a subject of interest for many researchers. On the experimental side, several experiments have been performed to detect these doubly-excited resonances of Li^+. One may cite for example an earlier experiment by Bruch *et al* (1975) [1], using the so-called beam-foil interaction mechanism. This group succeeded in determining the positions of the lowest $^{1,3}P^o$ doubly-excited states in Li^+. The energy spectrum of the emitted electrons was recorded and analyzed while the foil was moved along the beam axis. Due to the time

delay in the autoionization process, resonances were detected. Ziem et al (1975) [2] also determined the positions of the lowest ^1S and $^{1,3}P$ resonances in Li^+ by colliding H^+ and He^+ with Li^+. Carroll and Kennedy (1977) [3] performed a photo-absorption experiment for Li^+ and were able to determine the three lowest members of the doubly-excited-state resonances $^1P^o$. By looking at the ejected-electron spectra of highly-excited autoionization levels of Li^+ in their single collisions with neutral atoms and molecules such as He and CH_4 and with the guidance of the values obtained by theoretical calculations, Rodbro et al [4] were able to determine the positions of these doubly-excited states of Li^+

On the theoretical side, various research groups or individuals have carried out calculations, using different numerical methods, to determine these series of doubly-excited-state resonances of Li^+ in an attempt to verify their existence in this two-electron ionic atom as was predicted by theory (Cooper *et al*, 1963 [5]). One may cite for example the work by Bhatia (1977) [6] who employed the Feshbach projection-operator technique to determine the positions and widths of the three lowest-lying resonances of the various series below the N=2 excitation threshold of the hydrogenlike ion Li^{2+}. Ho (1981) [7] also determined a few lowest-lying doubly-excited resonances of Li^+ below the N=2 threshold, employing the complex coordinate rotation method (CCR) with the consideration of the Hylleraas-type wave functions. His results of position and width obtained for these resonances are in reasonable agreement with those by Bhatia, although the widths obtained by Ho are, at times, seen to deviate noticeably from those by Bhatia. Both these researchers determined a few lowest-lying resonances of these series only.

Bruch et al (1975) [1] was the research group who performed the calculations of the positions of higher-lying doubly-excited states, using the truncated diagonalization method (TDM) (1965, 1966) [8, 9]. For example, the positions of up to 11 resonances below the N=2 threshold were obtained by this group for the series of singlet S-wave resonances ($^1S^e$). However, the widths of only three lowest-lying doubly-excited-state resonances were calculated by Conneely and Lipsky (1978) [10] with the TDM. The widths obtained by them were found, in general, to differ considerably from those obtained by Bhatia and by Ho. More recently, Chung and Lin (1998) [11] carried out an extensive calculation of positions and widths for the doubly-excited-state resonances formed below the N=2, 3 thresholds in Li^+, using the complex-rotation method. For the singlet S-wave resonances of even parity below the N=2 threshold, they located altogether 16 of these resonances. Comparing the positions and widths of the low-lying S-wave resonances determined by this group to those by others, one finds that they agree reasonably well with those determined by Ho and also those by Bhatia, but their widths, in general, disagree with those obtained by Conneely and Lipsky considerably. The widths of the higher-lying resonances (especially those closer to the threshold) are usually considerably smaller than those of the lower-lying ones and should, thereby, be more difficult to be determined with accuracy. Unfortunately, as at present, Chung and Lin, to our knowledge, has been the only research group who determined the widths for these higher-lying resonances in Li^+. It would, therefore, be interesting to try to determine these resonances using, however, a completely different (and reliable) numerical method for comparison with their results and also to resolve the discrepancy existing among the widths of the low-lying resonances calculated by these various research groups or

individuals. It is also interesting to try to determine the doubly-excited states lying even higher (and closer to the N=2 threshold of Li^{2+}) than those located by Chung and Lin, that nobody has yet attempted to.

This thesis presents the results of our investigation of S-wave doubly-excited states of Li^{+} below the N=2 excitation threshold of Li^{2+}, employing a completely different numerical method developed earlier by Gien (1995 [12, 13]) within the Harris-Nesbet variational calculation (1980 [14]) of electron and positron collisions with H and with hydrogenlike ions. As will be seen in subsequent discussions of the thesis, this method is quite reliable for this task. We focus our attention to the singlet S-wave only, however.

1.2 Outline of the thesis.

The content of the thesis is organized as follows. In Chapter 2, we make a review on the Harris-Nesbet method for electron (positron) collisions with atomic targets. We also show how the method is applied to the case of electron scattering from a hydrogenlike ion target. In chapter 3, we present our results with discussion and compare them to those obtained by other research groups. We also discuss in this chapter the details of the Harris-Nesbet calculation carried out for electron-Li^{2+} scattering and the numerical procedure through which the positions and widths of the doubly-excited-state resonances below the N=2 excitation threshold of Li^{2+} in Li^{+} are determined. We summarize the results of the research work of the thesis in chapter 4.

Chapter 2

Harris-Nesbet Variational method

In order to improve the stability of the Kohn-Hulthe'n variational method (1944, 1948, 1948) [15-17] when applied to a collision process (Schwartz, 1961) [18], Harris (1967) [19] proposed a method of expansion of the trial wave function, which, later on, has been known as the Harris variational method. The detail of this method will be described in section 2.1 below. As will be seen in 2.1, the Harris method can provide the variational phase shifts of the collision process at a specific set of scattering energies only. They are eigenenergies of the set of basis functions selected in advance for the bound part of the trial wave function. Nesbet (1968, 1969, 1973) [20-22] subsequently proposed an extension of the Harris method which enables the calculation of phase shifts and cross sections at any arbitrary scattering energies. This method has been, later on, known as the Harris-Nesbet variational method in collision theory. In section 2.2, we shall describe, in some detail, the Harris-Nesbet variational method in the case of single-channel collision as well as multi-channel collision. Finally, in section 2.3, we discuss the Harris-Nesbet variational method for electron-hydrogenlike-ion collisions.

2.1 Harris variational method

The Schrödinger equation which governs the dynamics of a collision process is

$$(H - E)\Psi = 0 \tag{2.1}$$

Thus the functional of the collision process should be, as usual, defined as (Harris (1967) [19]):

$$\Xi = \langle \psi | H - E | \psi \rangle \tag{2.2}$$

According to Harris [19], the form of the trial function Ψ in the variational method should be selected to be an expansion as follows,

$$\Psi = \Phi + \alpha_0 S + \alpha_1 C \tag{2.3}$$

where Φ is the bound part of the trial wave function which represents the collision system at short distance while S and C are the sin and cos functions which form the free part of the trial function. The free part, together with α_0 and α_1, describes the collision system in the asymptotic region.

A set of numerable bound-state functions η_i are then chosen. They can be canonically transformed into the basis functions φ_i which diagonalize H. In practice, φ_i are obtained by solving the finite matrix equation below

$$(H - ES)X = 0 \tag{2.4}$$

where $H_{ij} = \langle \eta_i | H | \eta_j \rangle$ and overlap matrix S has elements $S_{ij} = \langle \eta_i | \eta_j \rangle$. X is an unknown column matrix, with its jth element representing the component of the state vector $|X\rangle$ on $|\eta_j\rangle$.

The bound part Φ can then be expanded in terms of this basis set of φ_i

$$\Phi = \sum_i C_i \varphi_i \tag{2.5}$$

Thus, the bound-part function Φ is normalizable and does not affect the asymptotic behavior of Ψ.

The well-known variational conditions imposed on the functional (2.2) with C_i^* as variational variables are equivalent to requiring that the state function on the left-hand side of (2.1) has no component in the subspace spanned by the basis of φ_i, i.e.,

$$\langle \varphi_i | H - E | \psi \rangle = 0 \qquad i = 1,2..n \tag{2.6}$$

or equivalently,

$$\sum_j \langle \varphi_i | H - E | \varphi_j \rangle C_j = -\langle \varphi_i | H - E | \alpha_0 S + \alpha_1 C \rangle \tag{2.7}$$

At an eigen-energy $E=E_i$, the left-hand side of (2.7) vanishes and Eq. (2.7) reduces to

$$\alpha_0 \langle \varphi_i | H - E | S \rangle + \alpha_1 \langle \varphi_i | H - E | C \rangle = 0 \tag{2.8}$$

By solving Eq. (2.8), one obtains the ratio α_1/α_0 which is, as usual, nothing else but the tangent of the phase shift at scattering energy $E=E_i$.

In practice, the following four steps should be carried out in order to obtain the Harris variational phase shift at a scattering energy $E=E_i$.:

i. Choose a set of η_i and diagonalize H to obtain the basis functions and their energy eigenvalues.

ii. Select an eigen energy E_i at which one wants to calculate the scattering phase shift

iii. Define S and C at this eigenenergy.

iv. Solve Eq (2.8) for α_1/α_0 to deduce the scattering phase shift.

2.2 Harris-Nesbet variational method.

In the following we shall discuss in some detail the Harris-Nesbet variational method in atomic collision theory.

2.2.1 Single-channel scattering

For convenience, Φ is split into two parts, Φ_S and Φ_C, which correspond to the function S and the function C respectively. Hence, equation (2.3) becomes in this case,

$$\Psi = \alpha_o(\Phi_S + S) + \alpha_1(\Phi_C + C) \tag{2.9}$$

where Φ_S and Φ_C are again expanded in terms of the set of φ_i,

$$\begin{aligned} \Phi_S &= \sum_{i=1}^{n} C_i^S \varphi_i \\ \Phi_C &= \sum_{i=1}^{n} C_i^C \varphi_i \end{aligned} \tag{2.10}$$

The variational conditions equivalent to (2.6) in this case are

$$\sum_j \langle \varphi_i | H - E | \alpha_0 \varphi_j \rangle C_j^S = -\langle \varphi_i | H - E | \alpha_0 S \rangle \tag{2.11a}$$

$$\sum_j \langle \varphi_i | H - E | \alpha_1 \varphi_j \rangle C_j^C = -\langle \varphi_i | H - E | \alpha_1 C \rangle \tag{2.11b}$$

They are used to determine C_i^S and C_i^C. Eqs (2.11a) and (2.11b) above enable the reduction of the functional Ξ (Eq(2.2)) to

$$\Xi = m_{00}\alpha_0^2 + (m_{01} + m_{10})\alpha_0\alpha_1 + m_{11}\alpha_1^2 \tag{2.12}$$

where

$$m_{00} = \langle S | H - E | \Phi_S + S \rangle \tag{2.13a}$$

$$m_{01} = \langle S | H - E | \Phi_C + C \rangle \tag{2.13b}$$

$$m_{10} = \langle C | H - E | \Phi_S + S \rangle \tag{2.13c}$$

$$m_{11} = \langle C | H - E | \Phi_C + C \rangle \tag{2.13d}$$

Now α_0 and α_1 act as variational parameters. Thus, the variational of the functional Ξ is

$$\delta\Xi = 2m_{00}\alpha_0\delta\alpha_0 + 2m_{11}\alpha_1\delta\alpha_1 + (m_{01} + m_{10})(\alpha_1\delta\alpha_0 + \alpha_0\delta\alpha_1) \tag{2.14}$$

In the Kohn variational method (Nesbet, 1980) [14], α_0 is chosen to be I. Then α_1 is nothing else but the one-dimensional R matrix [14] (note that R used here is to denote the collision reactance matrix which is also referred to as the K matrix),

$$\alpha_0 = I \qquad \alpha_1 = R \tag{2.15}$$

Therefore,

$$\delta\alpha_0 = 0 \qquad \delta\alpha_1 = \delta R \tag{2.16}$$

Substituting into (2.12) and (2.14), one has,

$$\Xi = m_{00} + (m_{01} + m_{10})R + m_{11}R^2 \tag{2.17}$$

$$\delta\Xi = 2m_{11}R\delta R + (m_{01} + m_{10})\delta R \tag{2.18}$$

One can prove the following relation between m_{10} and m_{01}:

$$m_{01} - m_{10}^{+} = \frac{1}{2}I \tag{2.19}$$

where 1 is an one-by-one unit matrix. In the single channel scattering case, $m_{10} = m_{10}^{+}$. Using these two relations, (2.18) becomes

$$\delta\Xi = 2(m_{10} + m_{11}R)\delta R + \frac{1}{2}\delta R \tag{2.20}$$

By choosing R_0 which satisfies the relation

$$m_{10} + m_{11} R_0 = 0 \tag{2.21}$$

or

$$R_0 = m_{10} m_{11}^{-1} \tag{2.22}$$

as a trial function for R, (2.20) will be reduced to

$$\delta \Xi = \frac{1}{2} \delta R_0 \text{ or } \delta\left(\Xi - \frac{1}{2} R_0 \right) = 0 \tag{2.23}$$

Eq. (2.23) indicates that the functional [R] defined for the one-dimensional R-matrix as $[R] = R_0 - 2\Xi(R_0)$ is stationary. Thus, [R] should be the one-dimensional variational R-matrix of the collision process, namely the tangent of the scattering phase shift. [R] can be expressed in terms of the m-matrices as,

$$[R] = -2\left(m_{00} - m_{10}^{+} m_{11}^{-1} m_{10}\right) \tag{2.24}$$

Equation (2.24) has been known to be the Kohn formula of the R-matrix in the Harris-Nesbet variational method. By evaluating the appropriate m-matrices, one can deduce the Kohn variational value of the tangent of the scattering phase shift through Eq. (2.24).

In a similar fashion, one chooses in the inverse Kohn method (Nesbet,1980)[14],

$$\alpha_0 = R^{-1} \qquad \alpha_1 = I \tag{2.25}$$

Thus

$$\delta\alpha_0 = \delta R^{-1} \qquad \delta\alpha_1 = 0 \tag{2.26}$$

Substitute (2.25) and (2.26) into (2.14) one obtains the variational of Ξ as

$$\delta\Xi = 2(m_{01} + m_{00}R^{-1})\delta R^{-1} + \frac{1}{2}\delta R^{-1} \tag{2.27}$$

One can also choose a trial function $R_0^{-1} = -m_{00}^{-1}m_{01}$ for R^{-1}, so that

$$m_{01} + m_{00}R^{-1} = 0 \tag{2.28}$$

With this choice, one can immediately see, through (2.19), that the functional $[R^{-1}]$ defined by

$$[R^{-1}] = R_0^{-1} + 2\Xi(R_0^{-1}) \tag{2.29}$$

is stationary. By substituting the expression of the trial function of R_0^{-1} (2.28) into equation (2.29) above, one obtains an explicit formula for the inverse reactance matrix in the inverse Kohn variational method which, by the way, is also the cotangent of the scattering phase shift in the elastic scattering case,

$$[R^{-1}] = 2(m_{11} - m_{01}^{+}m_{00}^{-1}m_{01}) \tag{2.30}$$

2.2.2 Multi-channel scattering

Let Ψ^s be the wave function of the collision system in the channel s, while Ψ^t that of the collision system in the channel t. Hence, the functional Ξ^{st} in the multi-channel scattering case, that involves the s and t channels, is:

$$\Xi_{st} = \langle \Psi_s | H - E | \Psi_t \rangle \tag{2.31}$$

For a certain energy E, if the system has n_C open scattering channels, the wave function of the system in the s channel can be written as:

$$\Psi^s = \sum_p^{n_C} \{ \Phi_p + \alpha_{0p}^s S_p + \alpha_{1p}^s C_p \} \tag{2.32}$$

p stands for a specific channel. Again, as in the case of single scattering channel, one can split the bound part Φ_p into two, Φ_{Sp} and Φ_{Cp} , corresponding to the S and C functions respectively,

$$\Psi^s = \sum_p^{n_C} \{ \alpha_{0p}^s (\Phi_{Sp} + S_p) + \alpha_{1p}^s (\Phi_{Cp} + C_p) \} \tag{2.33}$$

$$\Phi_{Sp} = \sum_{i=1}^{n_p} C_{p,i}^S \varphi_{p,i} \tag{2.34a}$$

$$\Phi_{Cp} = \sum_{i=1}^{n_p} C_{p,i}^C \varphi_{p,i} \tag{2.34b}$$

Substituting (2.33) into (2.31), one obtains

$$\Xi_{st} = \sum_{ip} \sum_{jq} \alpha_{ip}^s m_{ij}^{pq} \alpha_{jq}^t \tag{2.35}$$

In this equation, p and q represent different scattering channels. i,j =0,1 correspond to

the free functions S, C. The explicit form for m_{ij}^{pq} is

$$m_{ij}^{pq} = M_{ij}^{pq} - \sum_{\mu}\sum_{\nu} M_i^{p\mu}\left(M^{-1}\right)_{\mu\nu} M_j^{\nu q} \tag{2.36}$$

Eq.(2.36) can also be written as

$$m_{ij}^{pq} = M_{ij}^{pq} - \sum_{k} M_i^{pk}\left(E - E_k\right)^{-1} M_j^{kq} \tag{2.37}$$

by diagonalizing the bound-bound matrix M. Note that if Ψ_t is the exact solution, $\sum_{jq} m_{ij}^{pq}\alpha_{jq}^{t} = 0$

In equation (2.36) the M matrices are either a bound-bound matrix with its element connecting a bound state to a bound state

$$M_{\mu\nu} = \left\langle \Phi_\mu \middle| H - E \middle| \Phi_\nu \right\rangle \tag{2.38}$$

or a bound-free matrix with its element connecting a bound state to a free state which is either an S or a C function

$$M_S^{pk} = \left\langle S_p \middle| H - E \middle| \Phi_k \right\rangle \tag{2.39}$$

$$M_C^{pk} = \left\langle C_p \middle| H - E \middle| \Phi_k \right\rangle \tag{2.40}$$

$$M_S^{kq} = \left\langle \Phi_k \middle| H - E \middle| S_q \right\rangle \tag{2.41}$$

$$M_C^{kq} = \left\langle \Phi_k \middle| H - E \middle| C_q \right\rangle \tag{2.42}$$

or a free-free matrix with its element connection a free state to a free state,:

$$M_{SS}^{pq} = \langle S_p | H - E | S_q \rangle \tag{2.43}$$

$$M_{SC}^{pq} = \langle S_p | H - E | C_q \rangle \tag{2.44}$$

$$M_{CS}^{pq} = \langle C_p | H - E | S_q \rangle \tag{2.45}$$

$$M_{CC}^{pq} = \langle C_p | H - E | C_q \rangle \tag{2.46}$$

In matrix notation, define a $2n_c$ x $2n_c$ m-matrix as.

$$m = \begin{pmatrix} m_{00} & m_{01} \\ m_{10} & m_{11} \end{pmatrix} \tag{2.47}$$

From equation (2.37), the explicit forms for the elements of the matrices m_{ij} are

$$m_{00}^{pq} = M_{SS}^{pq} - \sum_k M_S^{pk} (E - E_k)^{-1} M_S^{kq} \tag{2.48}$$

$$m_{01}^{pq} = M_{SC}^{pq} - \sum_k M_S^{pk} (E - E_k)^{-1} M_C^{kq} \tag{2.49}$$

$$m_{10}^{pq} = M_{CS}^{pq} - \sum_k M_S^{pk} (E - E_k)^{-1} M_S^{kq} \tag{2.50}$$

$$m_{11}^{pq} = M_{CS}^{pq} - \sum_k M_S^{pk} (E - E_k)^{-1} M_C^{kq} \tag{2.51}$$

An α matrix is defined as

$$\alpha = \begin{pmatrix} \alpha_0 \\ \alpha_1 \end{pmatrix} \tag{2.52}$$

Hence, α is a $2n_c$ x n_c matrix and α^+, its Hermitian conjuguate. α^+ is given by

$$\alpha^+ = \begin{pmatrix} \alpha_0^+ & a_1^+ \end{pmatrix} \tag{2.53}$$

Thus, the functional Ξ_{st} becomes

$$\Xi_{st} = \alpha^+ m \alpha \tag{2.54}$$

$$\Xi_{st} = \alpha_0^+ (m_{00}\alpha_0 + m_{01}\alpha_1) + \alpha_1^+ (m_{10}\alpha_0 + m_{11}\alpha_1) \tag{2.55}$$

One then deduces the variational of Ξ_{st} as

$$\delta\Xi_{st} = \delta\alpha^+ m\alpha + \alpha^+ m\delta\alpha + \alpha^+ m^+ \delta\alpha - \alpha^+ m^+ \delta\alpha \tag{2.56}$$

$$\delta\Xi_{st} = \delta\alpha^+ m\alpha + (m\alpha)^+ \delta\alpha + \alpha^+ (m - m^+)\delta\alpha \tag{2.57}$$

Note that there exist among the m-matrices the following relations,

$$m_{01} - m_{10}^+ = \frac{1}{2} I \tag{2.58a}$$

$$m_{10} - m_{01}^+ = -\frac{1}{2} I \tag{2.58b}$$

whereas, m_{00} and m_{11} are Hermitian matrices. Therefore,

$$\alpha^{+}\left(m-m^{+}\right)\delta\alpha=\begin{pmatrix}\alpha_0^{+} & \alpha_1^{+}\end{pmatrix}\begin{pmatrix}m_{00}-m_{00}^{+} & m_{01}-m_{10}^{+}\\ m_{10}-m_{01}^{+} & m_{11}-m_{11}^{+}\end{pmatrix}\begin{pmatrix}\delta\alpha_0\\ \delta\alpha_1\end{pmatrix}$$
$$=\frac{1}{2}\begin{pmatrix}\alpha_0^{+} & \alpha_1^{+}\end{pmatrix}\begin{pmatrix}0 & I\\ -I & 0\end{pmatrix}\begin{pmatrix}\delta\alpha_0\\ \delta\alpha_1\end{pmatrix} \tag{2.59}$$
$$=\frac{1}{2}\left(\alpha_0^{+}\delta\alpha_1-\alpha_1^{+}\delta\alpha_0\right)$$

Eq. (2.57) becomes

$$\delta\Xi_{st}=\delta\alpha^{+}m\alpha+\left(m\alpha\right)^{+}\delta\alpha+\frac{1}{2}\left(\alpha_0^{+}\delta\alpha_1-\alpha_1^{+}\delta\alpha_0\right) \tag{2.60}$$

In the Kohn variational method α_0 and α_1 are chosen as follows

$$\alpha_0=I \qquad\qquad \alpha_1=R \tag{2.61}$$

Hence,

$$\delta\alpha_0=0 \qquad\qquad \delta\alpha_1=\delta R \tag{2.62}$$

Substituting (2.61) and (2.62) into (2.59), one obtains

$$\delta\Xi_{st}=\delta R^{+}\left(m_{10}+m_{11}R\right)+\left(m_{10}+m_{11}R\right)^{+}\delta R+\frac{1}{2}\delta R \tag{2.63}$$

Then, one chooses a trial function R_0 for R such that

$$m_{10}+m_{11}R_0=0 \tag{2.64}$$

or

$$R_0=m_{10}m_{11}^{-1} \tag{2.65}$$

Eq. (2.63) becomes

$$\delta\Xi_{st}(R_0)=\frac{1}{2}\delta R_0 \tag{2.66}$$

or

$$\delta[R_0-2\Xi_{st}(R_0)]=0 \tag{2.67}$$

This equation indicates that the functional [R] should be defined as

$$[R]=R_0-2\Xi_{st}(R_0) \tag{2.68}$$

and it is stationary. By substituting (2.65) into (2.66), one obtains the formula of [R] in terms of the m-matrices,

$$[R]=-2\left(m_{00}-m_{10}^{+}m_{11}^{-1}m_{10}\right) \tag{2.69}$$

which should be the variational value for the exact R matrix in the Harris-Nesbet Kohn variational method.

Similarly, in the inverse Kohn variational method, one chooses

$$\alpha_0=R^{-1} \qquad\qquad \alpha_1=I \tag{2.70}$$

Thus

$$\delta\alpha_0=\delta R^{-1} \qquad\qquad \delta\alpha_1=0 \tag{2.71}$$

Substitute (2.70) into (2.60) one obtains the variational of Ξ_{st} as follows,

$$\delta\Xi_{st}=\delta R^{-1}\left(m_{01}+m_{00}R^{-1}\right)+\left(m_{01}+m_{00}R^{-1}\right)^{+}\delta R^{-1}-\frac{1}{2}\delta R^{-1} \tag{2.72}$$

Thus, one can also choose a trial expression R_0^{-1} for R_0^{-1}, $R_0^{-1} = -m_{00}^{-1} m_{01}$ such that

$$m_{01} + m_{00} R^{-1} = 0 \tag{2.73}$$

With this choice, the functional $[R^{-1}]$ of the inverse reactance matrix R^{-1} should be

$$[R^{-1}] = R_0^{-1} + 2\Xi(R_0^{-1}) \tag{2.74}$$

and it is stationary. By substituting the expression of R_0^{-1} into equation (2.74), one obtains the formula for the inverse reactance matrix in the Harris-Nesbet inverse Kohn variational method as

$$[R^{-1}] = 2(m_{11} - m_{01}^{+} m_{00}^{-1} m_{01}) \tag{2.75}$$

2.3 Harris-Nesbet method for eletron-hydrogenlike ion collisions

In this section, we shall present the formalism for electron-hydrogenlike-atom scattering within the context of the Harris-Nesbet variational method (Gien, 2002) [23]. The Hamiltonian of the collision system is

$$\hat{H} = -\frac{1}{2}\vec{\nabla}_{r_1}^2 - \frac{1}{2}\vec{\nabla}_{r_2}^2 - \frac{Z}{r_1} - \frac{Z}{r_2} + \frac{1}{|\vec{r}_1 - \vec{r}_2|} \tag{2.76}$$

where

$$\vec{\nabla}^2 = \frac{\partial^2}{\partial r^2} + \frac{2}{r}\frac{\partial}{\partial r} - \frac{\hat{L}^2}{r^2} \tag{2.77}$$

$$\vec{L}^2 = \frac{1}{r^2 \sin\theta}\frac{\partial}{\partial\theta}\left(\sin\theta\frac{\partial}{\partial\theta}\right)+\frac{1}{\sin^2\theta}\frac{\partial^2}{\partial\varphi^2} \tag{2.78}$$

Here, the atomic units are used, hence ħ = 1, m = 1.

In electron scattering from atomic targets, the L-S coupling scheme is usually considered for the collision system. Within the L-S coupling scheme, to total orbital angular momentum L and the total spin S of the system are good quantum numbers. Thus, triplet states of the two-electron system correspond to S=1 while singlet states to S=0. The total wave function of this collision system with a definite value for L and for S is, therefore, given by (Gien, 2002) [23].

$$\Psi_{L,S}(\vec{r}_1,\vec{r}_2) = \frac{1}{\sqrt{2}}\left(1 \pm \hat{P}_{12}\right)\sum_{n_1 l_1 l_2} u_{n_1 l_1}(r_1) F_{n_1 l_1 l_2}(r_2) Y^{M_L}_{L l_1 l_2}(\hat{r}_1,\hat{r}_2) \tag{2.79}$$

where n_1 is the principal quantum number of the hydrogenlike ion, ℓ_1, ℓ_2 are the orbital angular momentum of the bound electron and scattered electron respectively. Here, a scattering channel is specified by a set of (n_1, ℓ_1, ℓ_2) denoted by p. $u_{n_1 l_1}(r_1)$ is the radial wave function of the hydrogenlike ion. $Y^{M_L}_{L l_1 l_2}(\hat{r}_1,\hat{r}_2)$ is a bipolar spherical harmonics representing the total orbital angular momentum state of the collision system. The total orbital angular momentum wave function $Y^{M_L}_{L l_1 l_2}(\hat{r}_1,\hat{r}_2)$ are obtained by coupling the two orbital angular momenta of the individual electrons,

$$Y^{M_L}_{L l_1 l_2}(\hat{r}_1,\hat{r}_2) = \sum_{m_1, m_2} C(L, l_1, l_2, m_1, m_2, M_L) Y_{l_1 m_1}(\hat{r}_1) Y_{l_2 m_2}(\hat{r}_2) \tag{2.80}$$

where $C(L,l_1,l_2,m_1,m_2,M_L)$ are the relevant Clebsch-Gordan coefficients. $F_{n_1l_1l_2}(r_2)$ is the wave function of the scattered electron in the channel $p(n_1,\ell_1,\ell_2)$. The trial form for $F_{n_1l_1l_2}(r_2)$ is composed of two parts, a bound part and a free part,

$$F_p(r_2)=\Phi_p(r_2)+\alpha_{0p}S_p(r_2)+\alpha_{1p}C_p(r_2) \tag{2.81}$$

The bound part Φ_p can be expanded in terms of a set of basis functions which are usually chosen to be of a Slater-type function. Thus,

$$\Phi_p(r_2)=\sum_i C_{p,i}\varphi_{p,i}=\sum_i \beta_{p,i}e^{n_{i2}}r^{-\alpha_{i2}r_2} \tag{2.82}$$

For the case of electron scattering from hydrogenlike ion, the free wave function S_p is given by

$$S_p(r_2)=k_p\Im_{l_2}(k_pr_2) \tag{2.83}$$

where $\Im_{l_2}(k_pr_2)$ is the Coulomb-Bessel function [24]. $k_p^{\,2}=2(E-E_p)$. E_p is the energy of the bound electron. The free function C_p in this case is a Coulomb-Neumann function $N_{l_2}(k_pr_2)$ [24] weighted by the factor $\left(1-e^{-\beta r_2}\right)^{2l_2+1}$

$$C_p(r_2)=k_p\left(1-e^{-\beta r_2}\right)^{2l_2+1}N_{l_2}(k_pr_2) \tag{2.84}$$

This weighting is to provide correct behaviours of the C_p function near the coordinate origin (r_2=0). Another form, which is the so-called Armstead-type form [25, 26], can also be chosen to represent the free function C_p,

$$C_p(r_2) = k_p\left(\left(\frac{\eta}{\ell_2+1}\right)\Im_{l_2}(k_p r_2) + \sqrt{1+\left(\frac{\eta}{\ell_2+1}\right)^2}\,\Im_{l_2+1}(k_p r_2)\right) \tag{2.85}$$

and can also provide correct behaviours of C_p near the coordinate origin (r_2=0) as well as at large r_2.

In order to improve the accuracy of the results of calculation, one may add a set of the correlation functions to the expansion of $\Psi_{LS}(\vec{r}_1,\vec{r}_2)$. This is, to some extent, equivalent to increasing the number of basis functions employed to expand the bound part of the trial function $F_{n_1 l_1 l_2}(r_2)$. With the addition of these correlation terms,

$$\Psi_{L,S}(\vec{r}_1,\vec{r}_2) = \frac{1}{\sqrt{2}}\left(1 \pm \hat{P}_{12}\right)\sum_{n_1 l_1 l_2} u_{n_1 l_1}(r_1) F_{n_1 l_1 l_2}(r_2) Y_{L l_1 l_2}^{M_L}(\hat{r}_1,\hat{r}_2) + \sum_i c_i \chi_i(r_1,r_2) Y_{L l_1 l_2}^{M_L}(\hat{r}_1,\hat{r}_2) \tag{2.86}$$

The correlation functions $\chi_i(r_1,r_2)$ can be chosen to be in the form of a product of two Slater-type functions.

As was seen in the previous sections, the R matrix (or in the case of elastic scattering, the scattering phase shift) can be calculated by using the formulas of (2.24) and (2.69) in the Kohn variational method or the formulas of (2.30) and (2.75) in the inverse Kohn variational method. This, in turn, requires the evaluations of the bound-bound, bound-free, and free-free matrix elements. In the case of electron scattering from a hydrogenlike-ion target, elements of bound-bound matrix M_{pq} are given by

$$M_{pq} = B_{i2}B_{j2} \times$$
$$\left\langle u_{n_{i1}l_{i1}}(r_1) r_2^{n_{i2}} e^{-\alpha_{i2}r_2} Y^{M_L}_{Ll_{i1}l_{i2}}(\hat{r}_1,\hat{r}_2) \middle| \left(\hat{H}-E\right)\left(1 \pm \hat{P}_{12}\right) \middle| u_{n_{j1}l_{j1}}(r_1) r_2^{n_{j2}} e^{-\alpha_{j2}r_2} Y^{M_L}_{Ll_{j1}l_{j2}}(\hat{r}_1,\hat{r}_2) \right\rangle \tag{2.87}$$

where B_{i2} and B_{j2} are normalization constants.

Elements of bound-free matrices are given by

$$M_{pS} = B_{i2}k_{j2} \times$$
$$\left\langle u_{n_{i1}l_{i1}}(r_1) r_2^{n_{i2}} e^{-\alpha_{i2}r_2} Y^{M_L}_{Ll_{i1}l_{i2}}(\hat{r}_1,\hat{r}_2) \middle| \left(\hat{H}-E\right)\left(1 \pm \hat{P}_{12}\right) \middle| u_{n_{j1}l_{j1}}(r_1) \Im_{l_{j2}}(k_{j2}r_2) Y^{M_L}_{Ll_{j1}l_{j2}}(\hat{r}_1,\hat{r}_2) \right\rangle \tag{2.88}$$

$$M_{pC} = B_{i2}\left\langle u_{n_{i1}l_{i1}}(r_1) r_2^{n_{i2}} e^{-\alpha_{i2}r_2} Y^{M_L}_{Ll_{i1}l_{i2}}(\hat{r}_1,\hat{r}_2) \middle| \left(\hat{H}-E\right)\left(1 \pm \hat{P}_{12}\right) \middle| u_{n_{j1}l_{j1}}(r_1) C_q(r_2) Y^{M_L}_{Ll_{j1}l_{j2}}(\hat{r}_1,\hat{r}_2) \right\rangle \tag{2.89}$$

while elements of free-free matrices, by

$$M_{SS} = k_{i2}k_{j2}\left\langle u_{n_{i1}l_{i1}}(r_1) \Im_{l_{i2}}(k_{i2}r_2) Y^{M_L}_{Ll_{i1}l_{i2}}(\hat{r}_1,\hat{r}_2) \middle| \left(\hat{H}-E\right)\left(1 \pm \hat{P}_{12}\right) \middle| u_{n_{j1}l_{j1}}(r_1) \Im_{l_{j2}}(k_{j2}r_2) Y^{M_L}_{Ll_{j1}l_{j2}}(\hat{r}_1,\hat{r}_2) \right\rangle \tag{2.90}$$

$$M_{SC} = k_{i2}\left\langle u_{n_{i1}l_{i1}}(r_1) \Im_{l_{i2}}(k_{i2}r_2) Y^{M_L}_{Ll_{i1}l_{i2}}(\hat{r}_1,\hat{r}_2) \middle| \left(\hat{H}-E\right)\left(1 \pm \hat{P}_{12}\right) \middle| u_{n_{j1}l_{j1}}(r_1) C_q(r_2) Y^{M_L}_{Ll_{j1}l_{j2}}(\hat{r}_1,\hat{r}_2) \right\rangle \tag{2.91}$$

$$M_{CS} = k_{j2}\left\langle u_{n_{i1}l_{i1}}(r_1) C_p(r_2) Y^{M_L}_{Ll_{i1}l_{i2}}(\hat{r}_1,\hat{r}_2) \middle| \left(\hat{H}-E\right)\left(1 \pm \hat{P}_{12}\right) \middle| u_{n_{j1}l_{j1}}(r_1) \Im_{l_{j2}}(k_{j2}r_2) Y^{M_L}_{Ll_{j1}l_{j2}}(\hat{r}_1,\hat{r}_2) \right\rangle \tag{2.92}$$

$$M_{CC} = \left\langle u_{n_{i1}l_{i1}}(r_1) C_p(r_2) Y^{M_L}_{Ll_{i1}l_{i2}}(\hat{r}_1,\hat{r}_2) \middle| \left(\hat{H}-E\right)\left(1 \pm \hat{P}_{12}\right) \middle| u_{n_{j1}l_{j1}}(r_1) C_q(r_2) Y^{M_L}_{Ll_{j1}l_{j2}}(\hat{r}_1,\hat{r}_2) \right\rangle \tag{2.93}$$

At energies, below the first excitation threshold, only one elastic scattering channel exists for each partial wave L. Therefore, the matrix R_L obtained in the calculation is nothing else but the tangent of the phase shift δ_L in the Kohn variational method

$$\delta_L = \tan^{-1}(R_L) \tag{2.94}$$

or in the inverse Kohn method,

$$\delta_L = \text{cotan}^{-1}(R_L^{-1}) \tag{2.95}$$

Partial wave cross-sections can then be calculated, using the well known formula,

$$\sigma_L(k) = \frac{4\pi}{k^2}(2L+1)\sin^2\delta_L(k) \tag{2.96}$$

where $k^2 = 2E$.

Chapter 3

Determination of the singlet S-wave Doubly Excited States of Li^+ below the N=2 Excitation Threshold

3.1 Method of calculation

When an electron collides with a hydrogenlike ion such as Li^{2+}, it could elastically scatter from the ion, excite the ion to an excited state or even ionize the ion, depending on the energy that the incident electron can supply to the ion. In a purely elastic scattering process of electrons from Li^{2+} in its ground state for example, the incident electron can either just scatter off Li^{2+} or, at a suitable energy, be temporarily captured by Li^{2+} to form a two-electron atom Li^+ with both electrons staying in their excited states. One of the electrons of the atom is excited to the N=2 level while the other, to an *n*th excited state (with $n \geq N$) before being auto-ionized to a free electron, leaving behind the other electron de-excited to its ground state. Thus, the short-lived doubly excited states temporarily formed in an elastic scattering of electron from Li^{2+} are nothing else but doubly-excited auto-ionization states of Li^+ below the N=2 excitation threshold of Li^{2+}.

These doubly-excited-state resonances can, therefore, be located by simply looking at the region of energies where the partial wave phase shift of elastic electron-Li^{2+} scattering changes abruptly by π radian as the scattering energy crosses this energy position or equivalently where the relevant partial wave cross sections exhibit a peak. The positions of these resonances and their widths can, therefore, be determined with high accuracy by a numerical scattering method which can provide highly accurate partial wave phase shifts for electron scattering from Li^{2+}.

The calculations of phase shift and cross section at low energy using the Harris-Nesbet variational method [14] have been known to provide very accurate results for electron and positron collisions with (neutral) hydrogen atoms (see for example Gien and Gien et al [27-34]). Making use of the high accuracy that the method can provide for these scattering phase shifts at low energy, Gien (1995, 1996, 1998) [12, 13, 35-37] also employed this method to determine the positions and widths of the Feshbach resonances formed below the N=2 excitation threshold of H in both electron and positron collisions. Gien has indeed succeeded in determining the positions and widths for these resonances including those lying extremely close to the N=2 threshold of H. Recently, Gien [23, 36-40] also considered the Harris-Nesbet method for the calculations of phase shifts and cross sections for electron and positron collisions with hydrogenlike ions and succeeded in obtaining very accurate phase shifts for these ionic targets as well. Very recently, Gien, [41-45] also used the Harris-Nesbet method to determine with great success the doubly-excited-state resonances of He below the N=2 ionization threshold He^{+}.

We, therefore, consider here again the Harris-Nesbet method for the determination of the singlet S-wave doubly excited states formed below the N=2 threshold of Li^{2+} in the two-electron ionic atom Li^{+}. In the present calculation, the Harris-Nesbet variational method was first employed to obtain accurate values of S (L=0) singlet (S=0) partial wave phase shifts for electrons elastically scattered from Li^{2+} at energies below the N=2 excitation threshold of Li^{2+}. The detailed description of this method when applied to electron scattering from hydrogenlike ions had been given by Gien elsewhere [23, 40]. The so-called extended four-state (E4S) scheme, used in Gien's previous Harris-Nesbet calculations (Gien, 2002, 2003) [23, 40], has proved to provide very accurate results of phase shift for the scattering process and is again considered for the present calculation. The E4S scheme, as was discussed by Gien (2002, 2003) [23, 40], can represent well the long-ranged polarization potential effect of the electron-Li^{2+} collision system. A great number of correlation terms were added to the scheme to improve the accuracy of the long-ranged polarization potential effect as well as the short-ranged static potential effect of the electron-Li^{2+} collision system. In practice, the number of correlation terms added to the scheme was increased gradually until the phase shifts obtained no longer change significantly, i.e., when they already approach their convergent values. For the present calculation of singlet S-wave scattering, up to 108 correlation terms [44] were added to the scheme. Thus, the phase shifts obtained in the calculation are expected to be rather accurate. Furthermore, to obtain accurate results for the phase shifts at energies very close to the threshold where the highly-lying doubly-excited-state resonances are formed, we had to use a fairly large basis set of functions covering a wide spatial range that enables an adequate representation of the high-lying *n*th excited states of the second

electron [44]. A basis set of up to 33 Slater-type functions was considered for the present calculation. A very versatile and reliable computer code developed earlier by Gien [23] for the calculation of phase shifts and cross sections in electron (and positron) collisions with hydrogenlike ions within the Harris-Nesbet method was used for this calculation.

To determine the positions and widths of these doubly-excited-state resonances, we used a procedure which is fairly time consuming but has been proved in the past to be able to determine very accurately the positions and widths of the threshold resonances below the N=2 threshold in electron-H scattering (Gien 1996) [37], including those of extremely small width lying very close to the threshold that other numerical methods do not seem to be able to do. This procedure has also been used with great success in the determination of doubly excited states of He below the N=2 excitation threshold of He^+ mentioned above (Gien, 2005, 2006, 2007, 2008) [41-45]). We carefully swept through the energy regions where we sense the existence of a doubly-excited resonance with calculations of phase shifts at scattering energies slowly increased by a very small step and then gradually focused to the energy region around the position of that resonance. Finally, a great number of phase shifts at energies around the position of this resonance were calculated and these accurate phase shifts obtained were then fitted the Breit-Wigner formula,

$$\delta = \delta_o + \tan^{-1}\left[\frac{\Gamma/2}{E - E_o}\right] \qquad (3.1)$$

to determine the position E_o of the resonance and its width Γ. In Equation (3.1) above, δ_o is the partial wave phase shift of the background (non-resonant) scattering.

3.2 Results and discussion

As was well known, there are different classification schemes for the series of doubly excited states below the N=2 threshold and the correspondence among these different classification schemes have been discussed in the literature (see for example, Oza (1986) [46]). For ease of reference to these doubly excited states, we use the symbols of the classification scheme by Conneely and Lipsky [10] to label them. Thus, for the singlet S-wave doubly excited states $^1S^e$ below the excitation threshold N=2, there are two series of doubly excited states denoted by *a* and *b*. The *a*-series corresponds to the one which has its quantum numbers K=1 and T=0 in the configuration-mixed "doubly-excited symmetry basis" (DESB) classification scheme by Herrick and Sinanoglu (1975) [47] while the *b*-series, to the one which has its quantum numbers K=-1, T=0. It should be noted that it is quite straightforward to translate the designations of the doubly-excited states shown in Tables 3.1, 3.2, and 3.3 below within the classification scheme by Conneely and Lipsky [10] to those of the DESB scheme. Indeed, the doubly excited state $^1S^e$(2, 3a) for instance is just the second (n=3) lowest-lying of the series of doubly excited states of quantum numbers K=1 and T=0 in the DESB scheme.

Table 3.1 Doubly-excited-state resonances $^1S^e$ of the a, b series of Li^+ below the N=2 Li^{2+} threshold

Classification	[a] Energy	[b] Width	[c] Effective quantum number n*	[c] Reduced width $n^{*3}\Gamma$
K=1 T=0				
$^1S^e(2,2a)$	5.18843889	0.119(-1)	1.600	0.488(-1)
$^1S^e(2,3a)$	6.16906240	0.454(-2)	2.624	0.820(-1)
$^1S^e(2,4a)$	6.44282802	0.181(-2)	3.609	0.852(-1)
$^1S^e(2,5a)$	6.56109543	0.876(-3)	4.602	0.854(-1)
$^1S^e(2,6a)$	6.62234956	0.486(-3)	5.598	0.852(-1)
$^1S^e(2,7a)$	6.65804942	0.296(-3)	6.596	0.851(-1)
$^1S^e(2,8a)$	6.68064229	0.194(-3)	7.594	0.849(-1)
$^1S^e(2,9a)$	6.69584038	0.134(-3)	8.594	0.848(-1)
$^1S^e(2,10a)$	6.70658186	0.960(-4)	9.598	0.849(-1)
$^1S^e(2,11a)$	6.71456199	0.725(-4)	10.624	0.869(-1)
K=-1 T=0				
$^1S^e(2,2b)$	5.74890126	0.552(-3)	1.999	0.441(-2)
$^1S^e(2,3b)$	6.35331224	0.134(-3)	3.175	0.430(-2)
$^1S^e(2,4b)$	6.52201848	0.640(-4)	4.189	0.470(-2)
$^1S^e(2,5b)$	6.60159475	0.348(-4)	5.192	0.486(-2)
$^1S^e(2,6b)$	6.64569400	0.208(-4)	6.193	0.495(-2)
$^1S^e(2,7b)$	6.67269012	0.134(-4)	7.193	0.500(-2)
$^1S^e(2,8b)$	6.69041569	0.907(-5)	8.193	0.499(-2)
$^1S^e(2,9b)$	6.70268936	0.615(-5)	9.195	0.478(-2)
$^1S^e(2,10b)$	6.71158154	0.387(-5)	10.204	0.411(-2)
$^1S^e(2,11b)$	6.71835949	0.302(-5)	11.244	0.429(-2)

[a] Energy in Ryd and referred to the ground state of Li^{2+}
[b] Width in Ryd
[c] Conneely and Lipsky [10]

We succeeded in determining altogether 20 S-wave singlet doubly excited states $^1S^e$ of Li^+ below the N=2 excitation threshold of Li^{2+}, 10 belonging to the *a*-series (K=1, T=0) and another 10 belonging to the *b*-series (K=-1, T=0). This is the greatest number of doubly excited states $^1S^e$ determined below the N=2 excitation threshold for Li^+ so far. In Table 3.1, we display the positions and widths of doubly-excited states that we determined, together with their effective quantum number n* and their reduced widths $\gamma_n = n^{*3}\,\Gamma$ [10]. The fraction parts of n* are indeed almost the same for all the doubly excited states displayed [10]. In Tables 3.2 and 3.3, we tabulate, respectively, the positions and the widths that we determined for these doubly excited states together with those determined by other researchers employing different numerical methods for comparison. The energies and widths of the doubly-excited-state resonances are given in the units of Rydberg. The resonance energies E_r shown in this table are referred to the ground state of Li^{2+}. Because of the high accuracy of this method, we succeeded in determining doubly excited states very close to the N=2 threshold of Li^{2+}. Four of them, two belong to the *a*-series ($^1S^e$(2,10a) and $^1S^e$(2,11a)) and another two belonging to the *b*-series ($^1S^e$(2,10b) and $^1S^e$(2,11b)), were determined by us for the first time.

In general, the positions of the four lowest doubly excited states $^1S^e$ determined by the present work agree rather well with those determined by Ho, who employed the complex-coordinate-rotation (CCR) method. They also agree very well with those determined by Chung and Lin who also used the complex-rotation method. The positions of the three lowest-lying doubly excited states of the present calculation also agree reasonably well with those determined by Bhatia who employed the Feshbach projection-

Table 3.2 Energies (referred to the ground state of Li^{2+}) in Ryd of the doubly-excited-state resonances $^1S^e$ of the a, b series of Li^+ below the N=2 Li^{2+} threshold

Classification	This work	[a]Chung and Lin (1997)	[b]Bruch et al (1975)	[c]Ho (1981)	[d]Bhatia (1977)
K=1 T=0					
$^1S^e(2,2a)$	5.18843889	5.18843601	5.195788	5.1883068	5.1877556
$^1S^e(2,3a)$	6.16906240	6.16907430	6.176614	6.1688500	6.1694013
$^1S^e(2,4a)$	6.44282802	6.44287785	6.447654		
$^1S^e(2,5a)$	6.56109543	6.56115046	6.564172		
$^1S^e(2,6a)$	6.62234956	6.62243420	6.624356		
$^1S^e(2,7a)$	6.65804942	6.65817062	6.659376		
$^1S^e(2,8a)$	6.68064228	6.68082426			
$^1S^e(2,9a)$	6.69584038	6.69614137			
$^1S^e(2,10a)$	6.70658186				
$^1S^e(2,11a)$	6.71456198				
K=-1 T=0					
$^1S^e(2,2b)$	5.74890126	5.73977893	5.772498	5.7391223	5.7390268
$^1S^e(2,3b)$	6.35331224	6.35205096	6.360928	6.3517276	
$^1S^e(2,4b)$	6.52201848	6.52157322	6.525918		
$^1S^e(2,5b)$	6.60159475	6.60148396	6.603816		
$^1S^e(2,6b)$	6.64569400	6.64570198	6.647056		
$^1S^e(2,7b)$	6.67269012	6.67272794			
$^1S^e(2,8b)$	6.69041569	6.69042699			
$^1S^e(2,9b)$	6.70268936	6.70261761			
$^1S^e(2,10b)$	6.71158154				
$^1S^e(2,11b)$	6.71835949				

[a] Chung and Lin (1998) [11]
[b] Bruch et al. (1975) [1]
[c] Ho (1981) [7]
[d] Bhatia (1977) [6]

Table 3.3. Width Γ in Ryd of the doubly-excited-state resonances $^1S^e$ of the a, b series of Li^+ below the N=2 Li^{2+} threshold

Classification	This work	[a] Chung and Lin (1997)	[b] Conneely and Lipsky (1978)	[c] Ho (1981)	[d] Bhatia (1977)
K=1 T=0					
$^1S^e$(2,2a)	0.119(-1)	0.114(-1)	0.290(-1)	0.113(-1)	0.115(-1)
$^1S^e$(2,3a)	0.454(-2)	0.436(-2)	0.638(-2)	0.430(-2)	0.570(-2)
$^1S^e$(2,4a)	0.181(-2)	0.174(-2)			
$^1S^e$(2,5a)	0.876(-3)	0.845(-3)			
$^1S^e$(2,6a)	0.486(-3)	0.472(-3)			
$^1S^e$(2,7a)	0.296(-3)	0.290(-3)			
$^1S^e$(2,8a)	0.194(-3)	0.195(-3)			
$^1S^e$(2,9a)	0.134(-3)	0.137(-3)			
$^1S^e$(2,10a)	0.960(-4)				
$^1S^e$(2,11a)	0.725(-4)				
K=-1 T=0					
$^1S^e$(2,2b)	0.552(-3)	0.486(-3)	0.380(-3)	0.486(-3)	0.816(-3)
$^1S^e$(2,3b)	0.134(-3)	0.122(-3)		0.120(-3)	
$^1S^e$(2,4b)	0.640(-4)	0.590(-4)			
$^1S^e$(2,5b)	0.348(-4)	0.326(-4)			
$^1S^e$(2,6b)	0.208(-4)	0.195(-4)			
$^1S^e$(2,7b)	0.134(-4)	0.122(-4)			
$^1S^e$(2,8b)	0.907(-5)	0.780(-5)			
$^1S^e$(2,9b)	0.615(-5)	0.598(-5)			
$^1S^e$(2,10b)	0.387(-5)				
$^1S^e$(2,11b)	0.302(-5)				

[a] Chung and Lin (1998) [11]
[b] Bruch et al. (1975) [1]
[c] Ho (1981) [7]
[d] Bhatia (1977) [6]

operator formalism for his calculation. We believe that the positions determined by Bhatia for these doubly excited states are also fairly accurate, at least for these few low-lying ones. The positions of the three lowest-lying doubly excited states determined by Conneely and Lipsky [10] employing the truncated diagonalization method (TDM) are in reasonable agreement with those determined by the present calculation as well as with those by other research groups, but they tend the stay a bit higher than those determined by us as well as by other research groups (Ho [7], Bhatia [6], and Chung and Lin [11]). For higher-lying doubly excited states, the positions of the doubly excited states determined by us also seem to agree better with those determined by Chung and Lin than with those determined by Conneely and Lipsky.

The widths of the four lowest-lying resonances determined by us are found to agree reasonably well with those determined by Ho and by Chung and Lin. We believe that the widths determined by us are rather accurate. Indeed, we have double-checked these values by carrying out calculations with a smaller set of basis functions and found that the values of these widths do not vary significantly from one calculation to another. This fact indicates that the widths of these lowest-lying resonances that we obtained appear to have approached their convergent values and should, thereby, be rather accurate. The good agreement of the results of Ho with ours, obtained with a completely different numerical method, indicates that the CCR method can provide fairly accurate results for these resonance widths, at least for these low-lying doubly excited states. The widths obtained by Bhatia employing the Feshbach projection-operator formalism for his calculation can also be regarded as agreeing reasonably well with ours, although the

deviation of their values from ours is more noticeable. The widths obtained by Conneely and Lipsky, who employed the truncated diagonalization method with the static-exchange approximation for the continuum wave function, even for these lowest-lying resonances are found to disagree considerably with ours as well as with those determined by all other groups. This may be due to the fact that these researchers used the truncated diagonalization method (TDM) with a finite basis set of product of hydrogenlike wave functions for the Q space, excluding the effect of the continuum. The basis set of the Q space cannot, therefore, represent well all the interactions of the two-electron system including the long-ranged polarization potential effects, to which the accuracy of the resonance widths they calculated seems to be rather sensitive. Thus, the widths obtained by this group do not seem to be very accurate. Comparing the widths of the higher-lying doubly excited states obtained by Chung and Lin to those obtained by us, we found that their values agree rather well with ours (see Table 3.3). The widths of their resonances belonging to the *a*-series seem to agree somewhat better with ours than those of the resonances belonging to the *b*-series. This is as expected, since the widths of the resonances belonging to the *b*-series are at least one-order-of-smallness smaller than those of the *a*-series, and the accuracy of the calculations is, therefore, more difficult to achieve. On this basis, the widths of the higher-lying resonances of the *b*-series determined by Chung and Lin still can be regarded as agreeing with ours rather well and are, thereby, also rather accurate.

In Table 3.4, we show experimental data obtained for the positions and widths of the doubly-excited states $^1S^e$ of Li^+ below the N=2 threshold of Li^{2+}. These data still

Table 3.4 Experimental data for positions and widths in Ryd of the doubly-excited states $^1S^e$ of Li^+ below the N=2 excitation threshold of Li^{2+}

Classification	[a]Rodbro et al	[b]Ziem et al		Present calculation	
K=1 T=0	Position	Position	Width	Position	Width
$^1S^e(2,2a)$	5.19303538±0.00735	5.19083027±0.0022051	0.0073504±0.0022051	5.18843889	0.0119
$^1S^e(2,3a)$	6.17577965±0.00735			6.16906240	0.00454
K=-1 T=0					
$^1S^e(2,2b)$	5.74284295±0.00735			5.74890126	0.000552
$^1S^e(2,3b)$	6.35512865±0.01470			6.35331224	0.000134

[a] Experimental data by Rodbro et al (1979) [4]
[b] Experimental data by Ziem et al (1975) [2]

remain quite scarce. Ziem at al [2] reported the position and width measured by them for the lowest-lying doubly-excited state $^1S(2,2a)$, while Rodbro et al [4] only reported the positions of the four lowest-lying $^1S^e$. With the experimental errors (error bars) given for these data by these experimental groups, we see that the positions calculated by these various theoretical groups for these four doubly-excited states and shown in Table 3.2 (including ours) can all be regarded as agreeing well with experimental data. The sole experimental width provided by Ziem et al for the lowest-lying doubly-excited states $^1S^e(2,2a)$, considering its experimental errors given, can be regarded as agreeing only fairly with the theoretical widths calculated by various research groups. This is as expected, since experiments performed to measure these widths should be quite difficult, in view of the extreme smallness of the widths of most of these doubly-excited-state resonances. In this sense, accurate results of a reliable theoretical calculation should be quite useful in serving as benchmark values to guide these difficult experiments.

An advantage of the numerical method that we used to determine the doubly excited states presented in this thesis is that we can explicitly show them in graphical forms in order to see how exactly the shapes of these resonances would be. The graphical presentation of these doubly-excited-state resonances also, to some extent, provides a confirmation of their definite existence in the energy distribution of cross sections and phase shifts of the scattering process. We calculated a significantly great number of singlet S-wave elastic scattering phase shifts and cross sections around the positions of all the twenty doubly-excited states $^1S^e$ that we succeeded in locating, and plotted them in Figures 3.1 – 3.40. These graphs indicate that these resonances should belong to the same

family as they all have the same shape. They all start with a smooth increase of the cross sections on the left side to reach their peak and then end with a quick fall-off to nil on the right.

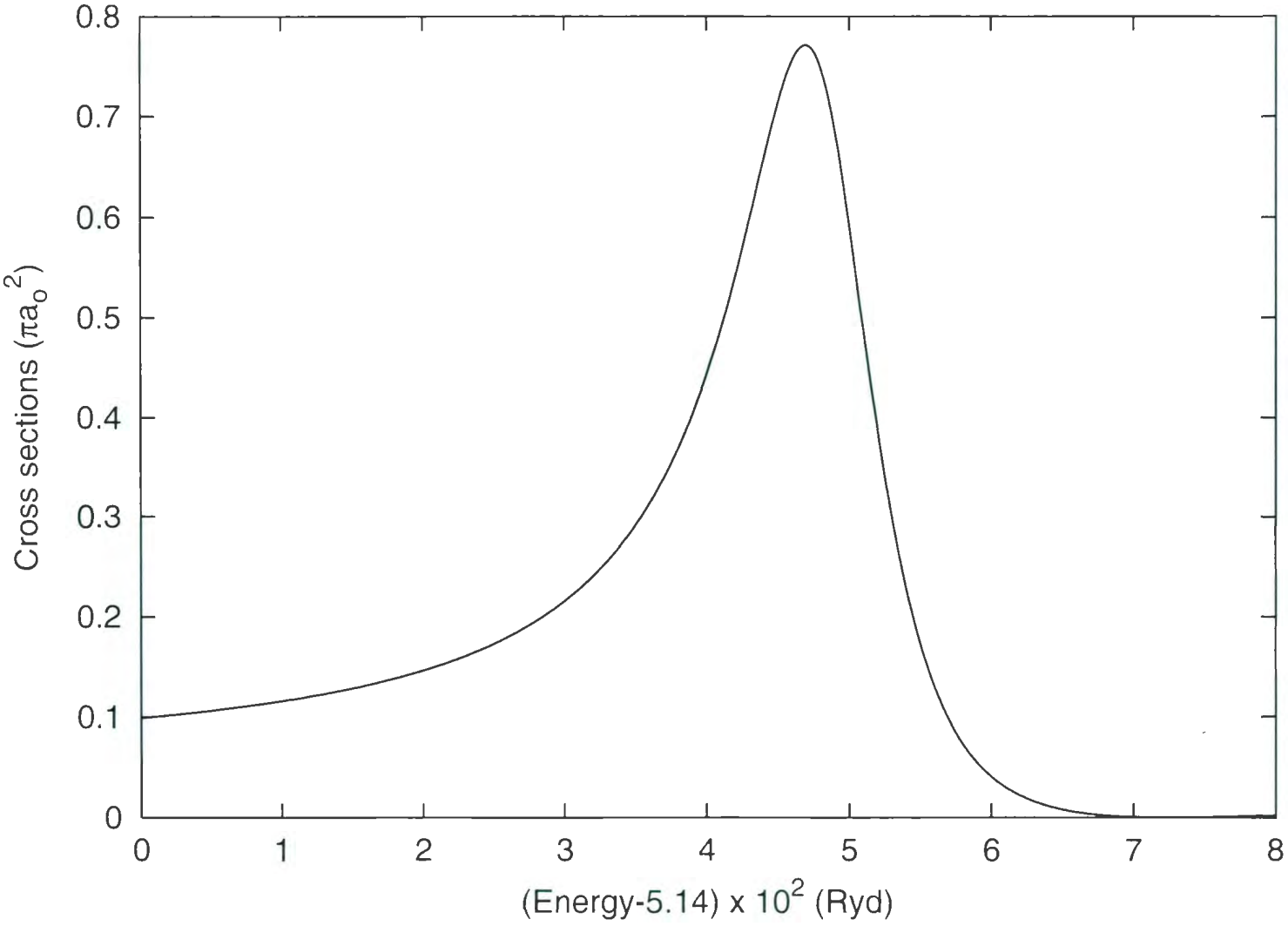

Figure 3.1. S-wave Cross-Sections of e^--Li^{2+} Singlet Scattering at $^1S^e$(2,2a)

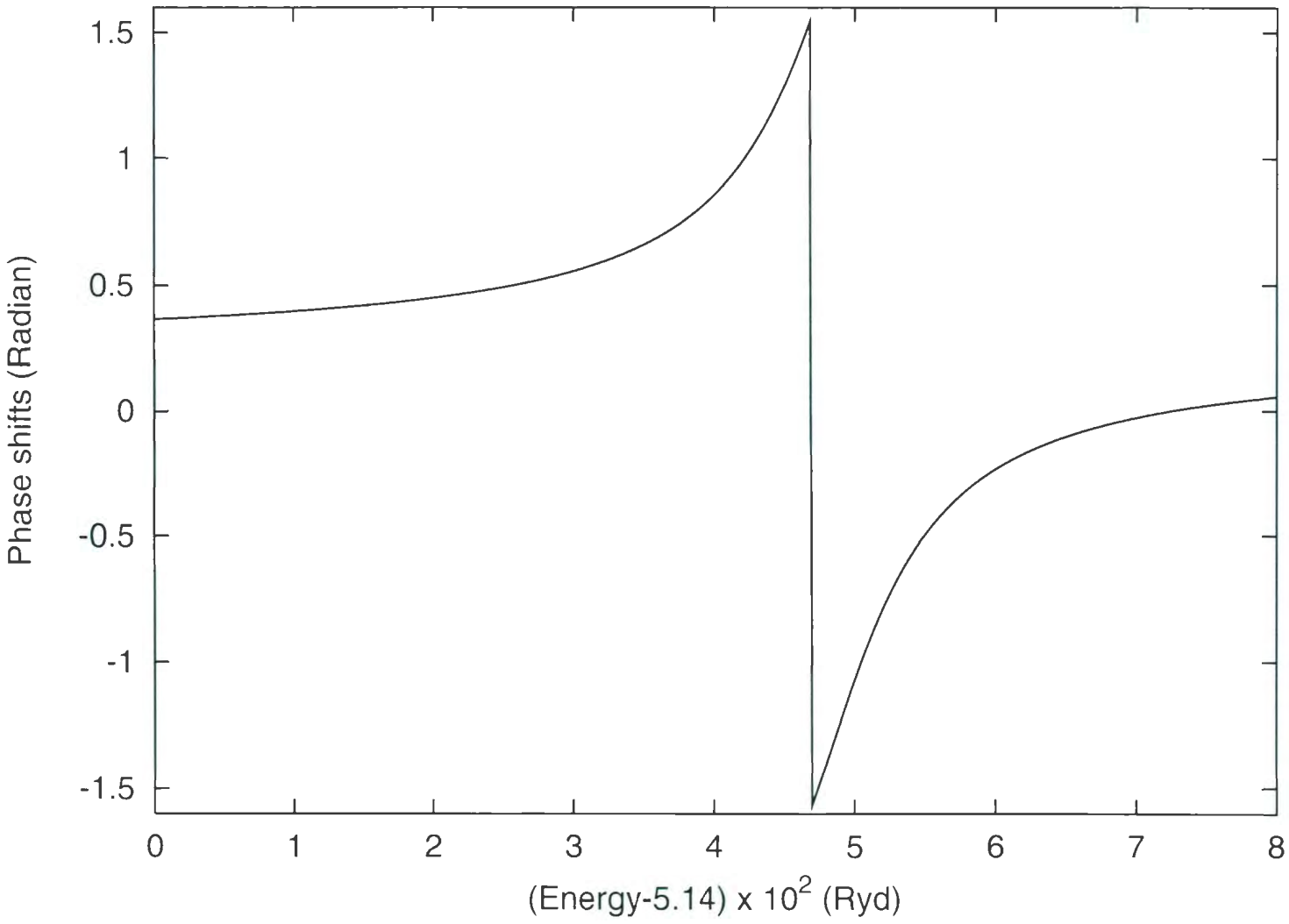

Figure 3.2. S-wave Phase Shifts of e^{-}-Li^{2+} Singlet Scattering at $^{1}S^{e}$(2,2a)

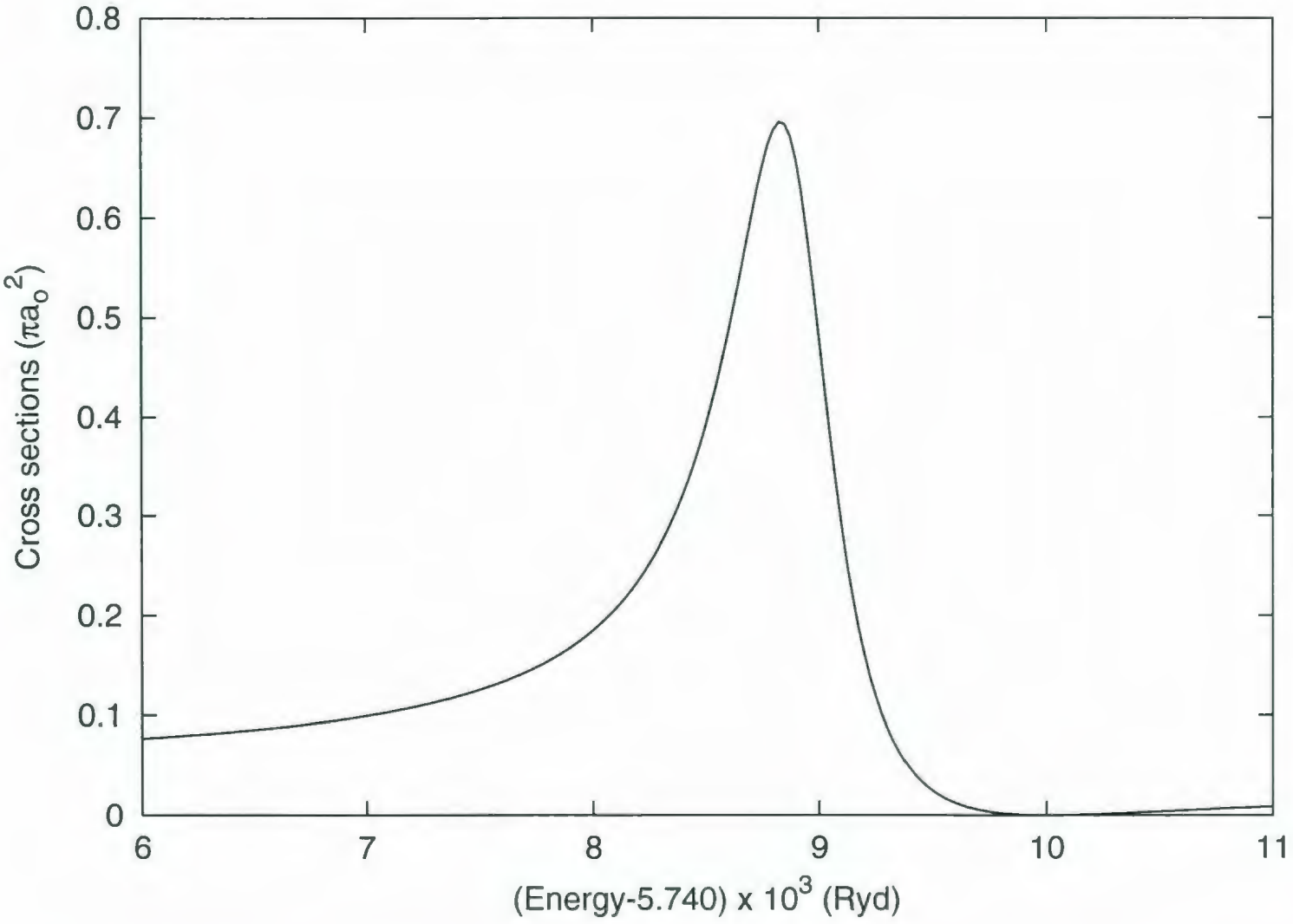

Figure 3.3. S-wave Cross-Sections of e^--Li^{2+} Singlet Scattering at $^1S^e$(2,2b)

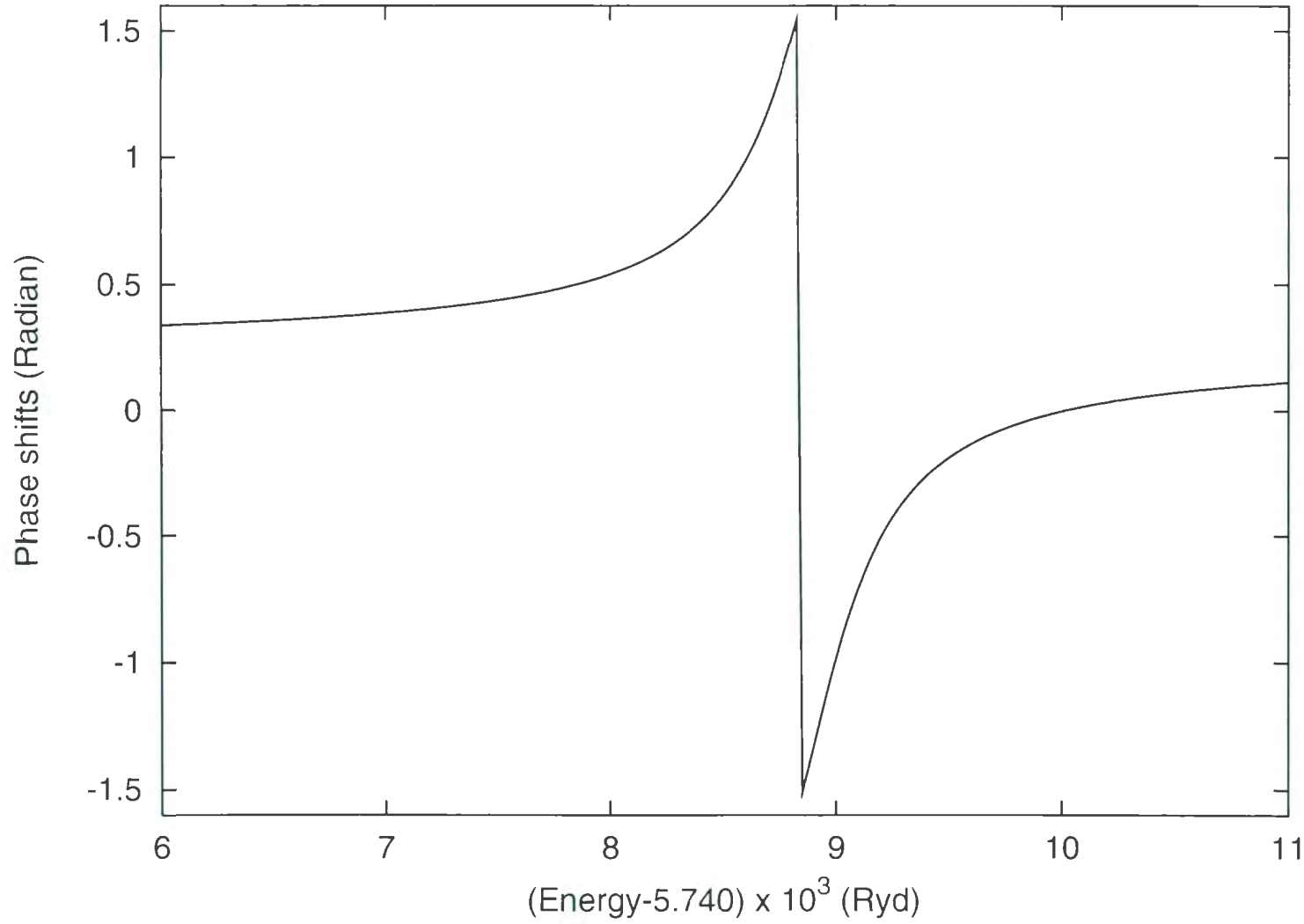

Figure 3.4. S-wave Phase Shifts of e^{-}-Li^{2+} Singlet Scattering at $^{1}S^{e}$(2,2b)

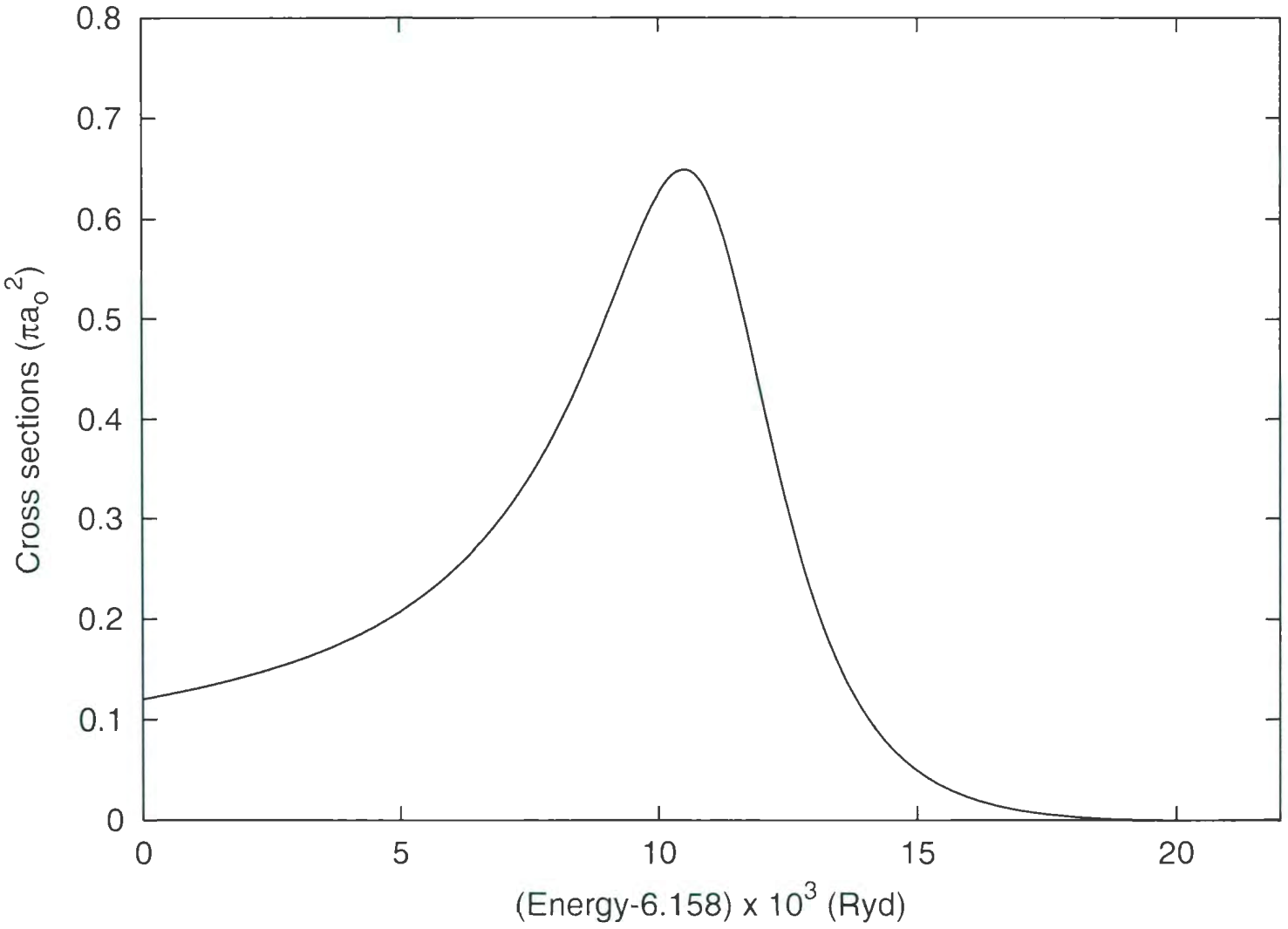

Figure 3.5. S-wave Cross-Sections of e^--Li^{2+} Singlet Scattering at $^1S^e$(2,3a)

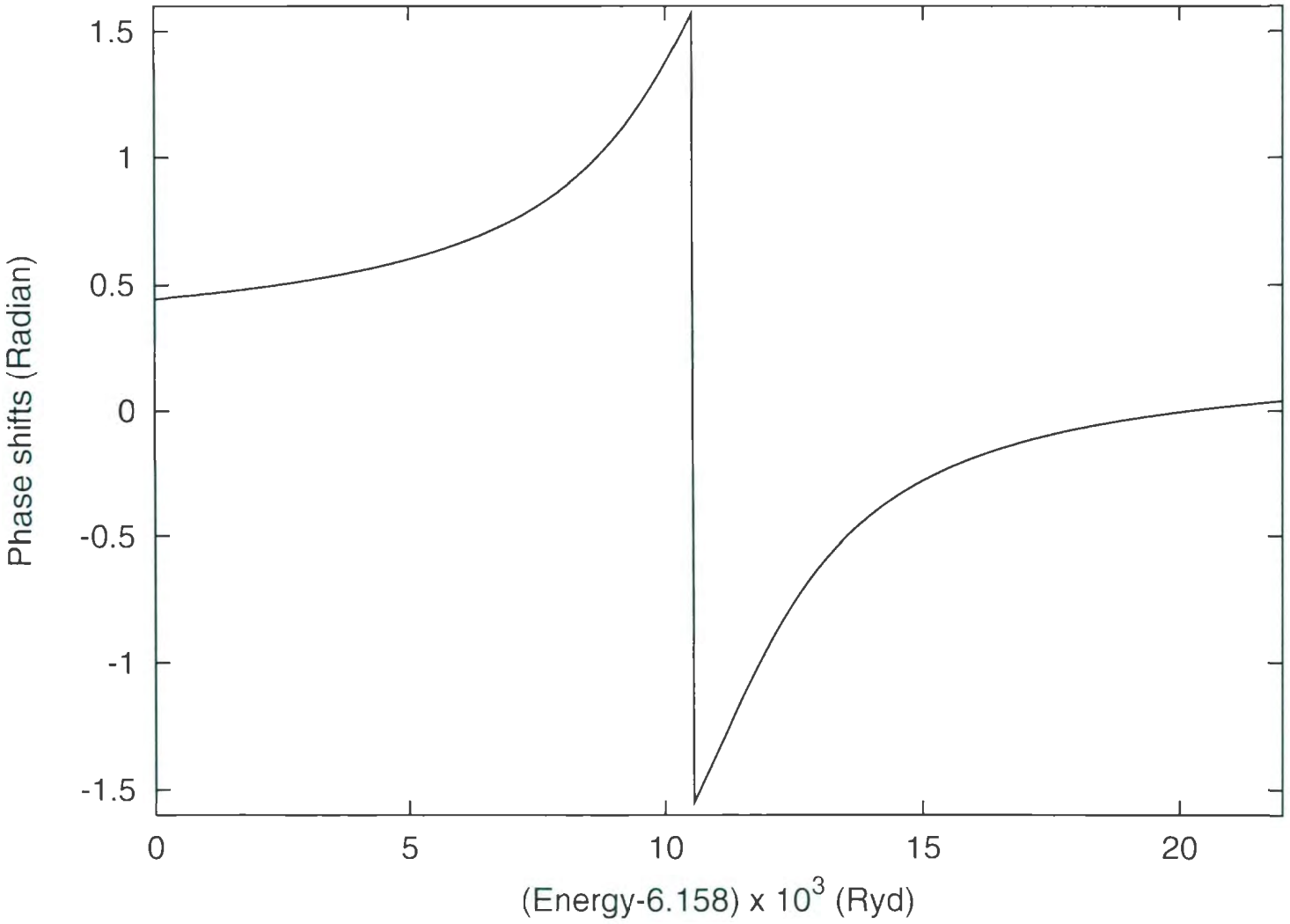

Figure 3.6. S-wave Phase Shifts of e^{-}-Li^{2+} Singlet Scattering at $^{1}S^{e}(2,3a)$

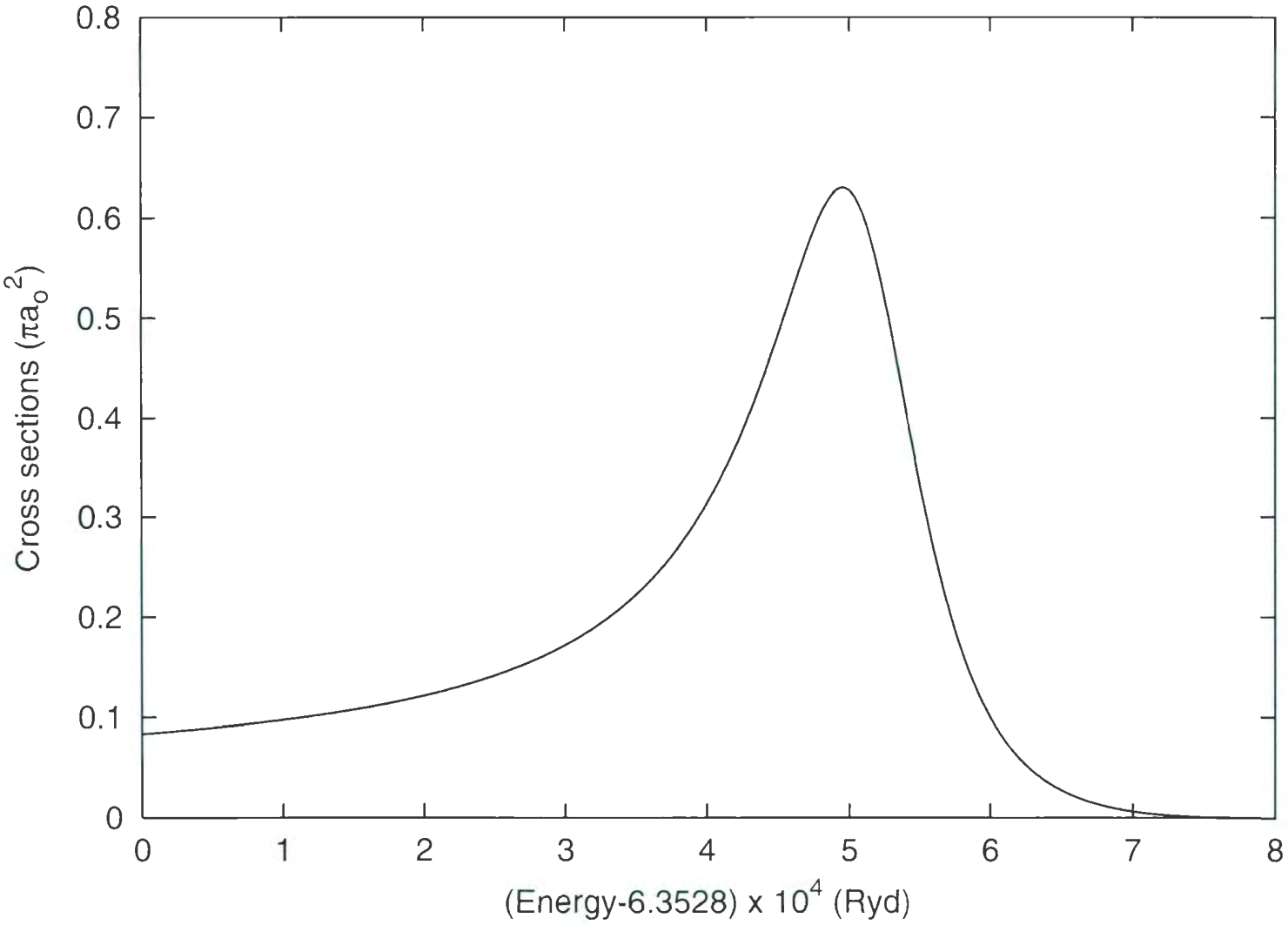

Figure 3.7. S-wave Cross-Sections of e^--Li^{2+} Singlet Scattering at $^1S^e$(2,3b)

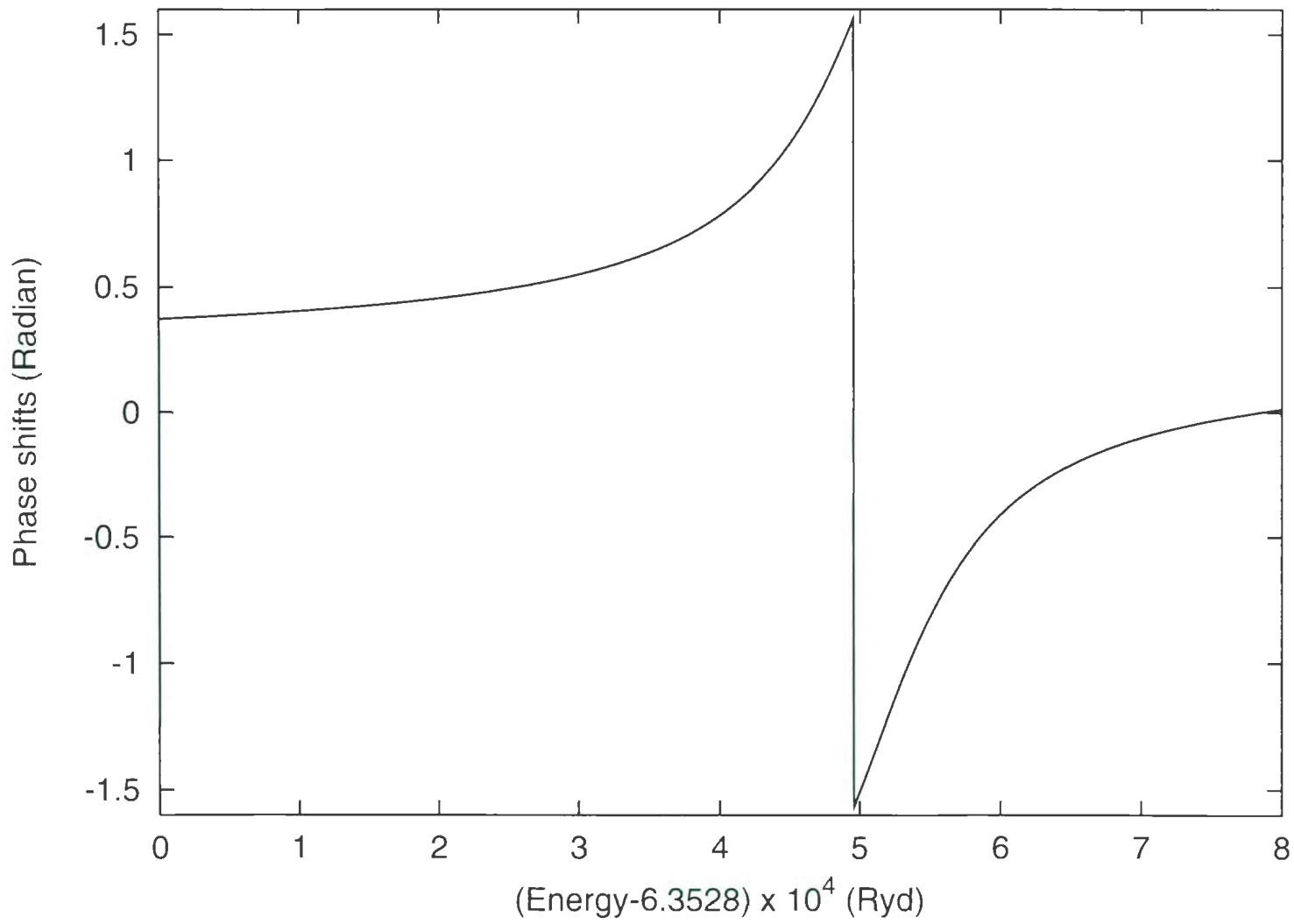

Figure 3.8. S-wave Phase Shifts of e^{-}-Li^{2+} Singlet Scattering at $^{1}S^{e}$(2,3b)

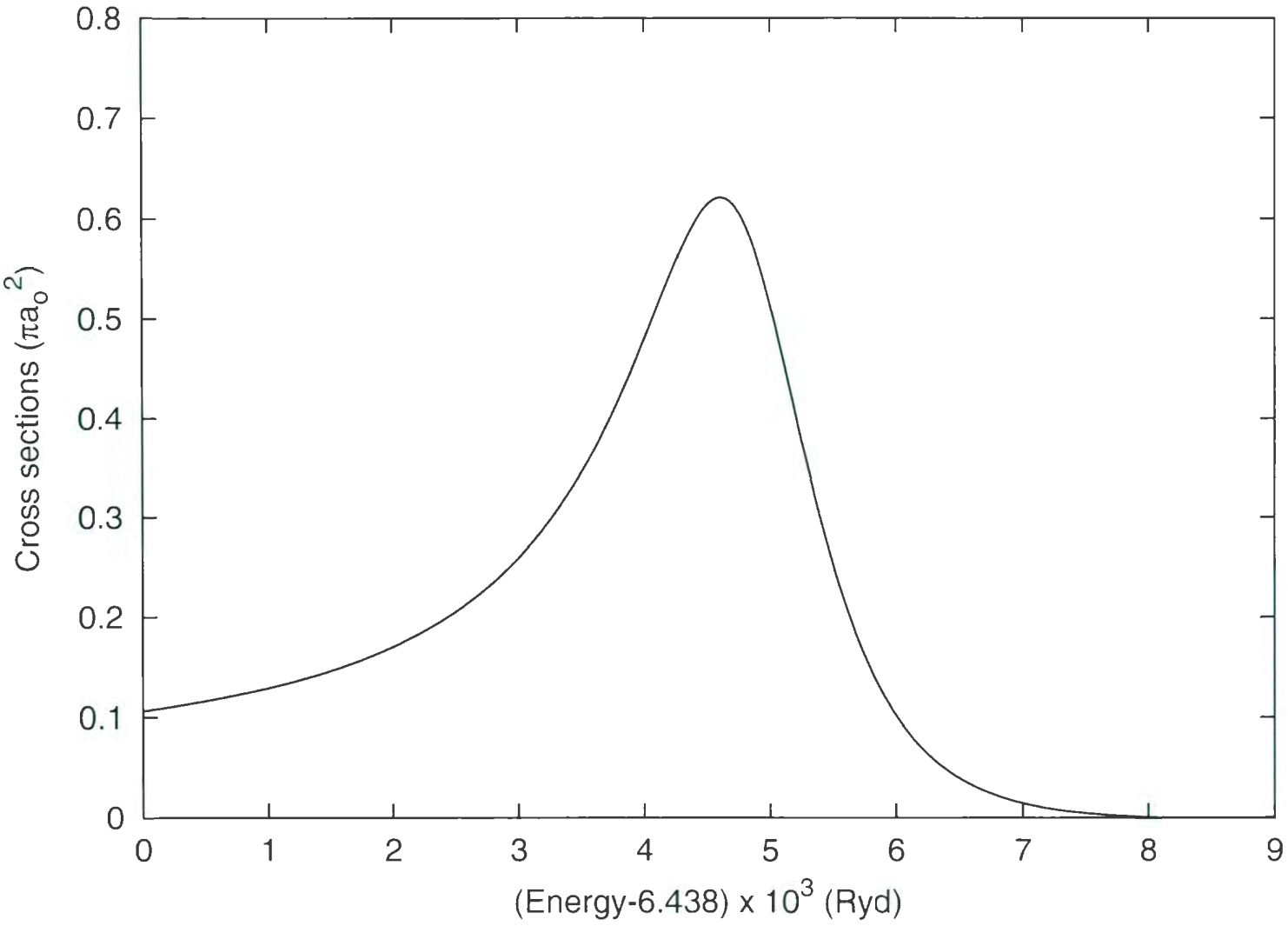

Figure 3.9. S-wave Cross-Sections of e^--Li^{2+} Singlet Scattering at $^1S^e$(2,4a)

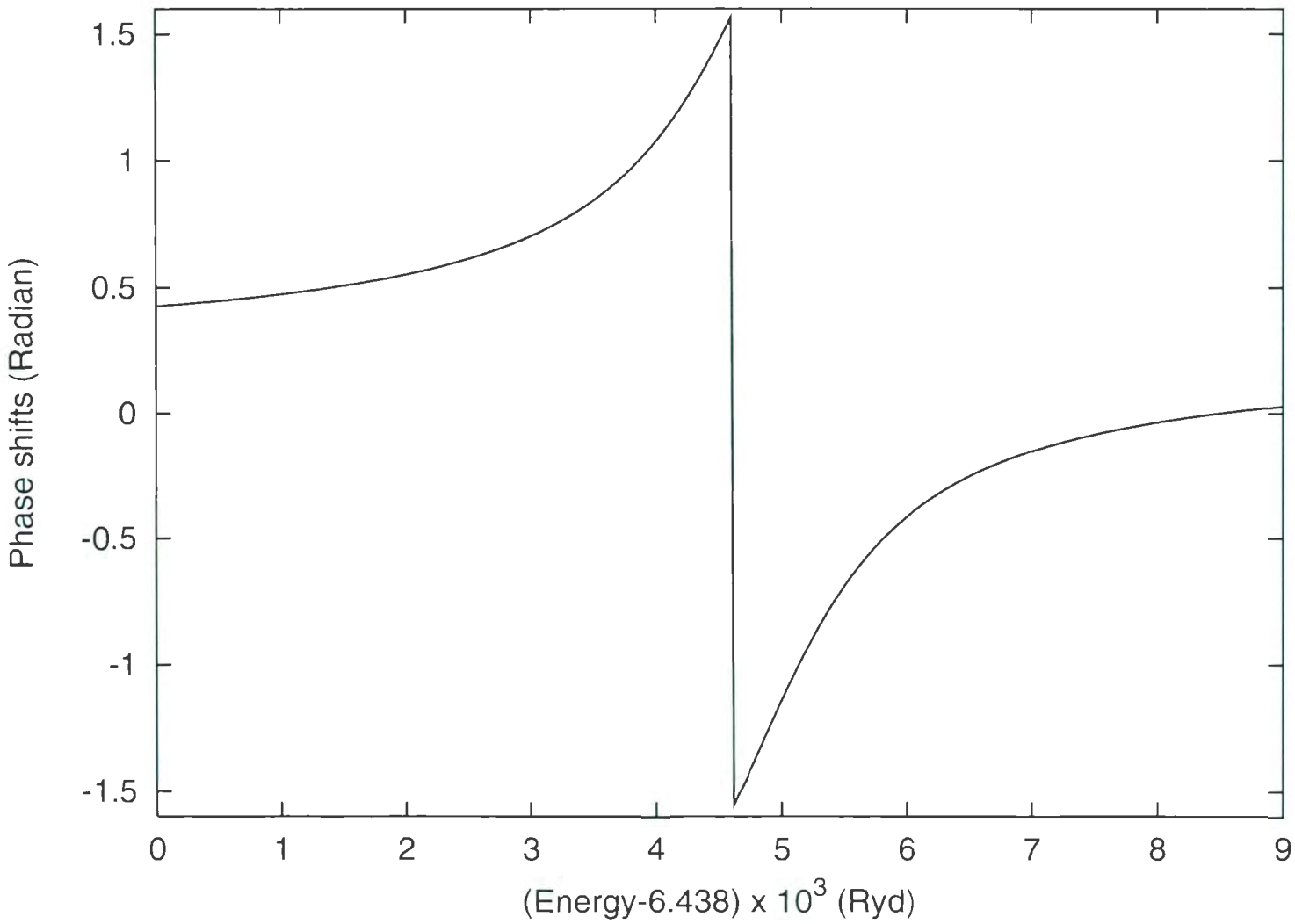

Figure 3.10. S-wave Phase Shifts of e^{-}-Li^{2+} Singlet Scattering at $^{1}S^{e}$(2,4a)

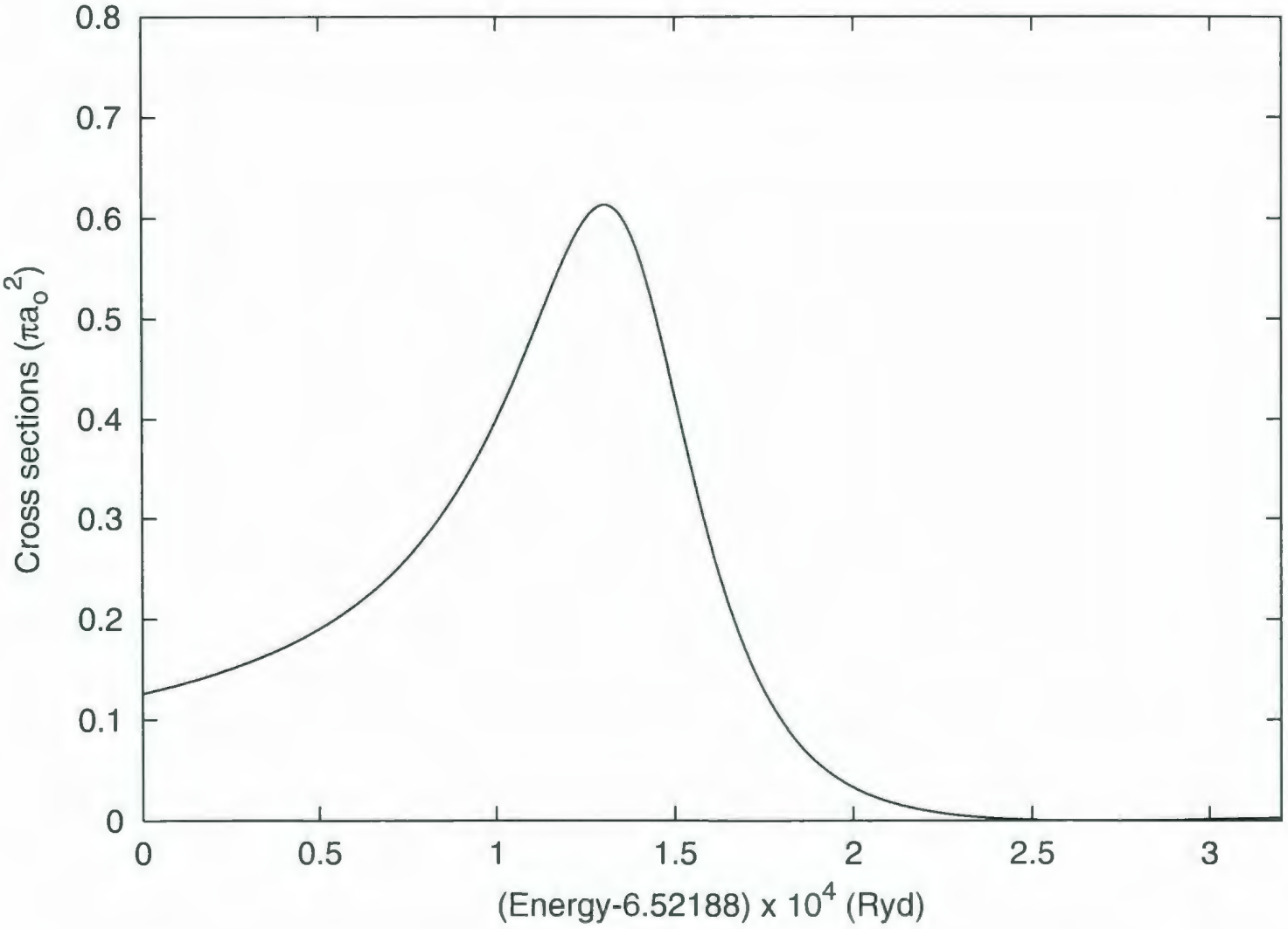

Figure 3.11. S-wave Cross-Sections of e^--Li^{2+} Singlet Scattering at $^1S^e$(2,4b)

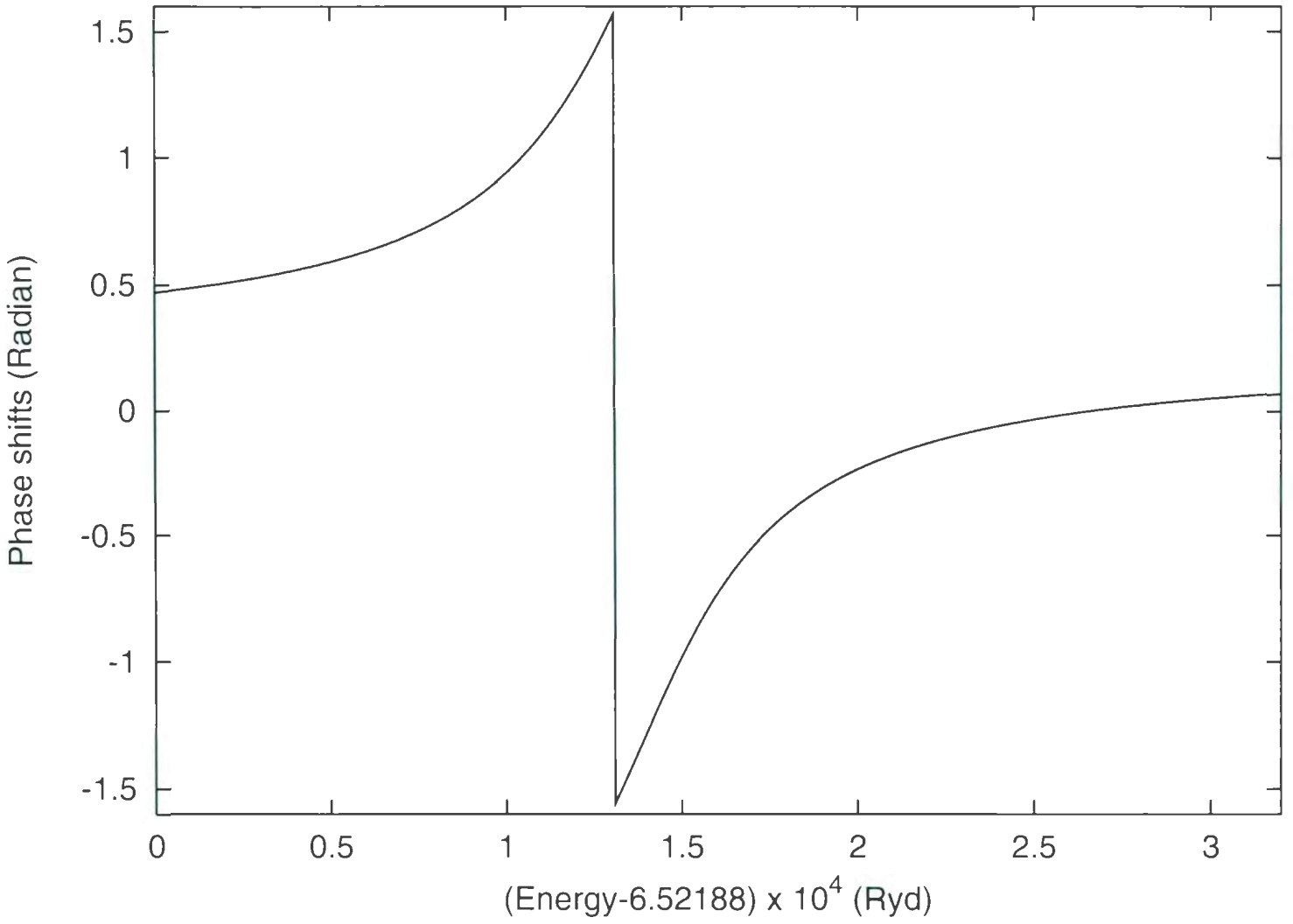

Figure 3.12. S-wave Phase Shifts of e^{-}-Li^{2+} Singlet Scattering at $^{1}S^{e}(2,4b)$

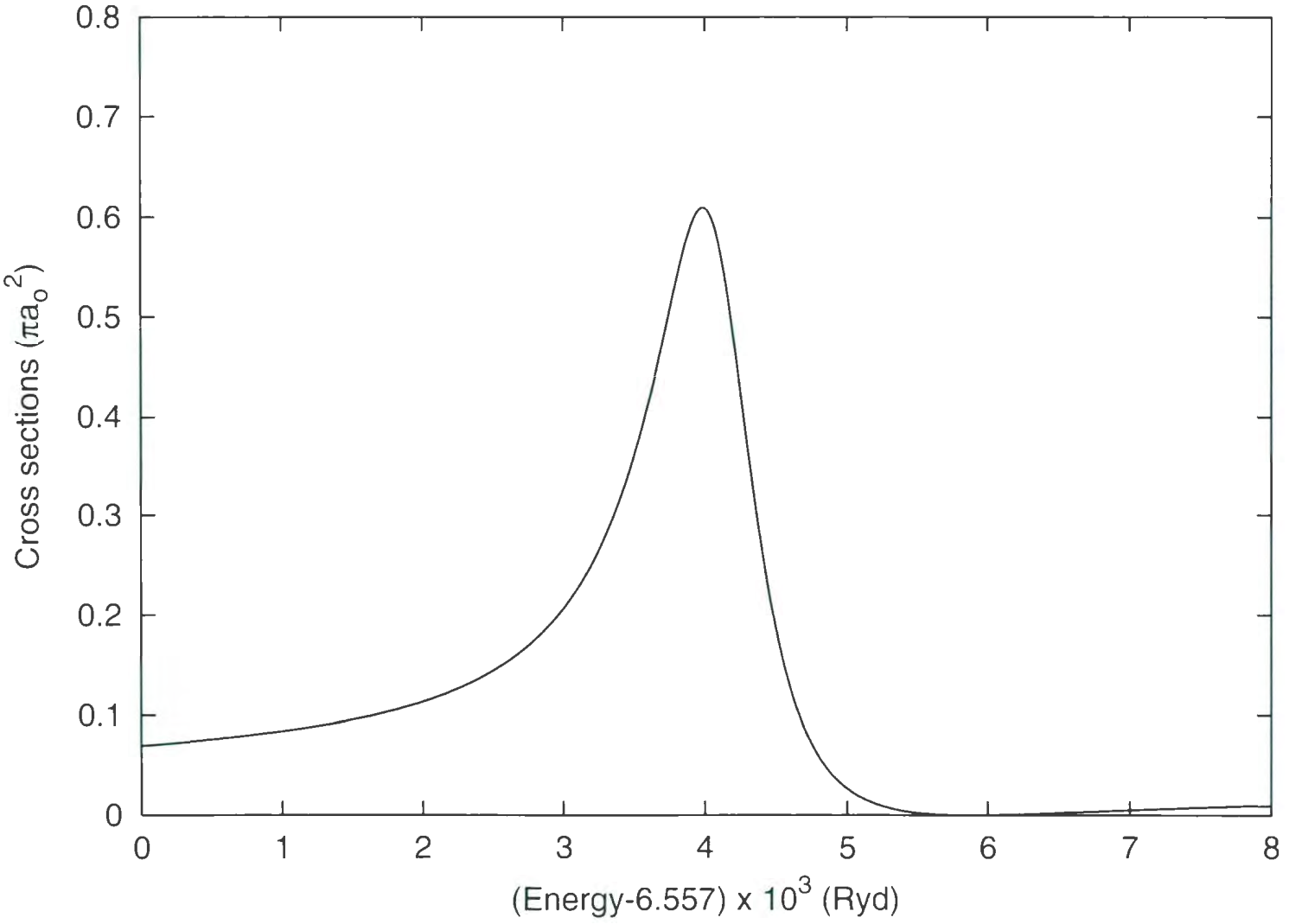

Figure 3.13. S-wave Cross-Sections of e^--Li^{2+} Singlet Scattering at $^1S^e$(2,5a)

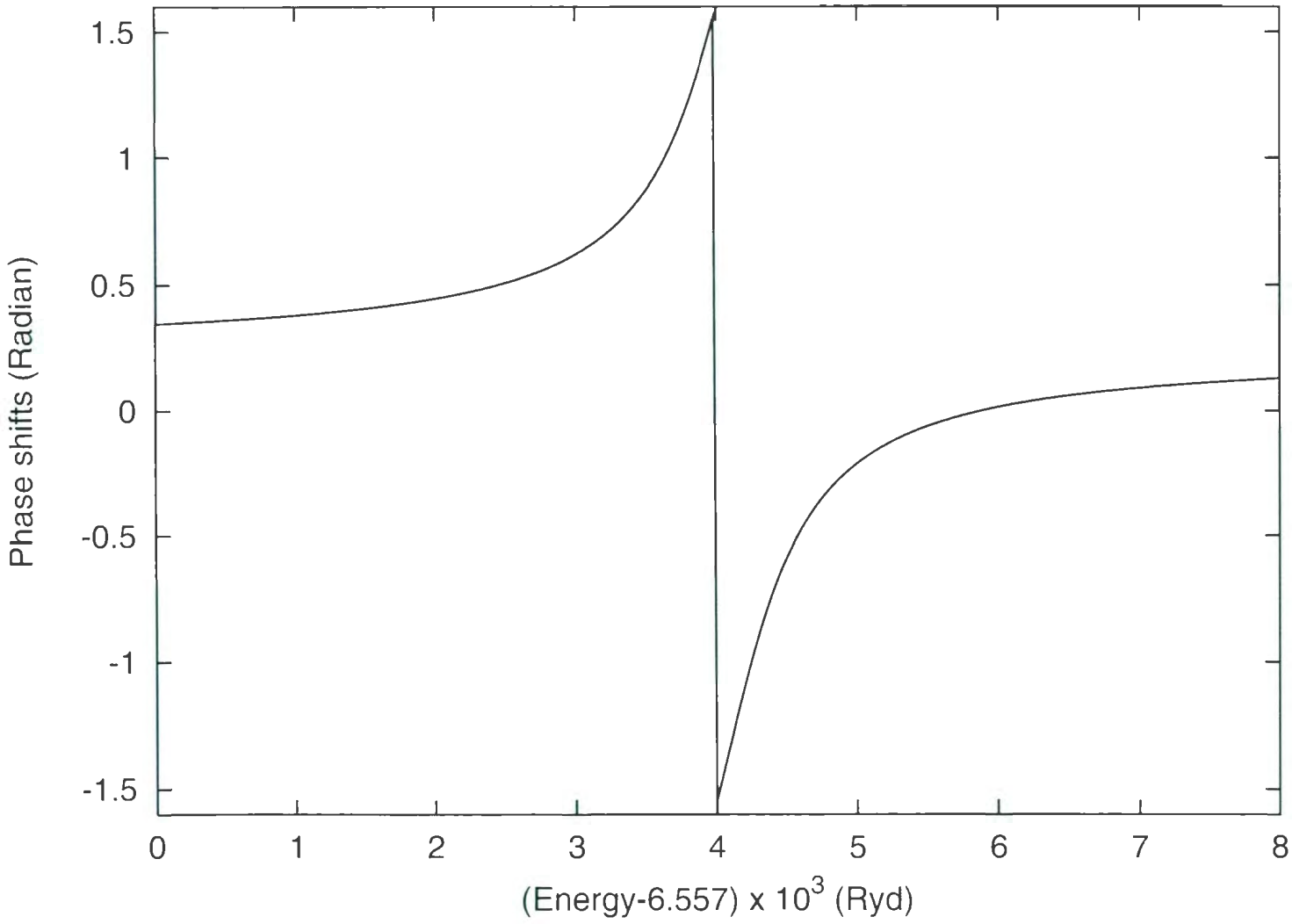

Figure 8.14. S-wave Phase Shifts of e^{-}-Li^{2+} Singlet Scattering at $^{1}S^{e}$(2,5a)

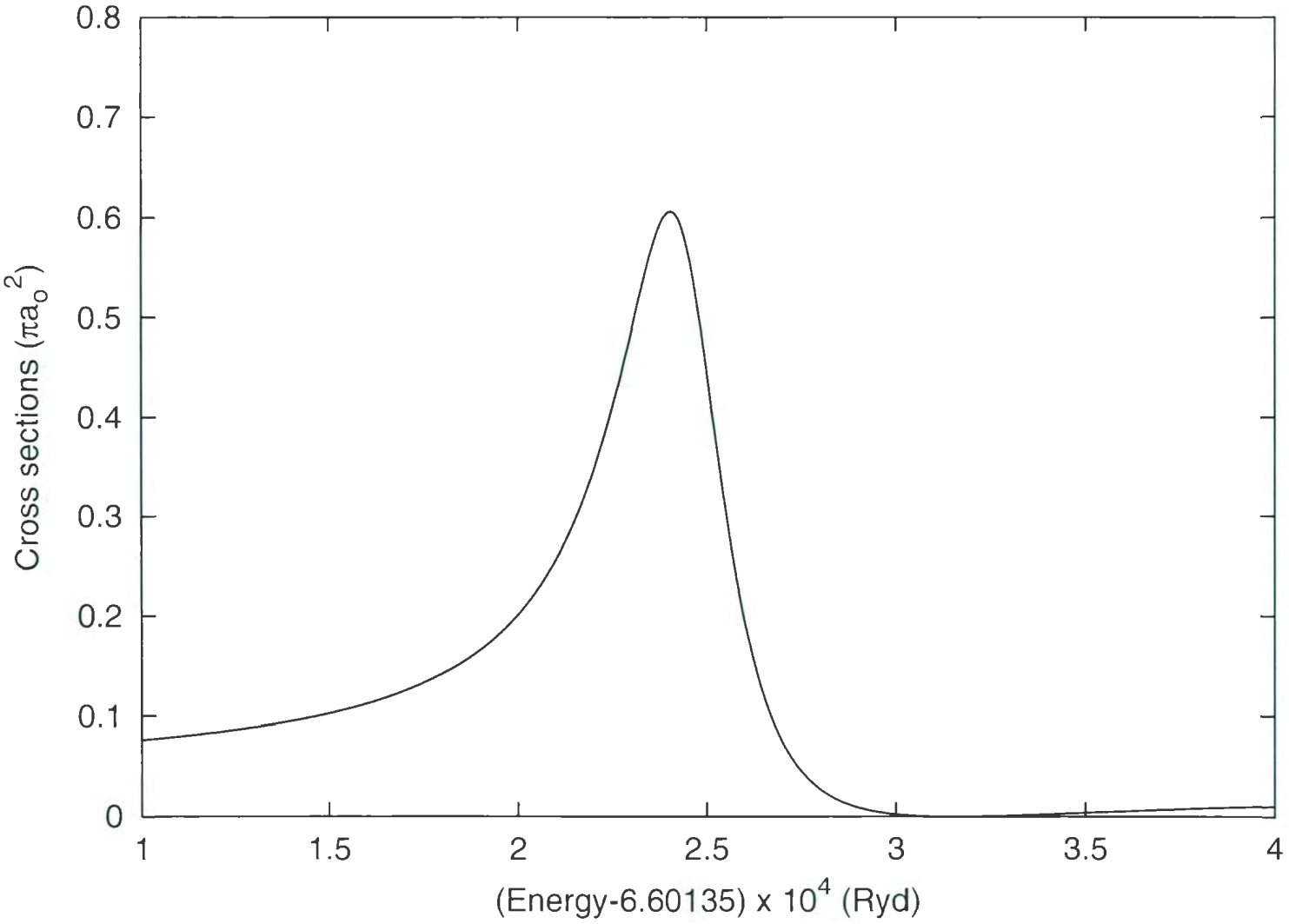

Figure 3.15. S-wave Cross-Sections of e^--Li^{2+} Singlet Scattering at $^1S^e$(2,5b)

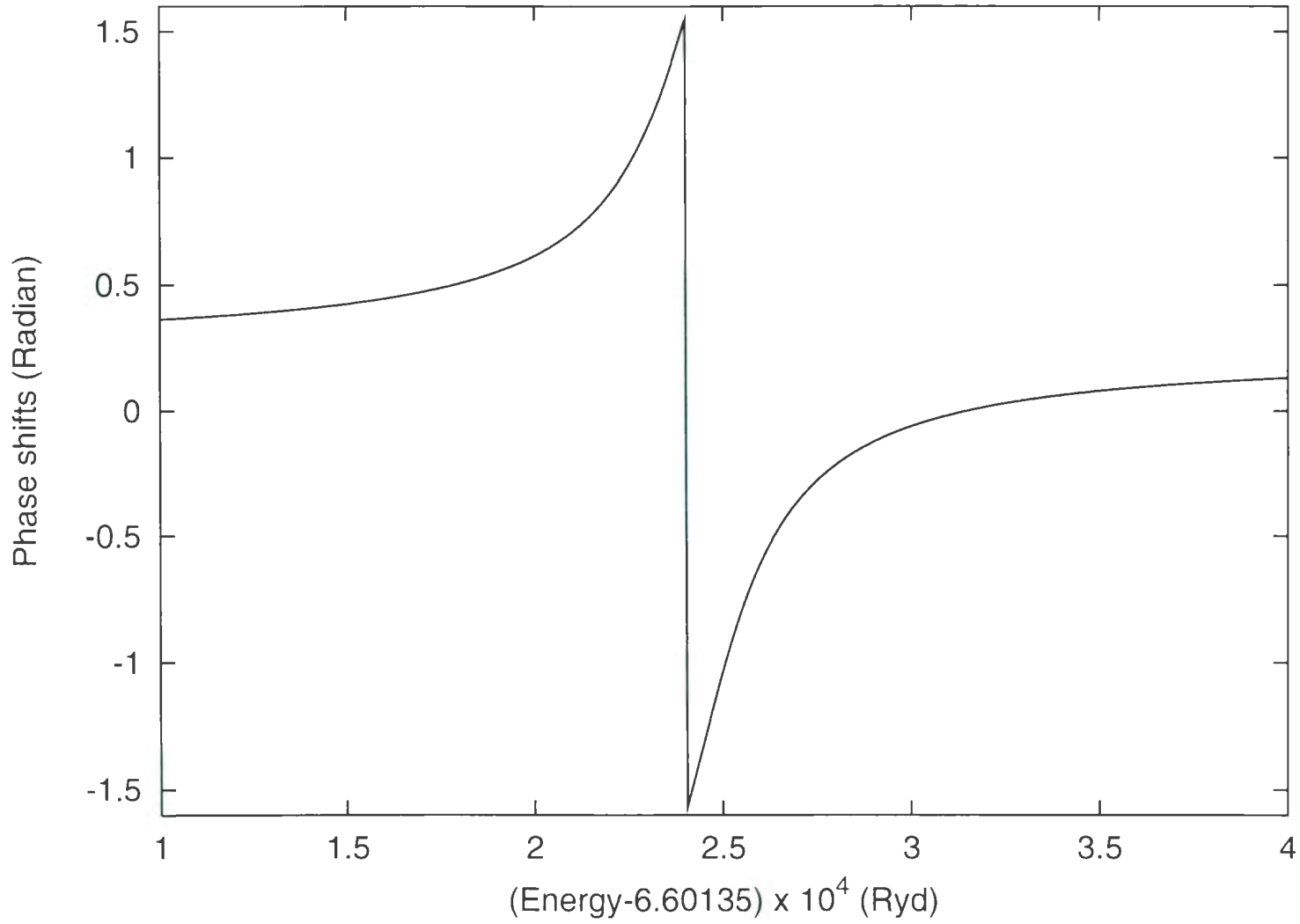

Figure 3.16. S-wave Phase Shifts of e^{-}-Li^{2+} Singlet Scattering at $^{1}S^{e}$(2,5b)

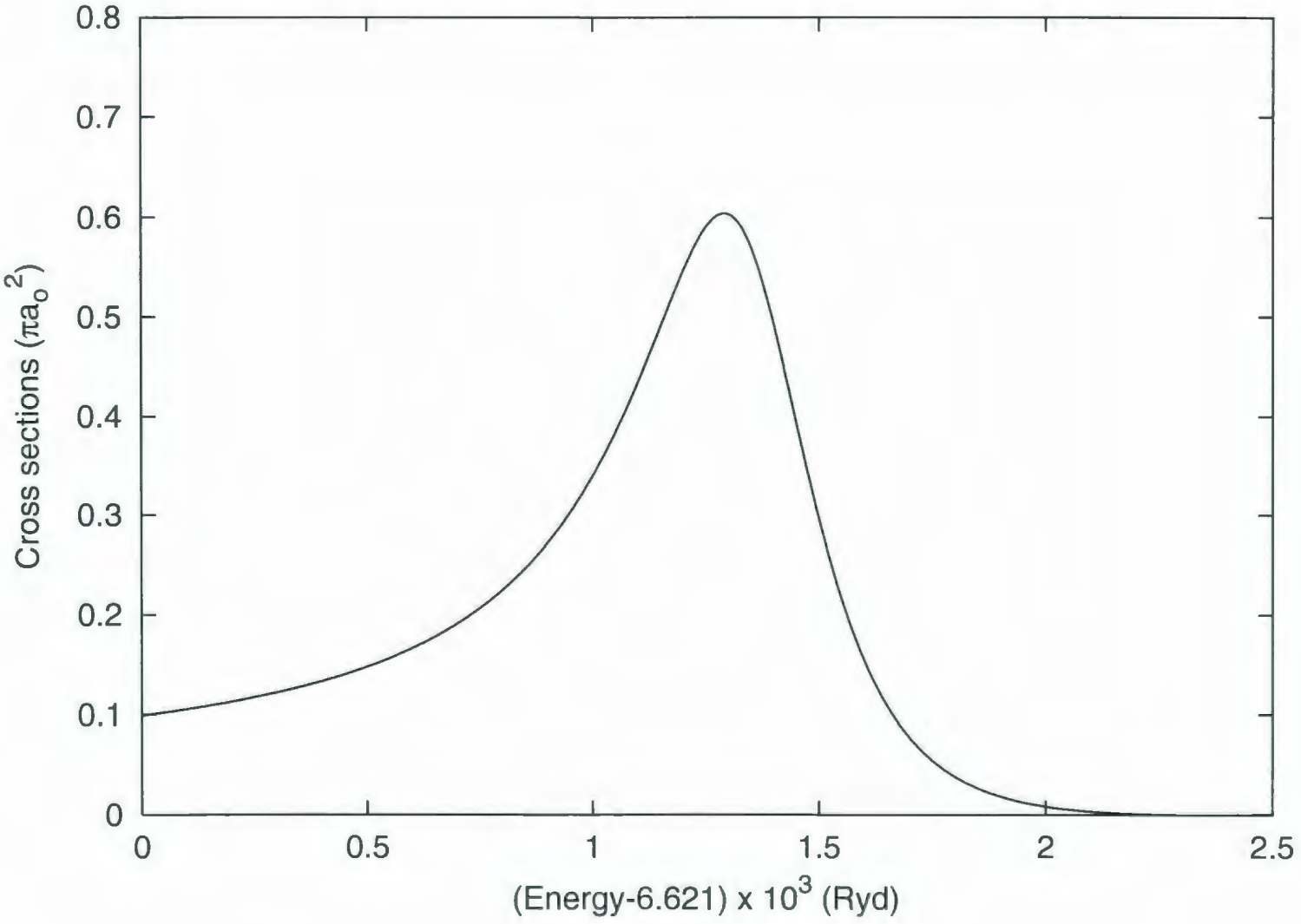

Figure 3.17. S-wave Cross-Sections of e^--Li^{2+} Singlet Scattering at $^1S^e$(2,6a)

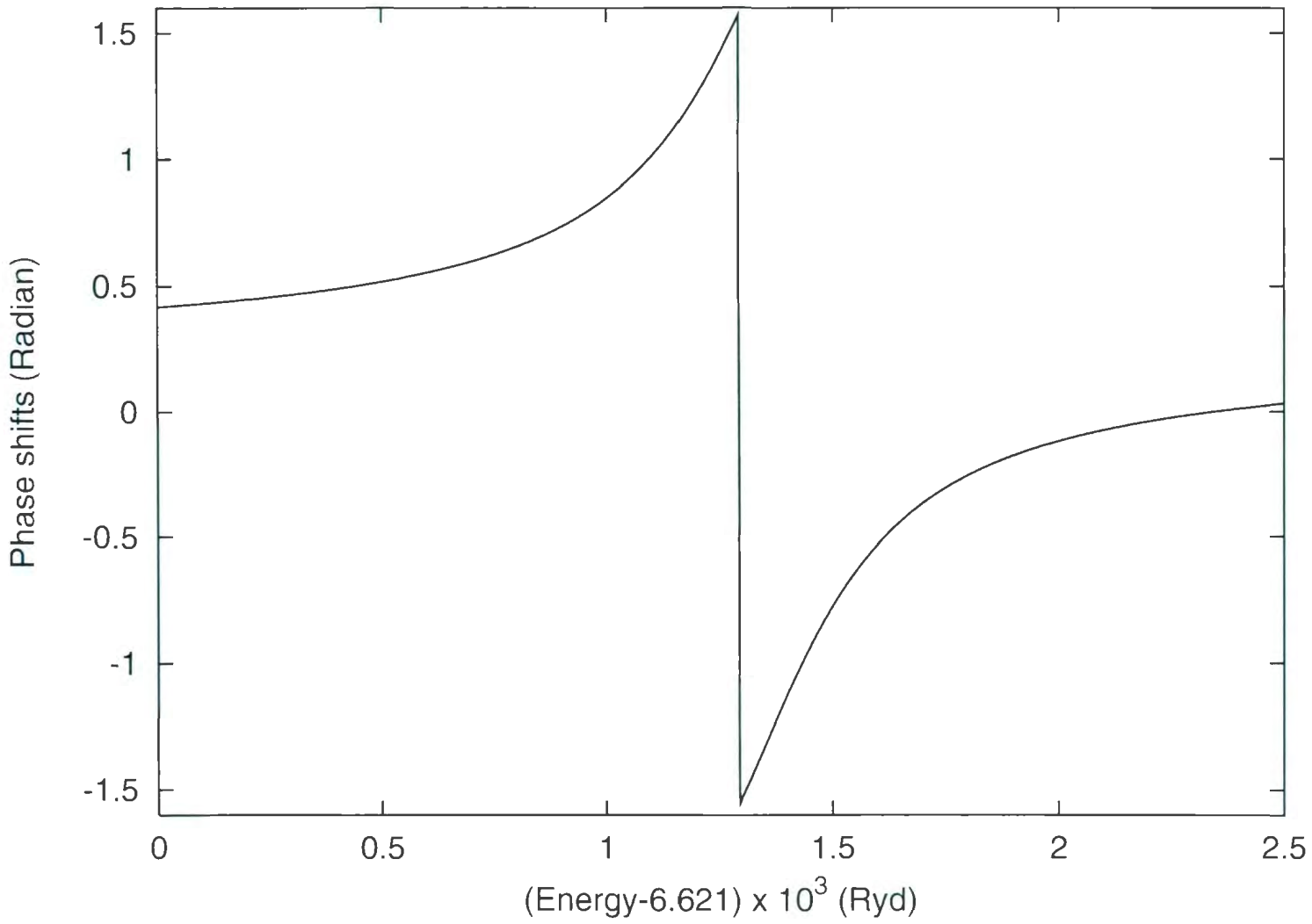

Figure 3.18. S-wave Phase Shifts of e^{-}-Li^{2+} Singlet Scattering at $^{1}S^{e}$(2,6a)

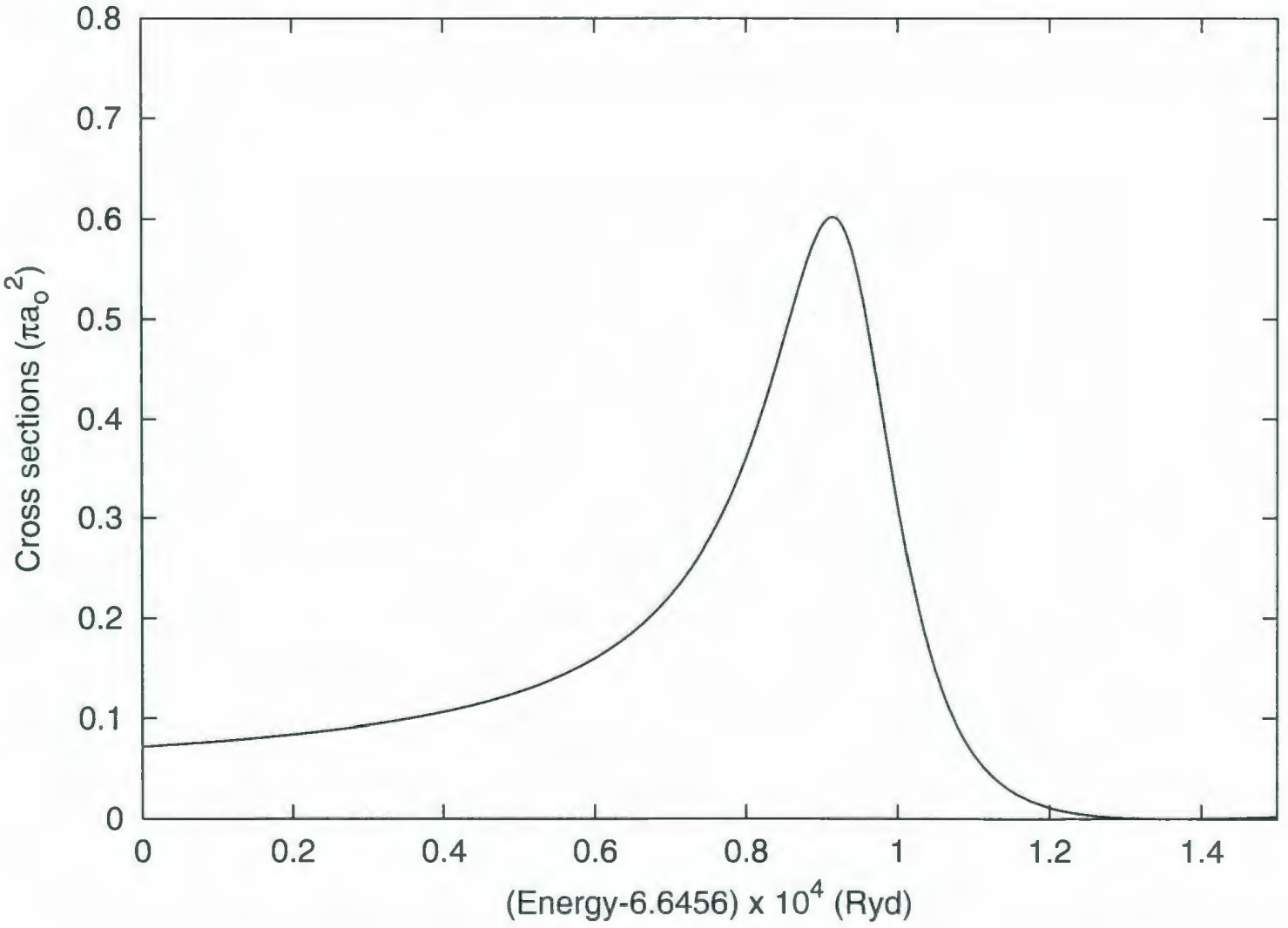

Figure 3.19. S-wave Cross-Sections of e^--Li^{2+} Singlet Scattering at $^1S^e$(2,6b)

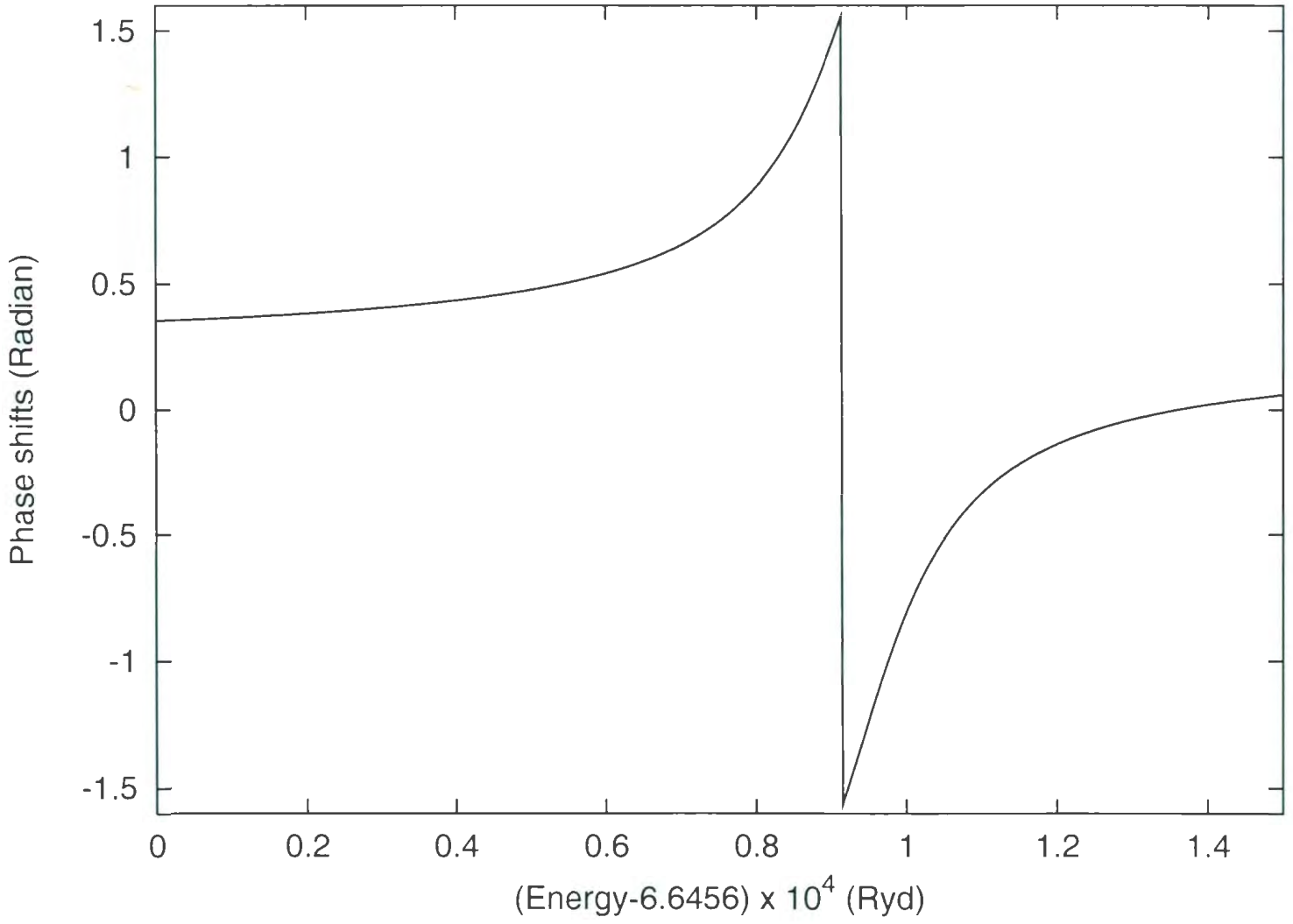

Figure 3.20. S-wave Phase Shifts of e^{-}-Li^{2+} Singlet Scattering at $^{1}S^{e}$(2,6b)

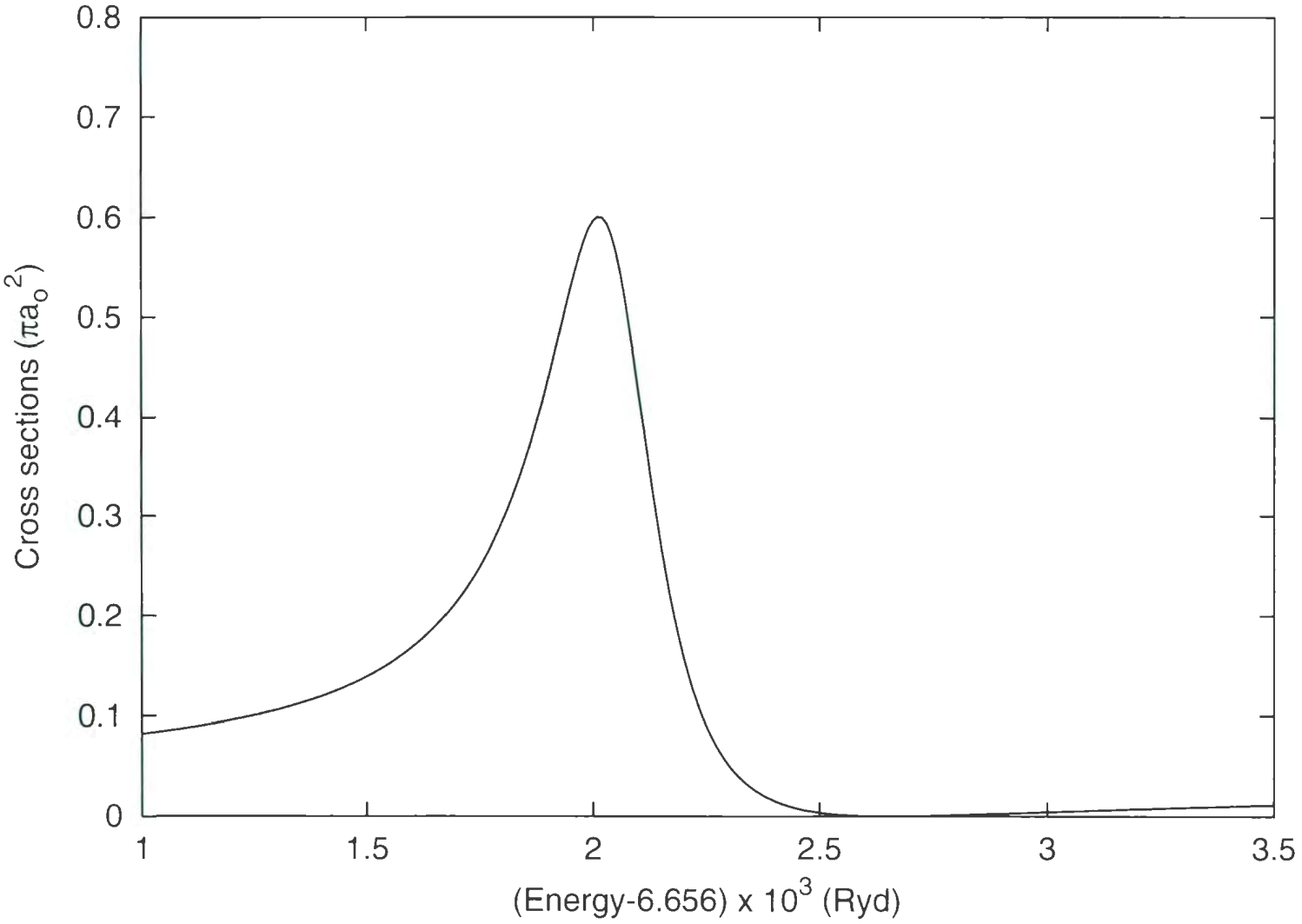

Figure 3.21. S-wave Cross-Sections of e^--Li^{2+} Singlet Scattering at $^1S^e$(2,7a)

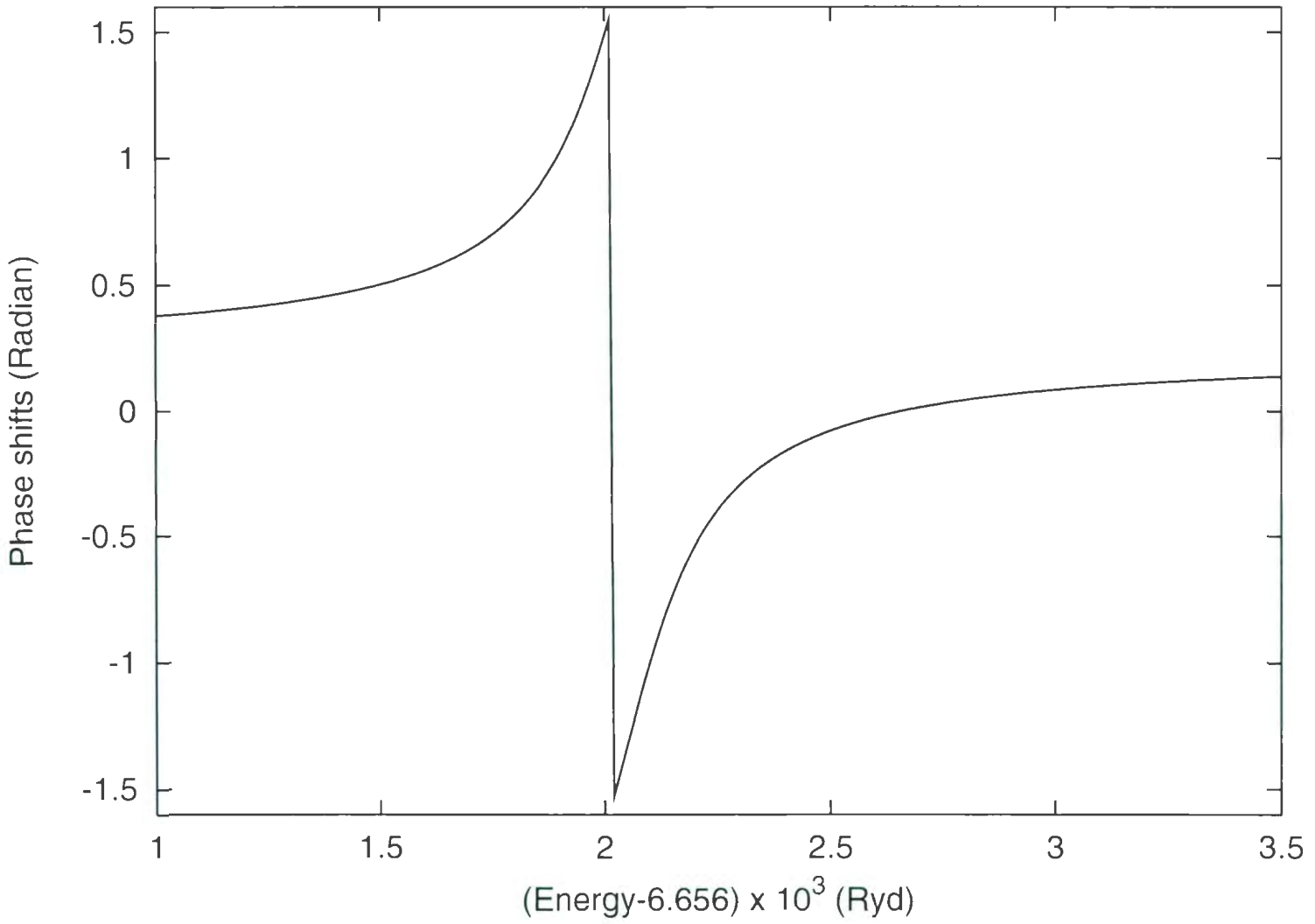

Figure 3.22. S-wave Phase Shifts of e^{-}-Li^{2+} Singlet Scattering at $^{1}S^{e}$(2,7a)

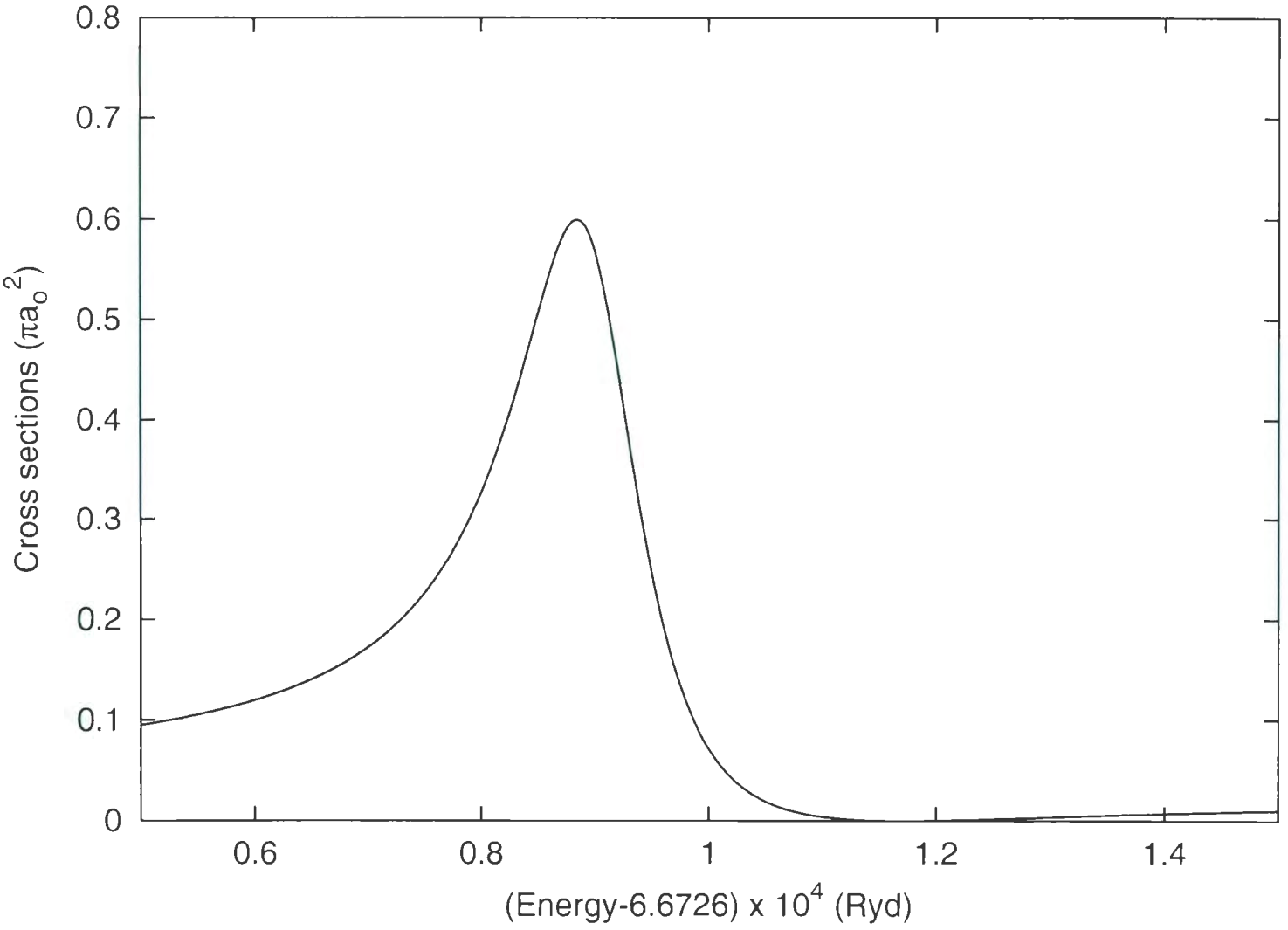

Figure 3.23. S-wave Cross-Sections of e^--Li^{2+} Singlet Scattering at $^1S^e$(2,7b)

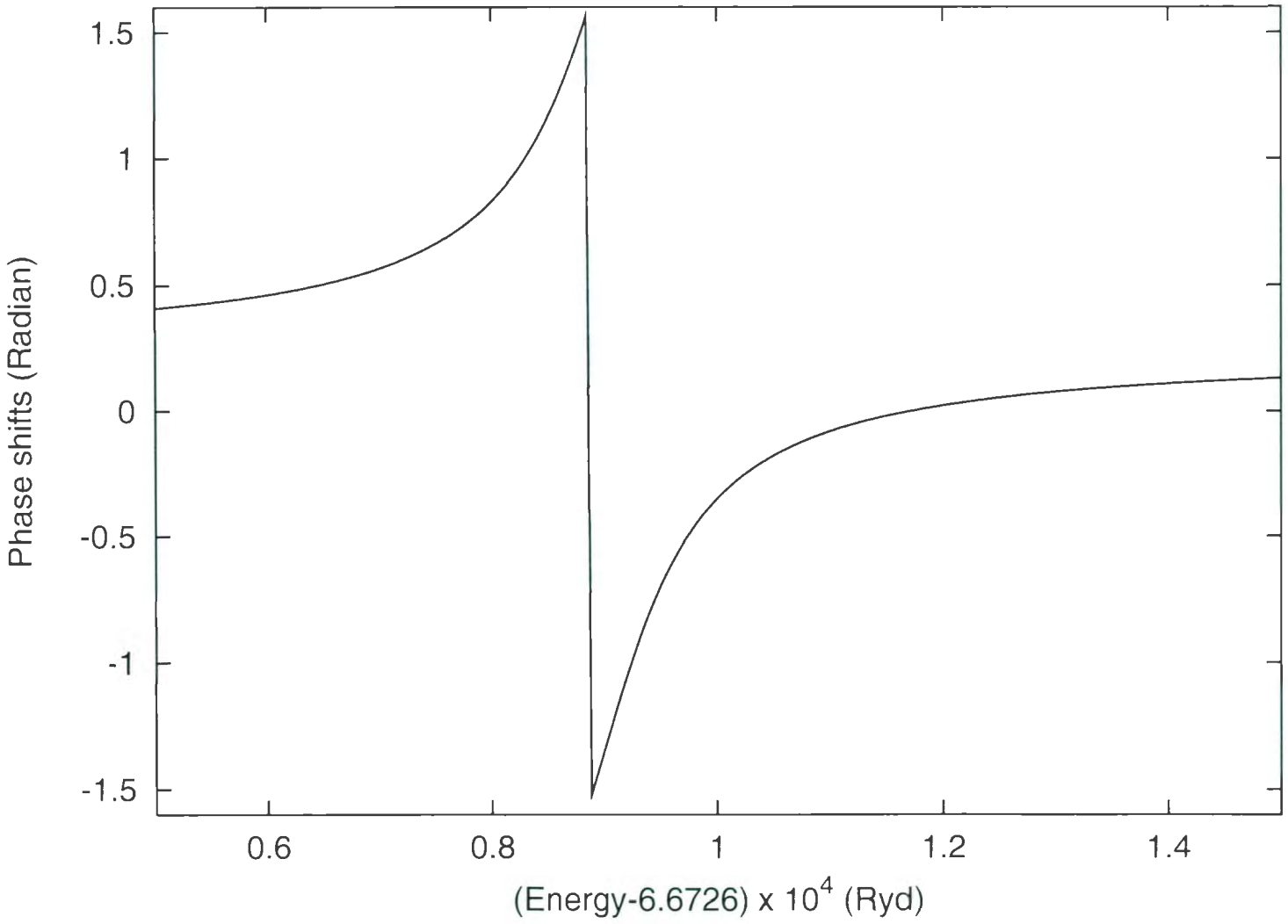

Figure 3.24. S-wave Phase Shifts of e^{-}-Li^{2+} Singlet Scattering at $^{1}S^{e}$(2,7b)

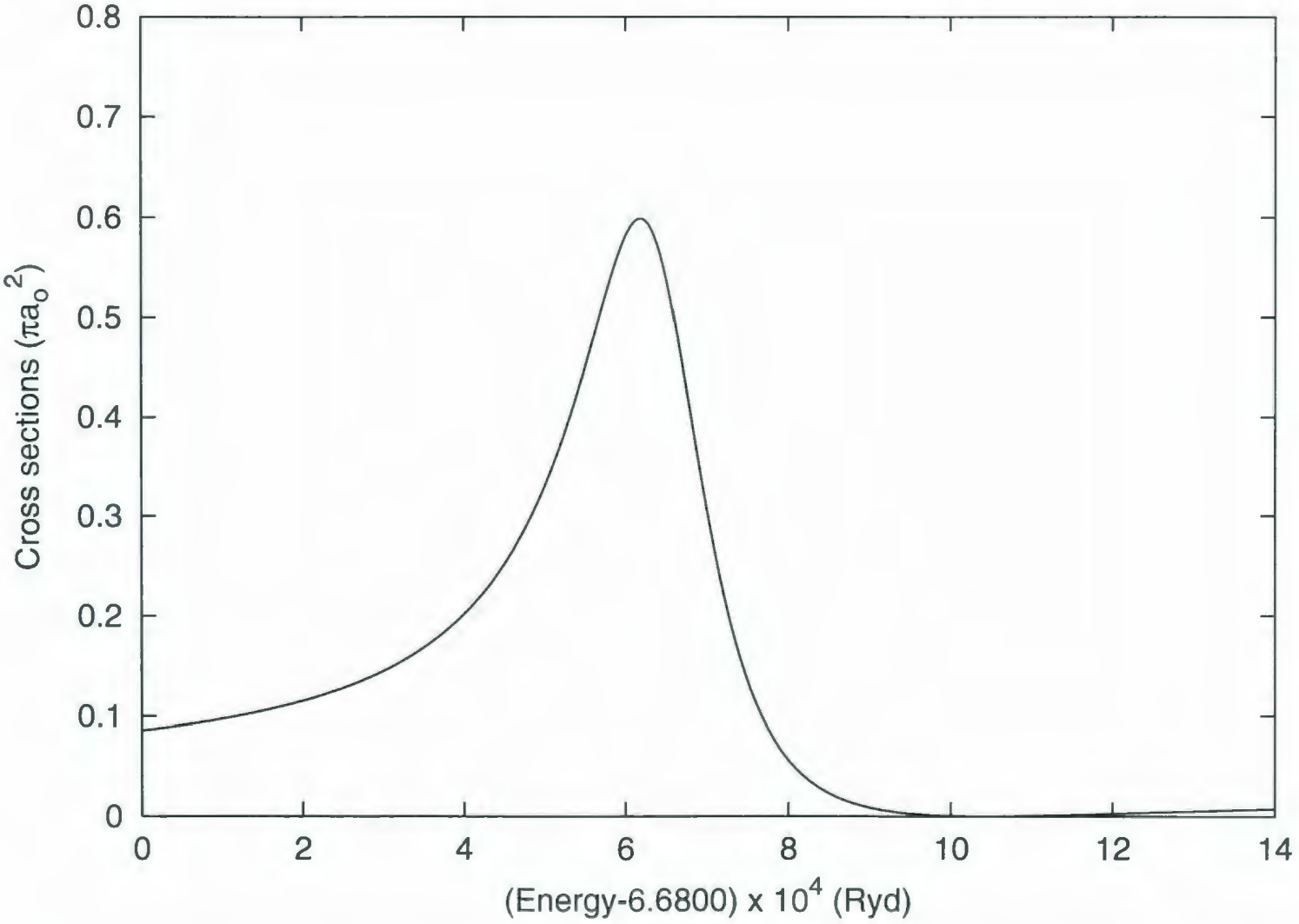

Figure 3.25. S-wave Cross-Sections of e^--Li^{2+} Singlet Scattering at $^1S^e$(2,8a)

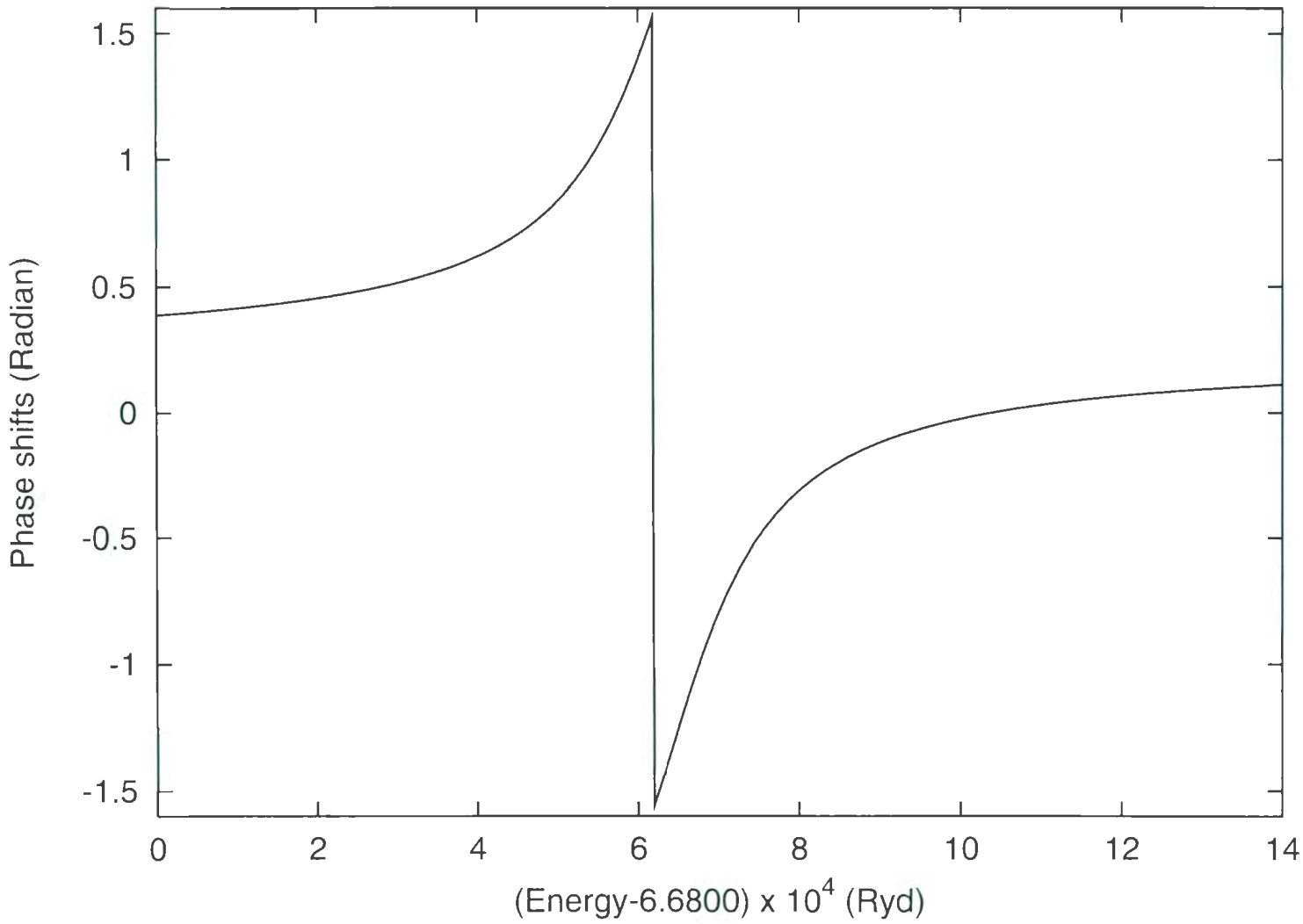

Figure 3.26. S-wave Phase Shifts of e^{-}-Li^{2+} Singlet Scattering at $^{1}S^{e}$(2,8a)

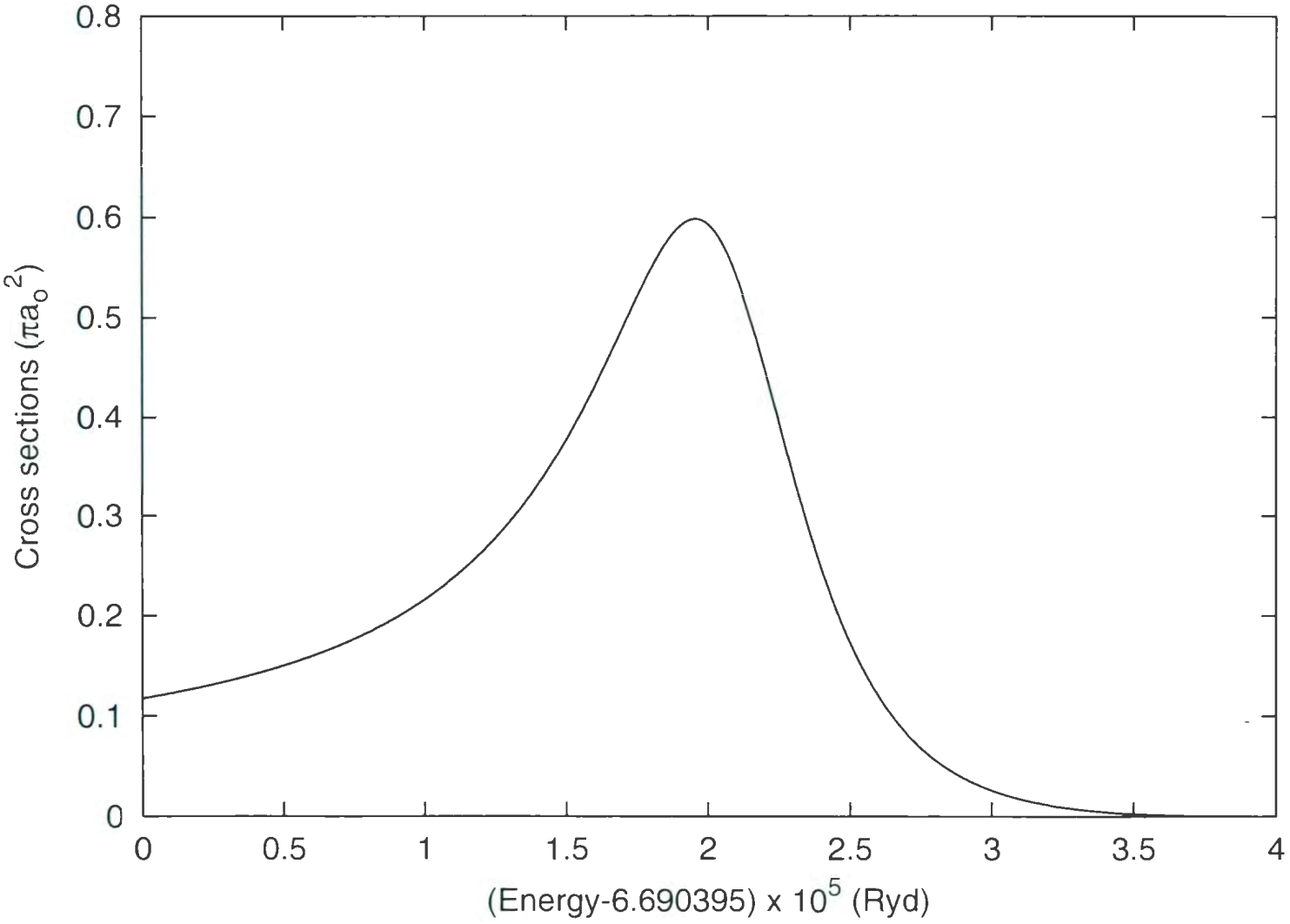

Figure 3.27. S-wave Cross-Sections of e^--Li^{2+} Singlet Scattering at $^1S^e$(2,8b)

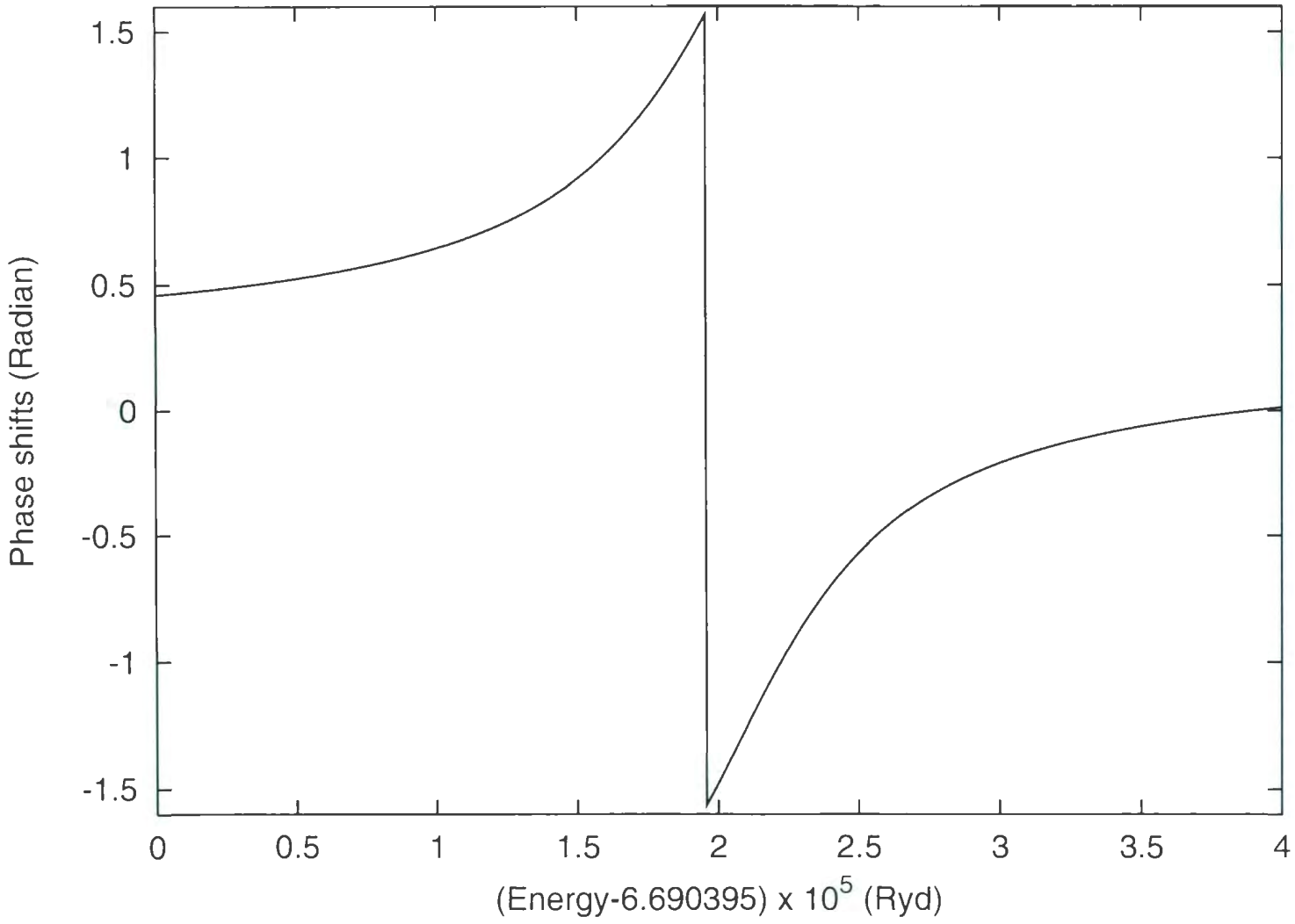

Figure 3.28. S-wave Phase Shifts of e^{-}-Li^{2+} Singlet Scattering at $^{1}S^{e}$(2,8b)

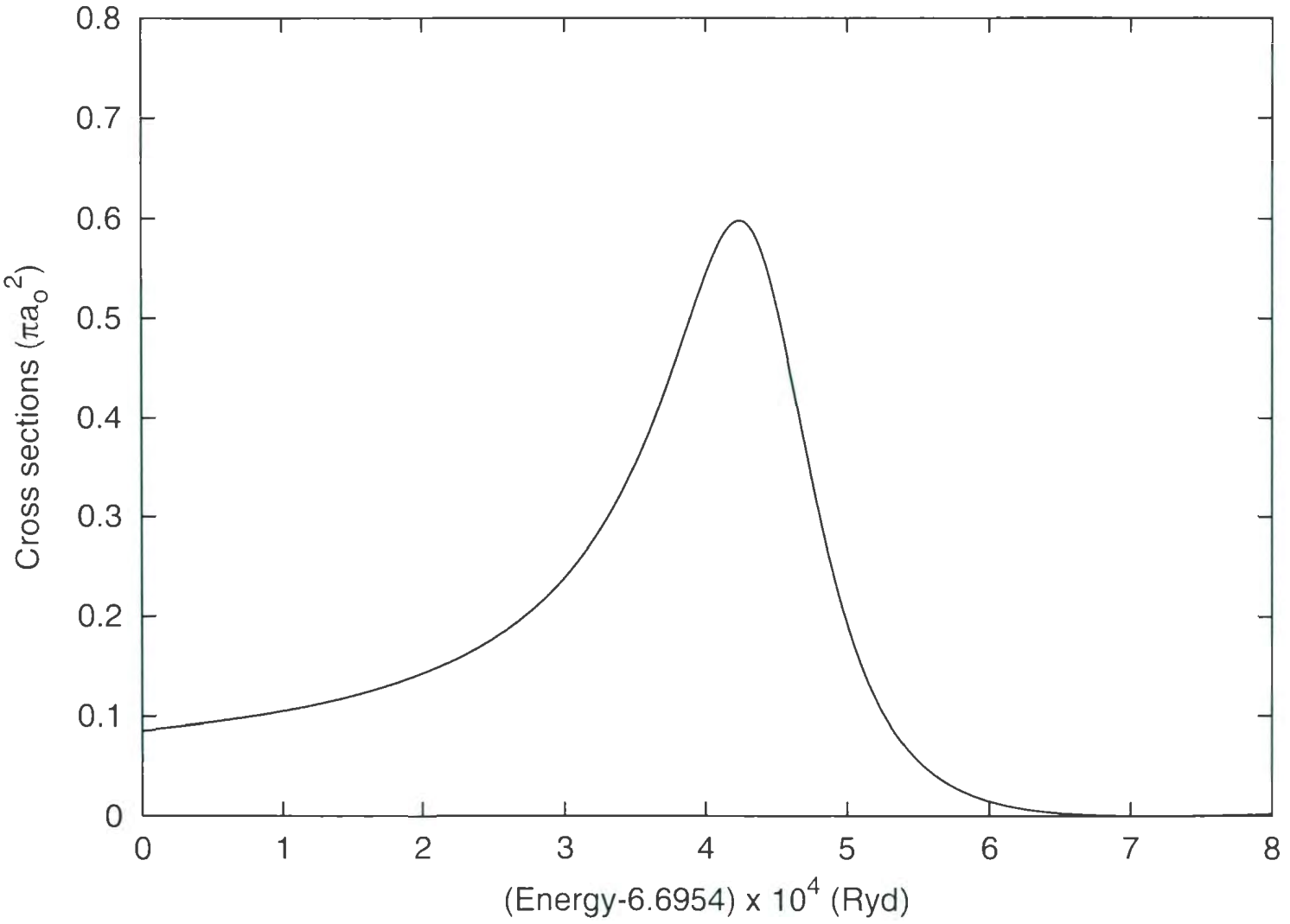

Figure 3.29. S-wave Cross-Sections of e^--Li^{2+} Singlet Scattering at $^1S^e$(2,9a)

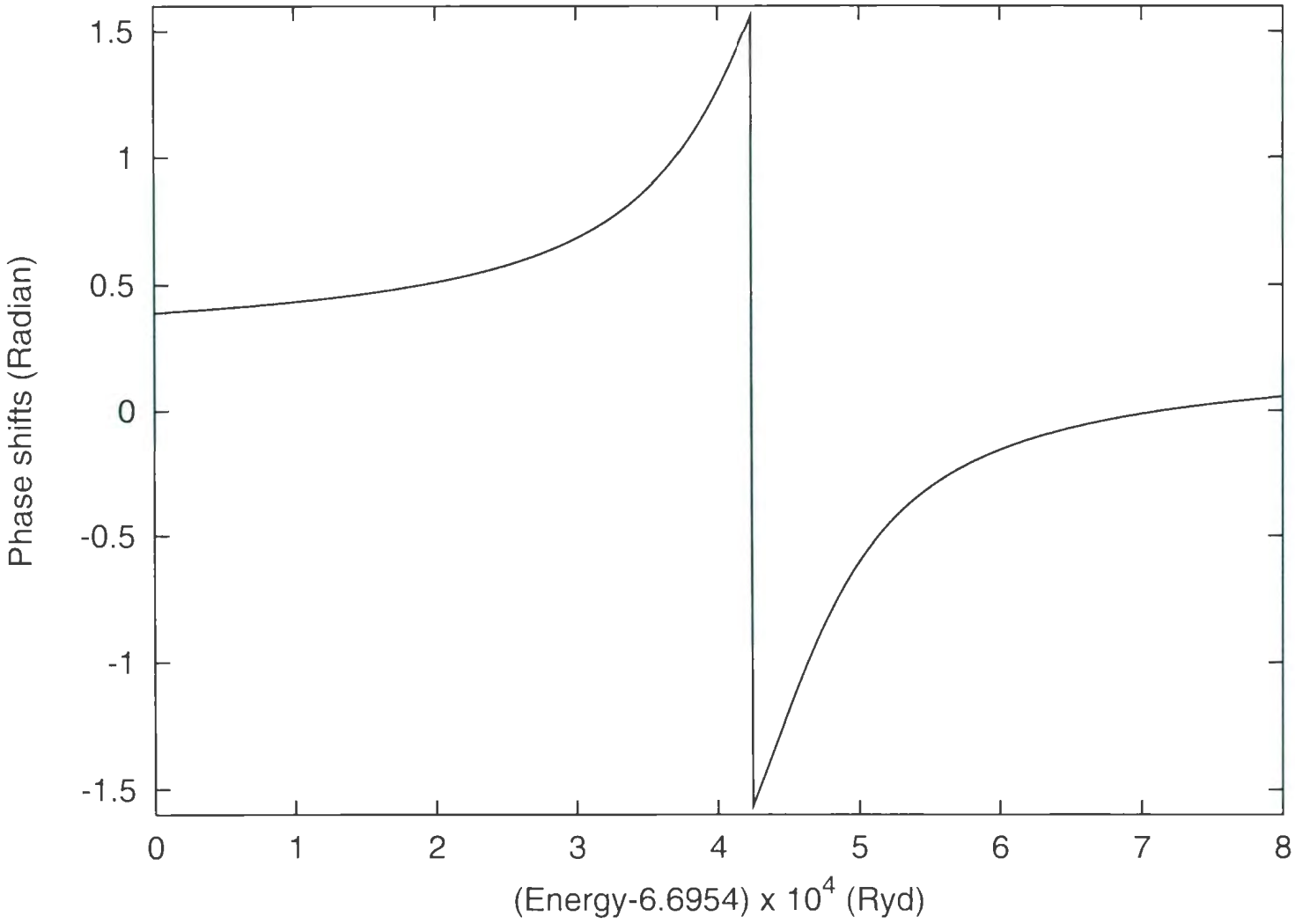

Figure 3.30. S-wave Phase Shifts of e^{-}-Li^{2+} Singlet Scattering at $^{1}S^{e}$(2,9a)

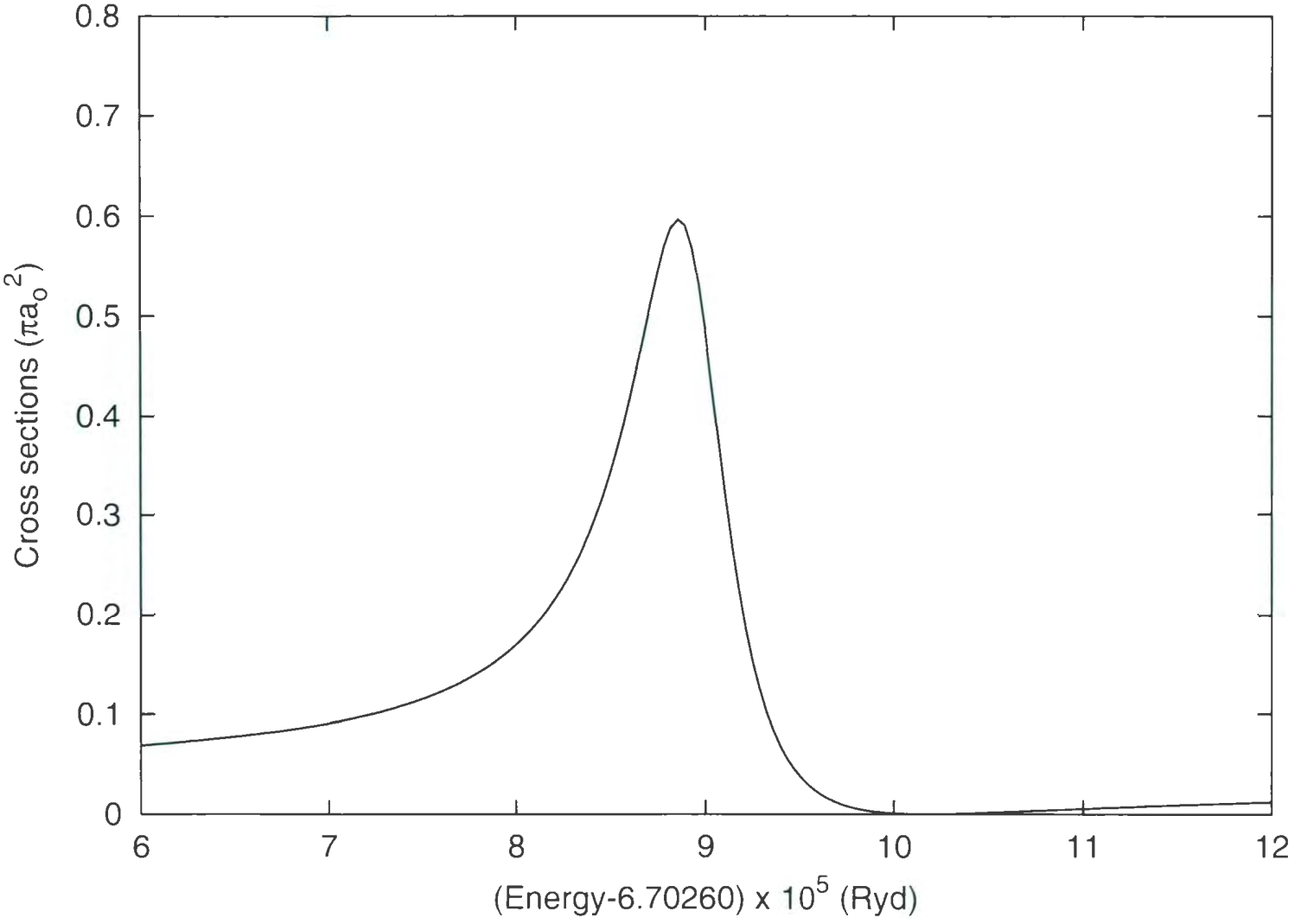

Figure 3.31. S-wave Cross-Sections of e^--Li^{2+} Singlet Scattering at $^1S^e$(2,9b)

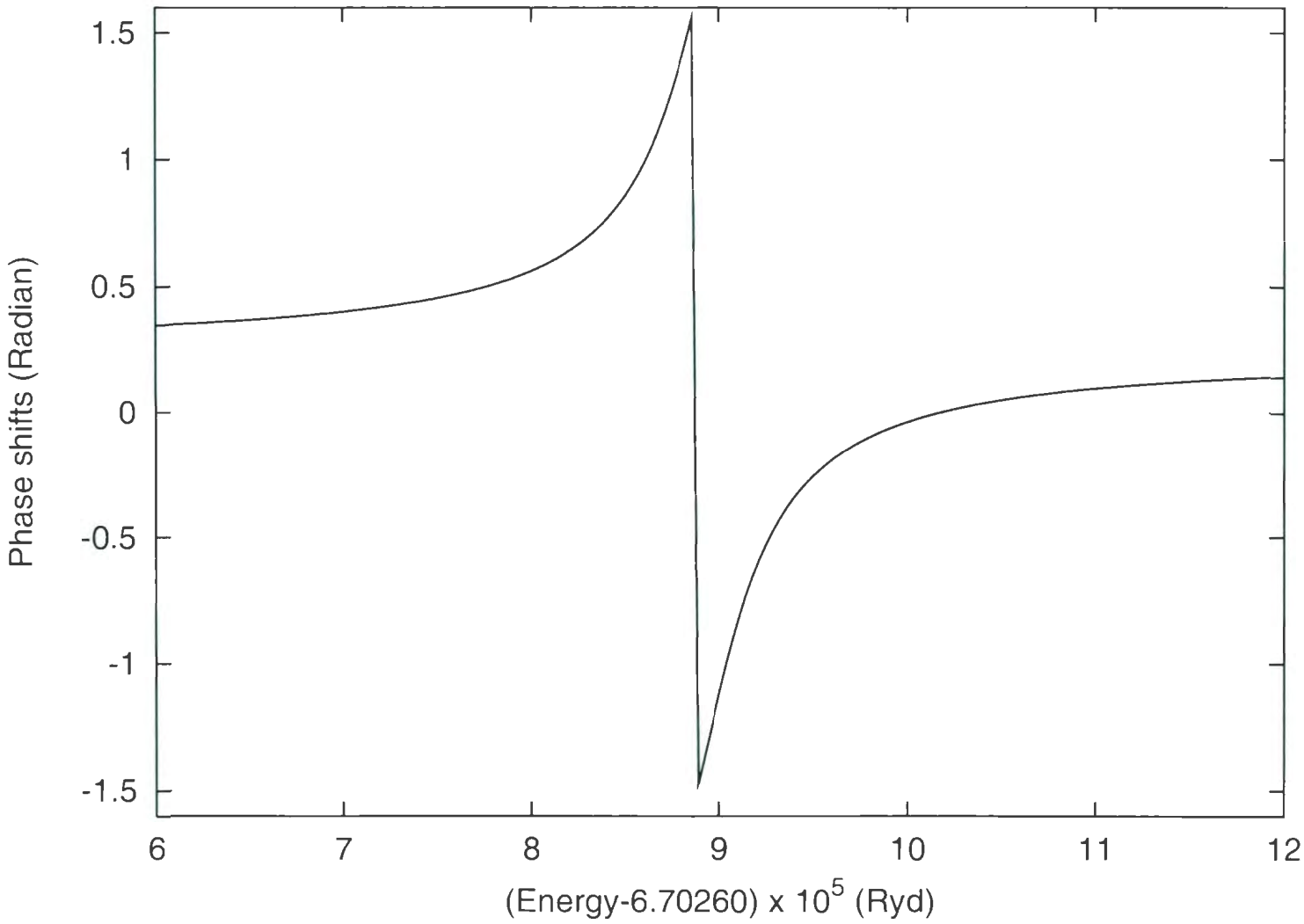

Figure 3.32. S-wave Phase Shifts of e^{-}-Li^{2+} Singlet Scattering at $^{1}S^{e}$(2,9b)

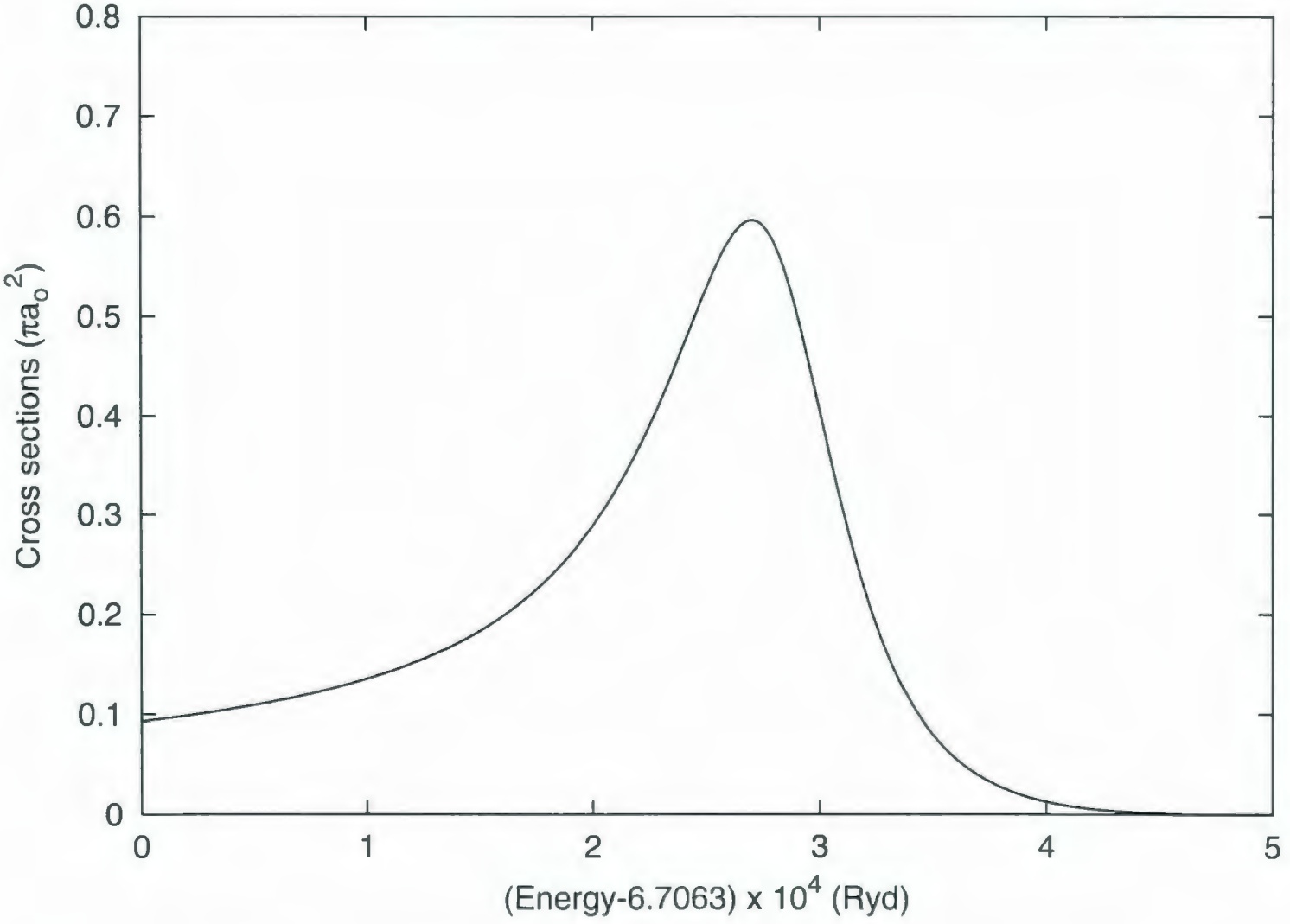

Figure 3.33. S-wave Cross-Sections of e^--Li^{2+} Singlet Scattering at $^1S^e$(2,10a)

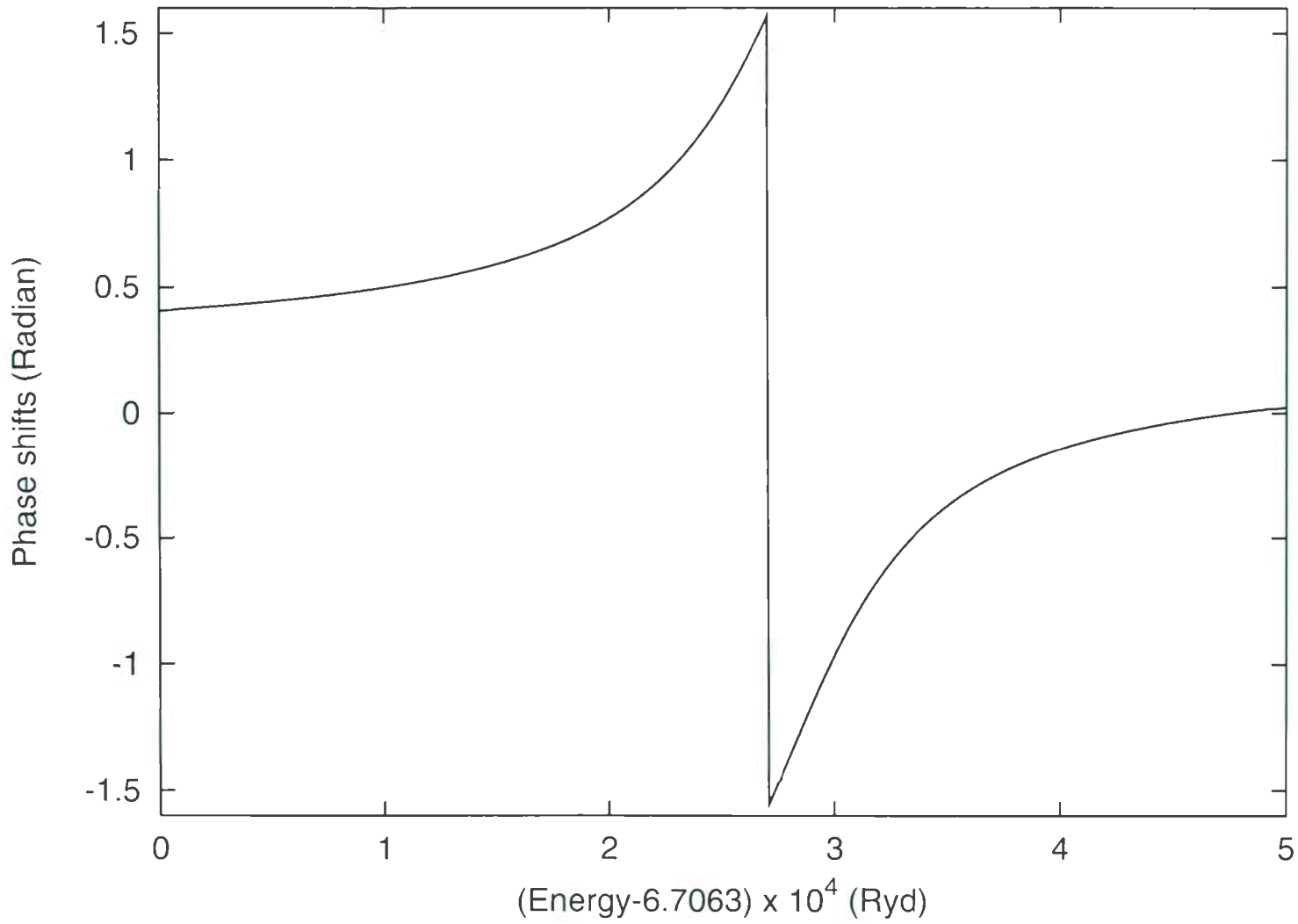

Figure 3.34. S-wave Phase Shifts of e^{-}-Li^{2+} Singlet Scattering at $^{1}S^{e}$(2,10a)

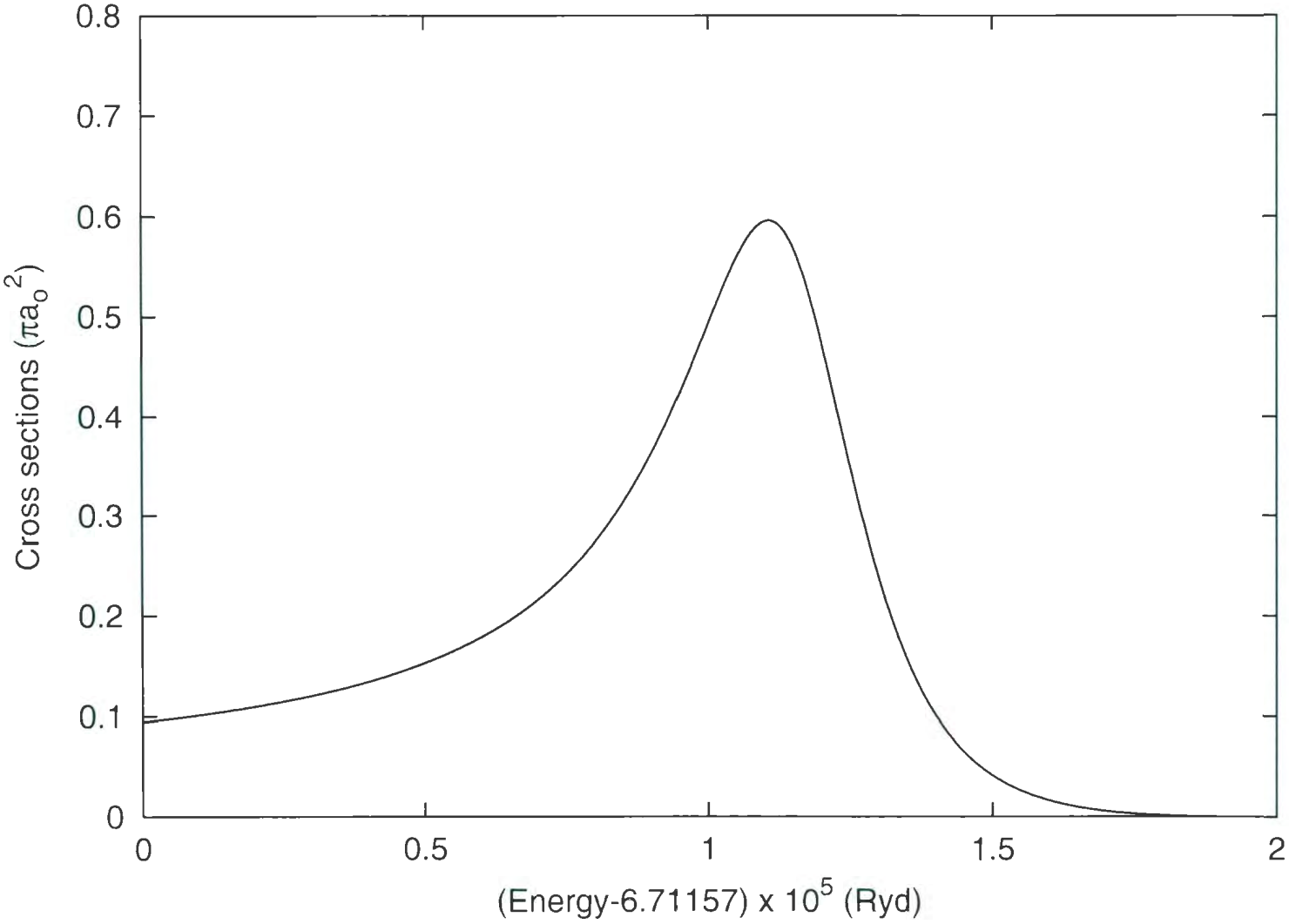

Figure 3.35. S-wave Cross-Sections of e^--Li^{2+} Singlet Scattering at $^1S^e$(2,10b)

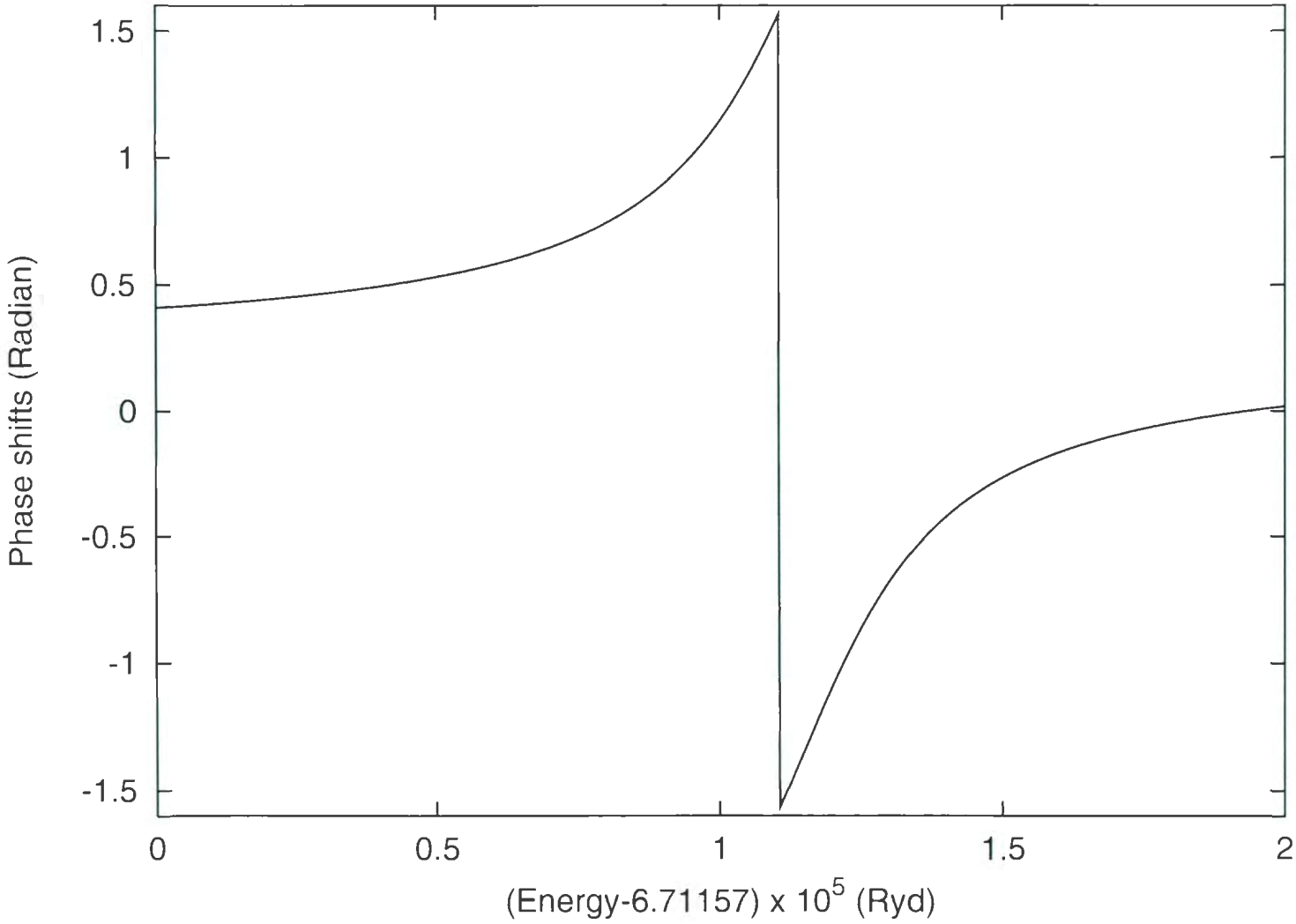

Figure 3.36. S-wave Phase Shifts of e^{-}-Li^{2+} Singlet Scattering at $^{1}S^{e}$(2,10b)

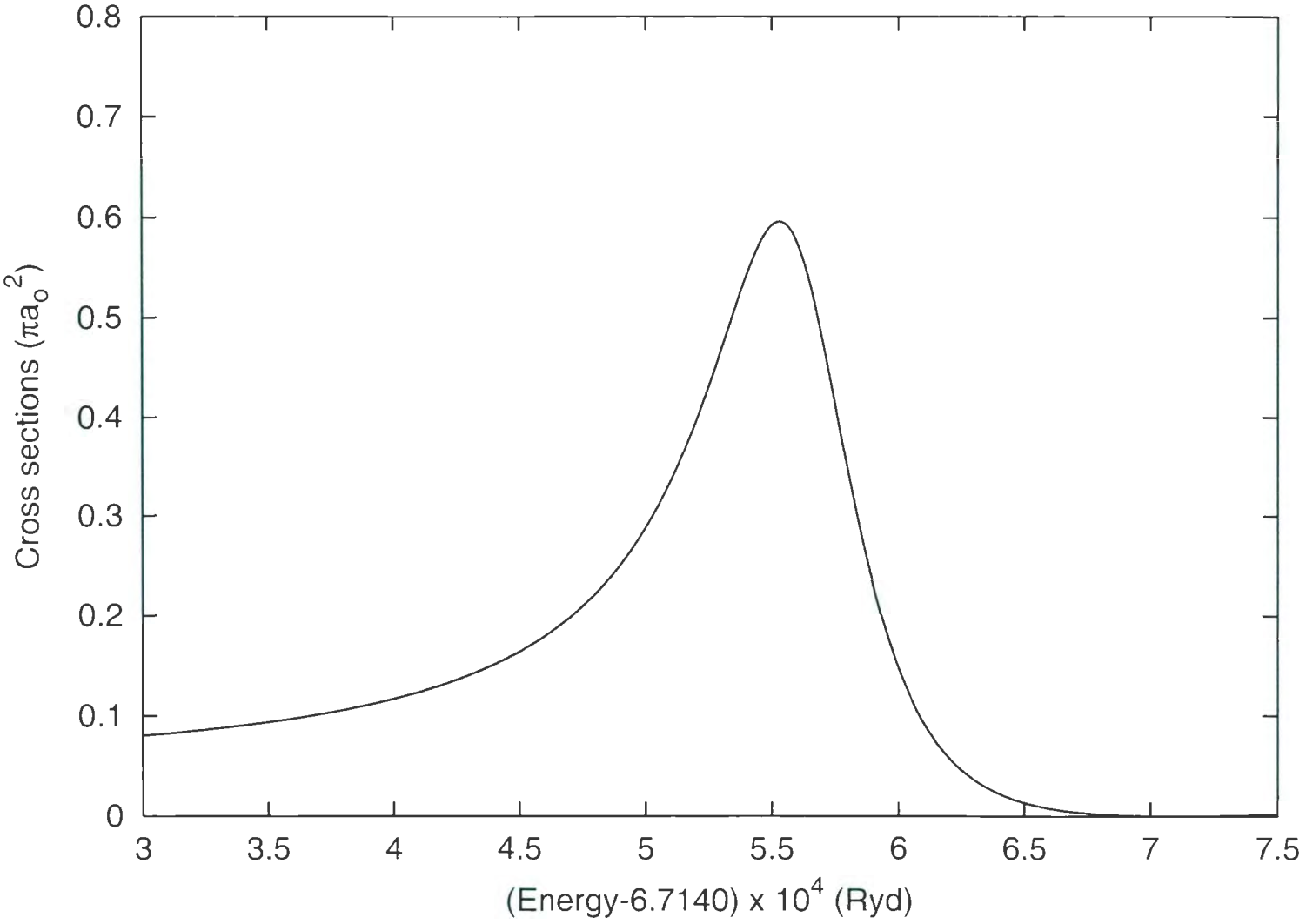

Figure 3.37. S-wave Cross-Sections of e^--Li^{2+} Singlet Scattering at $^1S^e$(2,11a)

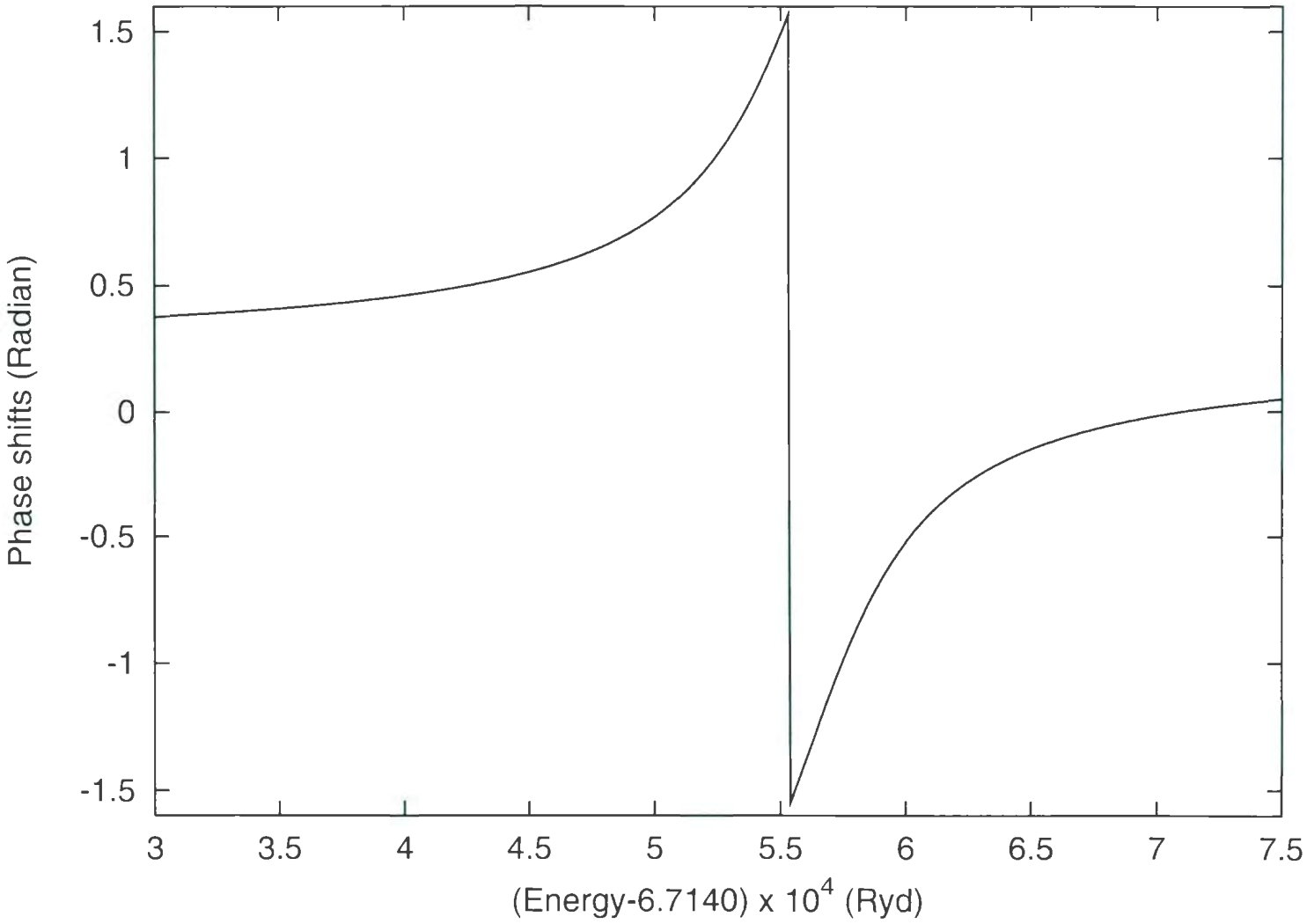

Figure 3.38. S-wave Phase Shifts of e^{-}-Li^{2+} Singlet Scattering at $^{1}S^{e}$(2,11a)

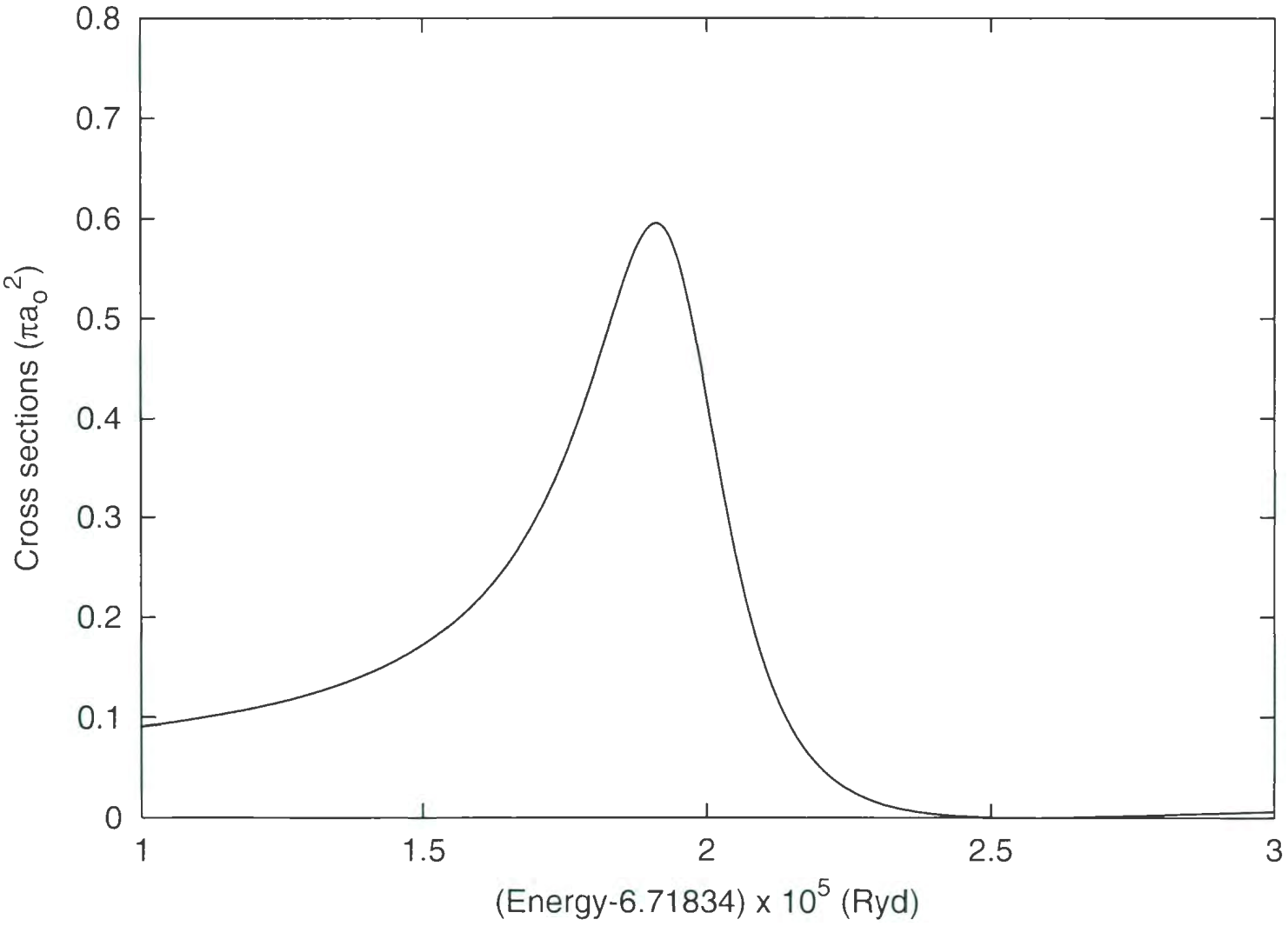

Figure 3.39. S-wave Cross-Sections of e^--Li^{2+} Singlet Scattering at $^1S^e$(2,11b)

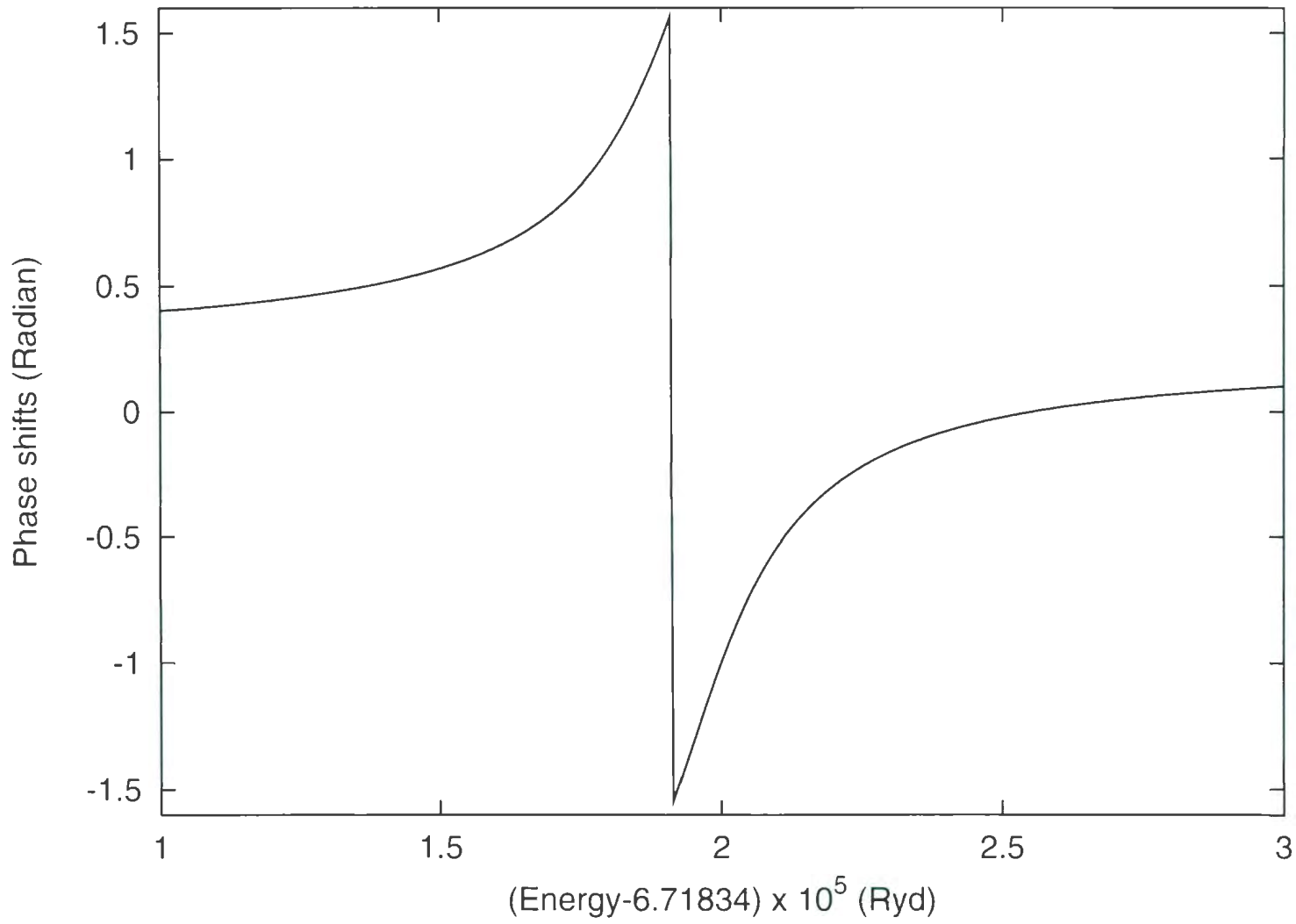

Figure 3.40. S-wave Phase Shifts of e^{-}-Li^{2+} Singlet Scattering at $^{1}S^{e}$(2,11b)

Chapter 4

Conclusion

In this thesis, we present the results of our determination of the S-wave singlet doubly-excited states $^1S^e$ of Li^+ below the N=2 excitation threshold of Li^{2+} using a numerical method developed earlier [12, 13] within the Harris-Nesbet variational calculation of electron-hydrogenlike-ion collisions. Altogether, we succeeded in locating 20 doubly-excited states $^1S^e$ of Li^+ below the N=2 threshold of Li^{2+}, 10 of them belonging to the *a*-series (K=1, T=0) and another 10 belonging to *b*-series (K=-1, T=0). This is the greatest number of singlet S-wave doubly excited states that have been determined below the threshold N=2 for Li^+ so far. Because of the high accuracy of this method, we were able to determine for the first time some of these doubly-excited states ($^1S^e$(2,10a) and $^1S^e$(2,11a) of the *a*-series and $^1S^e$(2,10b) and $^1S^e$(2,11b) of the *b*-series) which lie very close to the N=2 threshold. The results of the present calculation may also be used to resolve the discrepancy existing among the widths of a few lowest-lying doubly excited states $^1S^e$ determined by various other research groups employing different numerical methods. Our calculations also provide a large set of higher-lying $^1S^e$ resonances of Li^+

below the N=2 threshold for comparison with those determined by Chung and Lin. Our calculations confirm the existence of all the 16 doubly-excited states $^1S^e$ determined by this group and that the positions and widths determined by them seem to be also rather accurate. We are also able to display explicitly in graphs all the twenty doubly excited states $^1S^e$ that we determined, so that one can have a precise idea about the shape of these $^1S^e$ doubly-excited-state resonances. This work, together with numerous other works done in the past by Gien and Gien et al. [12, 13, 23, 27-45], again confirms that the Harris-Nesbet calculation is a reliable numerical method that can provide not only very accurate scattering phase shifts and cross sections for collisions of electron and positron with hydrogen atoms and hydrogenlike ions at low energy but also an accurate numerical procedure to be used in the determination of doubly excited states of two-electron (neutral or ionic) atoms. An interesting research work that could be done immediately is the determination of the triplet S-wave doubly excited states of Li^+ below the N=2 threshold of Li^{2+} using this very same numerical procedure.

Bibliography

[1] R. Bruch, G. Paul, J. Andra and Lester Lipsky, Phys. Rev A **12**: 1808, 1975

[2] P. Ziem, R. Bruch and N Stolterfoht, J. Phys. B: At. Mol. Phys **8**: L480, 1975

[3] P. K. Carrol and E. T. Kennedy, Phys. Rev. Lett. **38**: 1068, 1977

[4] M. Rodbro, R. Bruch and P. Bisgaard, J. Phys. B: At. Mol. Phys **12:** 2413, 1979

[5] J. W. Cooper, U. Fano and F. Prats, Phys. Rev. Lett. **10**: 518, 1963

[6] A. K. Bhatia, Phys. Rev. A **15**: 1315, 1977

[7] Y. K. Ho, Phys. Rev. A **23**: 2137, 1981

[8] P. L. Altick and E. N. Moore, Phys. Rev. Lett. **15**: 100, 1965

[9] L. Lipsky and A. Russek, Phys. Rev. **142**: 59, 1966

[10] M. J. Conneely and L Lipsky, J. Phys. B: At. Mol. Phys. **11**: 4135, 1978

[11] K. T. Chung and C. D. Lin, At. Data and Nucl. Data Tab. **69**: 101, 1998

[12] T. T. Gien, J. Phys. B: At. Mol. Opt. Phys. **28**: L313, 1995

[13] T. T. Gien, Proceedings of the Positron Workshop 1995, Vancouver, B. C., Canada, Can. J Phys. **74**: 343, 1996

[14] R. K. Nesbet, Variational Methods in Electron-Atom Scattering Theory, Plenum Press (New York), 1980

[15] L. Hulthe'n, Fysiogr. Sallsk. Lund Forhandl. **14**: 2, 1944

[16] L. Hulthe'n, Ark. Mat. Astr. Fys. **35A**, No 25, 1948

[17] W. Kohn, Phys. Rev. **74**:1763, 1948

[18] C. Schwartz, Ann. Phys.(N.Y.) **16**: 36, 1961

[19] F. E. Harris, Phys. Rev. Lett. **19**: 173, 1967

[20] R. K. Nesbet, Phys. Rev. **175**: 134, 1968

[21] R. K. Nesbet, Phys. Rev. **179**: 60, 1969

[22] R. K. Nesbet, Comput. Phys. Commun. **6**:275, 1973

[23] T. T. Gien, J. Phys. B: At. Mol. Opt. Phys. **35**: 4475, 2002

[24] M. Abramowitz, Handbook of Mathematical Functions (M. Abramowitz and I. A. Stegun, Eds.) p. 537 National Bureau of Standard, Washington, 1972

[25] S. E. A. Wakid and J. Callaway, Phys. Lett. **A78**: 137, 1980

[26] R. L. Armstead, Phys Rev. **171**: 91, 1968

[27] Guo-Guang Liu and T. T. Gien, Phys. Rev. A **46**: 3918, 1992

[28] T. T. Gien and G. G. Liu, Phys. Rev. A **48**: 3386, 1993

[29] T. T. Gien and G. G. Liu, J Phys. B: At. Mol. Opt. Phys. **27**: L179, 1994

[30] T. T. Gien, Phys. Rev. A **52**: 1186, 1995

[31] T. T. Gien, J. Phys. B: At. Mol. Opt. Phys. **28**: L321, 1995

[32] Y. R. Kuang and T. T. Gien, Phys. Rev. A **55**: 256, 1997

[33] T. T. Gien, J. Phys. B: At. Mol. Opt. Phys. **30**: L23, 1997

[34] T. T. Gien, Phys. Rev. A **56**: 1332, 1997

[35] T. T. Gien, J. Phys. B: At. Mol. Phys. **29**: 2127, 1996

[36] T. T. Gien, J. Phys. B: At. Mol. Opt. Phys. **31**: L629, 1998

[37] T. T. Gien, J. Phys. B: At. Mol. Opt. Phys. **31**: L1001, 1998. *Corrigendum*. J. Phys. B: At. Mol. Opt. Phys. **32**: 2295, 1999.

[38] T. T. Gien, J. Phys. B: At. Mol. Opt. Phys. **34**: L535, 2001

[39] T. T. Gien, J. Phys. B: At. Mol. Opt. Phys. **34**: 5103, 2001

[40] T. T. Gien, J. Phys. B: At. Mol. Opt. Phys. **36**: 2291, 2003

[41] T. T. Gien, ICPEAC 2005, XXIV International Conference on Photonic, Electronic, and Atomic Collisions, Rosario, Argentina July , 2005, Conference Abstracts p. 368

[42] T. T. Gien, J. Phys. B: At. Mol. Opt. Phys. **39**: 939, 2006

[43] T. T. Gien, J. Phys. B: At. Mol. Opt. Phys. **39**: 2969, 2006

[44] T. T. Gien, ECAMP IX, 9th European Conference on Atoms, Molecules, & Photons, Heraklion, Crete, Greece, 6-11 May 2007, Conferences Abstracts p Th2-46

[45] T. T. Gien, J. Phys. B: At. Mol. Opt. Phys. **41**: 035003, 2008

[46] D. H. Oza, Phys. Rev. A **33**: 824, 1986

[47] D. R. Herrick and O. Sinanoglu, Phys. Rev. A **11**: 97, 1975